Published by CERN in the Proceedings of the 2015 CERN–Latin-American School of High-Energy Physics, Ibarra, Ecuador, 4 – 17 March 2015, edited by M. Mulders and G. Zanderighi, CERN-2016-005 (CERN, Geneva, 2016)

Neutrino Physics

P. Hernández
IFIC, Universidad de València and CSIC, E-46071 Valencia, Spain

Abstract
This is the writeup of the lectures on neutrino physics delivered at various schools: TASI and Trieste in 2013 and the CERN-Latin American School in 2015. The topics discussed in this lecture include: general properties of neutrinos in the SM, the theory of neutrino masses and mixings (Dirac and Majorana), neutrino oscillations both in vacuum and in matter, as well as an overview of the experimental evidence for neutrino masses and of the prospects in neutrino oscillation physics. We also briefly review the relevance of neutrinos in leptogenesis and in beyond-the-Standard-Model physics.

Keywords
Neutrino; particle physics; lectures; neutrino oscillations; mixing; standard model.

1 Introduction

The history of neutrinos is tightly linked to that of the Standard Model. The discovery of neutrinos and the measurement of their tiny masses has been a scientific *tour de force*.

Neutrinos made their appearance at the beginning of the 20th century as *dark* particles in radioactive β-decay. In this process a nucleus undergoes a transition

$$ {}^{A}_{Z}X \rightarrow {}^{A}_{Z+1}X' + e^{-} \tag{1}$$

emitting an electron, which, by energy conservation, should have an energy equal to the difference of the parent and daughter nuclear masses, Q, see Fig. 1.

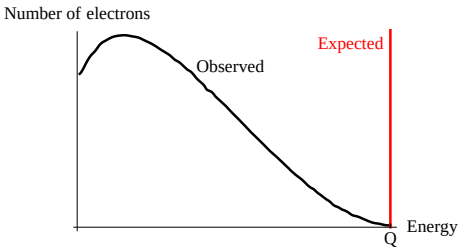

Fig. 1: Electron spectrum of β-decay.

The spectrum of the electrons was measured to be instead continuous with an end-point at Q. It took almost 20 years to come up with an explanation to this apparent violation of energy conservation. W. Pauli called for a *desperate remedy*, proposing that in the decay, a neutral and relatively light particle was being emitted together with the electron and escaped undetected. In that case the spectrum of the electron would indeed be continuous since only the sum of the energy of the electron and the phantom particle should equal Q. The dark particle got an italian name: *neutrino* in honour of E. Fermi, who was among the first to take seriously Pauli's hypothesis, from which he constructed the famous theory of β-decay [1]. In this theory, the interaction responsible for β-decay can be depicted as in Fig. 2,

https://doi.org/10.5170/CERN-2016-005.85

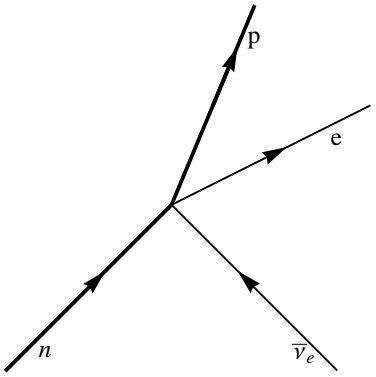

Fig. 2: Fermi four-fermion coupling responsible for β-decay.

a four-fermion interaction with strength given by G_F, the fermi constant. Such interaction implies that neutrinos should also scatter off matter through the inverse beta process, $\bar{\nu}\, p \to n e^+$. Bethe and Pearls [2] estimated the cross section for such process to be

$$\sigma_{\bar{\nu}} \leq 10^{-44}\ \text{cm}^2, \quad E_{\bar{\nu}} \simeq 2\ \text{MeV} \tag{2}$$

and concluded that *"it is absolutely impossible to observe processes of this kind"*. Indeed this tiny cross section implies that a neutrino has a mean free path of thousands of light-years in water.

Pontecorvo [3] however was among the first to realise that it was not so hopeless. One could get a few events per day in a ton-mass scale detector with a neutrino flux of $10^{11}\nu/\text{cm}^2/\text{s}$. Such is the neutrino flux of a typical nuclear reactor at a few tens of meters. Reines and Cowen (RC) succeeded [4, 5]. They were able to detect neutrinos via inverse beta decay in a very massive detector thanks to the extremely robust and clean signal which combines the detection of the positron and the neutron in delayed coincidence, see Fig. 3. This experiment not only lead to the discovery of anti-neutrinos, but introduced a detection technique that is still being used today in state-of-the-art reactor neutrino experiments, that continue to make discoveries in neutrino physics.

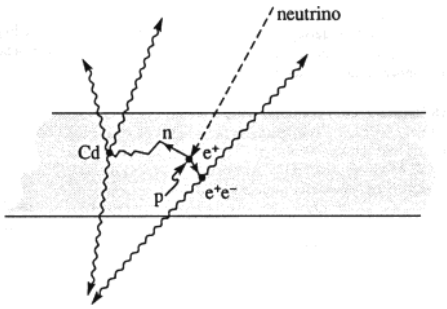

Fig. 3: Detection technique in the Reines-Cowan experiment.

Soon after anti-neutrinos were discovered, it was realised that they come in flavours. The muon had been discovered in cosmic rays much earlier, but it took a long time to understand that this particle was a heavier version of the electron and not the pion. The analogous of the β-process involving muons is pion decay

$$\pi^- \to \mu^- \bar{\nu}_\mu. \tag{3}$$

It was understood that also in this case a neutrino was being emitted but that such neutrino, accompanying the μ, had a different identity to that in β-decay. Since the energies involved in this process are higher than in β-decay and neutrino cross-sections grow fast with energy in the Fermi theory, it would actually be easier to detect this new type of neutrinos.

In 1962 Lederman, Schwartz and Steinberger (LSS) achieved this goal by creating the first accelerator neutrino beam [6]. In such a beam, an boosted proton beam hits a target producing pions and other hadrons that decay into neutrinos and other particles, mimicking what happens in cosmic rays. If a thick shield intercepts the beam, all particles except the neutrinos can be stopped, see Fig. 4. A neutrino detector is located behind the shield. A neutrino event will be seen from the appearance of a muon in the detector. Again this was such a great idea that we are still making discoveries with the modern versions of the LSS experiment, in the so-called conventional accelerator neutrino beams.

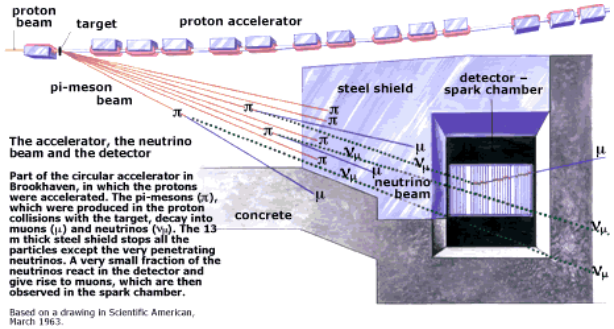

Fig. 4: Lederman, Schwartz, Steinberger experiment.

Kinematical effects of neutrino masses were searched for by measuring very precisely the end-point of the lepton energy spectrum in weak decays, that gets modified if neutrinos are massive. In particular the most stringent limit is obtained from tritium β-decay for the "electron" neutrino:

$$^3H \rightarrow ^3\mathrm{He} + e^- + \bar{\nu}_e. \tag{4}$$

Fig. 5 shows the effect of a neutrino mass in the end-point electron energy spectrum in this decay. The best limit has been obtained by the Mainz and Troitsk experiments. The PDG combination gives [7]:

$$m_{\nu_e} < 2\ \mathrm{eV}(95\%\mathrm{CL})\ . \tag{5}$$

The direct limits from processes involving μ, τ leptons are much weaker. The best limit on the ν_μ mass ($m_{\nu_\mu} < 170$ keV [8]) was obtained from the end-point spectrum of the decay $\pi^+ \rightarrow \mu^+\nu_\mu$, while that

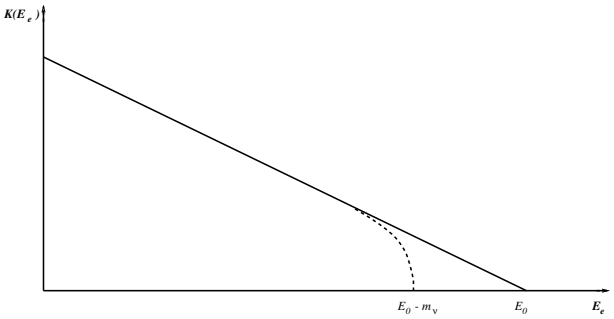

Fig. 5: Effect of a neutrino mass in the end-point of the lepton energy spectrum in β decay.

$(\mathbf{1},\mathbf{2})_{-\frac{1}{2}}$	$(\mathbf{3},\mathbf{2})_{-\frac{1}{6}}$	$(\mathbf{1},\mathbf{1})_{-1}$	$(\mathbf{3},\mathbf{1})_{-\frac{2}{3}}$	$(\mathbf{3},\mathbf{1})_{-\frac{1}{3}}$
$\begin{pmatrix}\nu_e\\ e\end{pmatrix}_L$	$\begin{pmatrix}u^i\\ d^i\end{pmatrix}_L$	e_R	u^i_R	d^i_R
$\begin{pmatrix}\nu_\mu\\ \mu\end{pmatrix}_L$	$\begin{pmatrix}c^i\\ s^i\end{pmatrix}_L$	μ_R	c^i_R	s^i_R
$\begin{pmatrix}\nu_\tau\\ \tau\end{pmatrix}_L$	$\begin{pmatrix}t^i\\ b^i\end{pmatrix}_L$	τ_R	t^i_R	b^i_R

Table 1: Irreducible fermionic representations in the Standard Model: $(d_{SU(3)}, d_{SU(2)})_Y$.

on the ν_τ mass was obtained at LEP ($m_{\nu_\tau} < 18.2$ MeV [9]) from the decay $\tau \to 5\pi\nu_\tau$. Neutrinos in the SM where therefore conjectured to be massless.

2 Neutrinos in the Standard Model

The Standard Model (SM) is a gauge theory based on the gauge group $SU(3) \times SU(2) \times U_Y(1)$. All elementary particles arrange in irreducible representations of this gauge group. The quantum numbers of the fermions $(d_{SU(3)}, d_{SU(2)})_Y$ are listed in table 1.

Under gauge transformations neutrinos transform as doublets of $SU(2)$, they are singlets under $SU(3)$ and their hypercharge is $-1/2$. The electric charge, given by $Q = T_3 + Y$, vanishes. They are therefore the only particles in the SM that carry no conserved charge.

The two most intriguing features of table 1 are its left-right or chiral asymmetry, and the three-fold repetition of family structures. Neutrinos have been essential in establishing both features.

2.1 Chiral structure of the weak interactions

The left and right entries in table 1 have well defined chirality, negative and positive respectively. They are two-component spinors or Weyl fermions, that is the smallest irreducible representation of the Lorentz group representing spin $1/2$ particles. Only fields with negative chirality (i.e. eigenvalue of γ_5 minus one) carry the $SU(2)$ charge. For free fermions moving at the speed of light (i.e., massless), it is easy to see that the chiral projectors are equivalent to the projectors on helicity components:

$$P_{R,L} \equiv \frac{1 \pm \gamma_5}{2} = \frac{1}{2}\left(1 \pm \frac{\mathbf{s}\cdot\mathbf{p}}{|p|}\right) + O\left(\frac{m_i}{E}\right), \tag{6}$$

where the helicity operator $\mathbf{\Sigma} = \frac{\mathbf{s}\cdot\mathbf{p}}{|p|}$ measures the component of the spin in the direction of the momentum. Therefore for massless fermions only the left-handed states (with the spin pointing in the opposite direction to the momentum) carry $SU(2)$ charge. This is not inconsistent with Lorentz invariance, since for a fermion travelling at the speed of light, the helicity is the same in any reference frame. In other words, the helicity operator commutes with the Hamiltonian for a massless fermion and is thus a good quantum number.

The discrete symmetry under CPT (charge conjugation, parity, and time reversal), which is a basic building block of any Lorentz invariant and unitary quantum field theory (QFT), requires that for any left-handed particle, there exists a right-handed antiparticle, with opposite charge, but the right-handed particle state may not exist. A Weyl fermion field represents therefore a particle of negative helicity and an antiparticle with positive one.

Parity however transforms left and right fields into each other, thus the left-handedness of the weak interactions implies that parity is maximally broken in the SM. The breaking is nowhere more obvious than for neutrinos where the parity partner of the neutrino does not exist. All the remaining fermions in the SM come in parity pairs, albeit with different $SU(2) \times U(1)$ charges. Since this gauge symmetry is spontaneously broken, the left and right fields combine into massive Dirac fermions, that is a four component representation of the Lorentz group and parity, which represents a particle and an antiparticle with either helicity.

The SM resolved the Fermi interaction as being the result of the exchange of the $SU(2)$ massive W boson as in Fig. 6.

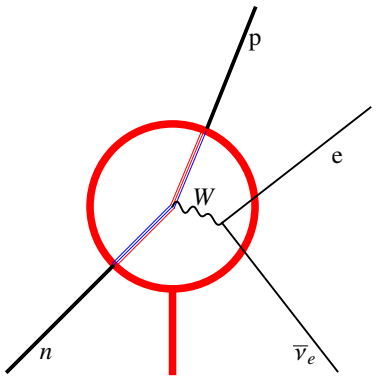

Fig. 6: β-decay process in the SM.

Neutrinos interact in the SM via charged and neutral currents:

$$\mathcal{L}_{SM} - \frac{g}{\sqrt{2}} \sum_{\alpha} \bar{\nu}_\alpha \gamma_\mu P_L l_\alpha W^+_\mu - \frac{g}{2\cos\theta_W} \sum_{\alpha} \bar{\nu}_\alpha \gamma_\mu P_L \nu_\alpha Z^+_\mu + h.c. \tag{7}$$

The weak current is therefore V–A since it only couples to the left fields: $\gamma_\mu P_L \propto \gamma_\mu – \gamma_\mu \gamma_5$. This structure is clearly seen in the kinematics of weak decays involving neutrinos, such as the classic example of pion decay to $e\ \bar{\nu}_e$ or $\mu \bar{\nu}_\mu$. In the limit of vanishing electron or muon mass, this decay is forbidden, because the spin of the initial state is zero and thus it is impossible to conserve simultaneously momentum and angular momentum if the two recoiling particles must have opposite helicities, as shown in Fig. 7. Thus the ratio of the decay rates to electrons and muons, in spite of the larger phase space in the former, is strongly suppressed by the factor $\left(\frac{m_e}{m_\mu}\right)^2 \sim 2 \times 10^{-5}$.

Another profound consequence of the chiral nature of the weak interaction is anomaly cancellation. The chiral coupling of fermions to gauge fields leads generically to inconsistent gauge theories due to chiral anomalies: if any of the diagrams depicted in Fig. 8 is non-vanishing, the weak current is conserved at tree level but not at one loop, implying a catastrophic breaking of gauge invariance. Anomaly cancellation is the requirement that all these diagrams vanish, which imposes strong constraints on the hypercharge assignments of the fermions in the SM, which are *miraculously* satisfied:

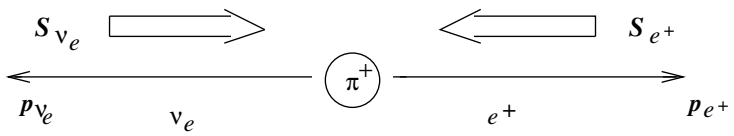

Fig. 7: Kinematics of pion decay.

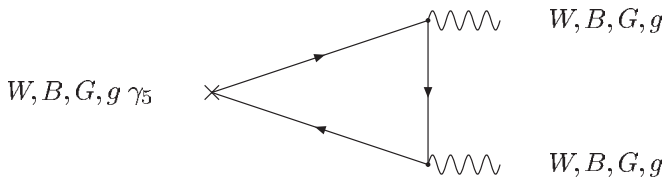

Fig. 8: Triangle diagrams that can give rise to anomalies. W, B, G are the gauge bosons associated to the $SU(2), U_Y(1), SU(3)$ gauge groups, respectively, and g is the graviton.

$$\overbrace{\sum_{i=\text{quarks}} Y_i^L - Y_i^R}^{GGB} = \overbrace{\sum_{i=\text{doublets}} Y_i^L}^{WWB} = \overbrace{\sum_i Y_i^L - Y_i^R}^{Bgg} = \overbrace{\sum_i (Y_i^L)^3 - (Y_i^R)^3}^{B^3} = 0, \tag{8}$$

where $Y_i^{L/R}$ are the hypercharges of the left/right components of the fermionic field i, and the triangle diagram corresponding to each of the sums is indicated above the bracket.

2.2 Family structure

Concerning the family structure, we know, thanks to neutrinos, that there are exactly three families in the SM. An extra SM family with quarks and charged leptons so heavy that cannot be produced, would also have massless neutrinos that would contribute to the invisible Z^0 decay:

$$Z^0 \to \bar{\nu}_\alpha \nu_\alpha. \tag{9}$$

The invisible width of the Z^0 has been measured at LEP with an impressive precision, as shown in Fig. 9. This measurement excludes any number of standard families different from three [7]:

$$N_\nu = \frac{\Gamma_{\text{inv}}}{\Gamma_{\bar{\nu}\nu}} = 2.984 \pm 0.008. \tag{10}$$

3 Massive Neutrinos

Neutrinos are ubiquitous in our surroundings. If we open our hand, it will be crossed each second by about $\mathcal{O}(10^{12})$ neutrinos from the sun, about $\mathcal{O}(10)$ from the atmosphere, about $\mathcal{O}(10^9)$ from natural radioactivity in the Earth and even $\mathcal{O}(10^{12})$ relic neutrinos from the Big Bang. In 1987, the Kamiokande detector in Japan observed the neutrino burst from a SuperNova that exploded in the Large Magellanic Cloud, at a distance of 168 thousand light years from Earth. For a few seconds, the supernova flux was of the same order of magnitude as the flux of solar neutrinos!

Using many of these sources as well as others man-made, a decade of revolutionary neutrino experiments have demonstrated that, for the time being, neutrinos are the less standard of the SM particles. They have tiny masses and this necessarily requires new degrees of freedom with respect to those in table 1.

A massive fermion necessarily has two states of helicity, since it is always possible to reverse the helicity of a state that moves at a slower speed than light by looking at it from a boosted reference frame. What is the right-handed state of the neutrino ? It turns out there are two ways to proceed.

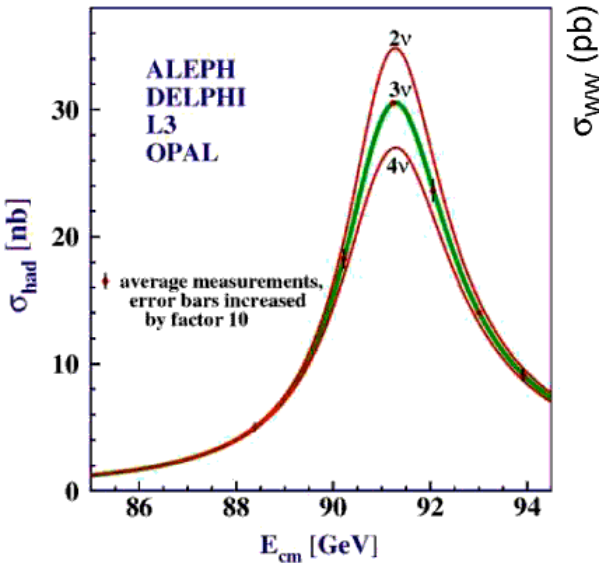

Fig. 9: Z^0 resonance from the LEP experiments. Data are compared to the case of $N_\nu = 2, 3$ and 4.

Let us consider the case of free fermions. A four-component Dirac fermion can be made massive adding the following mass term to the Lagrangian:

$$-\mathcal{L}_m^{Dirac} = m\bar{\psi}\psi = m(\overline{\psi_L + \psi_R})(\psi_L + \psi_R) = m(\overline{\psi_L}\psi_R + \overline{\psi_R}\psi_L). \tag{11}$$

A Dirac mass term couples the left-handed and right-handed chiral components of the fermion field, and therefore this coupling vanishes identically in the case of a Weyl fermion.

Can one give a mass to a two-component Weyl fermion ? As first realized by Majorana, this indeed can be done with the following mass term:

$$-\mathcal{L}_m^{Majorana} = \frac{m}{2}\overline{\psi^c}\psi + \frac{m}{2}\overline{\psi}\psi^c = \frac{m}{2}\psi^T C\psi + \frac{m}{2}\bar{\psi}C\bar{\psi}^T, \tag{12}$$

where

$$\psi^c \equiv C\bar{\psi}^T = C\gamma_0\psi^*. \tag{13}$$

It is easy to check that the Majorana mass term satisfies the required properties:

1) It can be constructed with a two-component spinor or Weyl fermion: if $\psi = P_L\psi \equiv (\psi_L, 0)$
$$\psi^T C\psi = \psi_L^T i\sigma_2\psi_L, \tag{14}$$
and it does not vanish in the absence of the right chiral component.
2) It is Lorentz invariant. It is easy to show, using the properties of the gamma matrices that under a Lorentz transformation ψ and ψ^c transform in the same way,
$$\psi \to e^{-\frac{i}{4}\omega_{\mu\nu}\sigma^{\mu\nu}}\psi \equiv S(\Lambda)\psi, \quad \psi^c \to S(\Lambda)\psi^c, \tag{15}$$
with $\sigma_{\mu\nu} \equiv= \frac{i}{4}[\gamma_\mu, \gamma_\nu]$, and therefore the bilinear $\overline{\psi^c}\psi$ is Lorentz invariant.
3) The equation of motion derived from eq. (12) for a free majorana fermion has plane wave solutions satisfying the relativistic relation for a massive fermion:
$$E^2 - \mathbf{p}^2 = m^2.$$

In the SM none of the mass terms of eqs. (11) and (12) are gauge invariant. Spontaneous symmetry breaking allows to generate the Dirac mass term from Yukawa couplings for all fermions in the SM, while the Majorana mass term can only be generated for neutrinos.

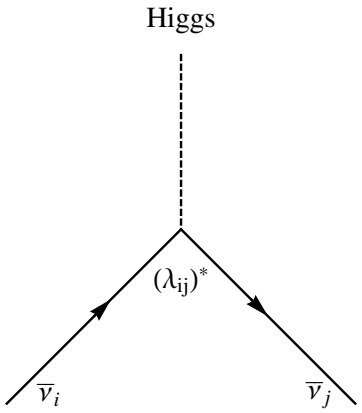

Fig. 10: Neutrino Yukawa coupling.

3.1 Massive Dirac neutrinos

We can enlarge the SM by adding a set of three right-handed neutrino, ν_R states, with quantum numbers $(1,1)_0$, ie singlets under all the gauge groups. A new Yukawa (Fig. 10) coupling of these new states with the lepton doublet is exactly gauge invariant and therefore can be added to the SM:

$$-\mathcal{L}_m^{Dirac} = \overline{L}\,\lambda\tilde{\Phi}\,\nu_R + \text{ h.c.} \tag{16}$$

where $L = (\nu\ l)$ is the lepton doublet, $\tilde{\Phi} \equiv i\sigma_2\phi^*$ and ϕ is the Higgs field, with quantum numbers $(\mathbf{1},\mathbf{2})_{-\frac{1}{2}}$. Upon spontaneous symmetry breaking the scalar doublet gets a vacuum expectation value $\langle\tilde{\Phi}\rangle = (\frac{v}{\sqrt{2}}\ 0)$, and therefore a neutrino Dirac mass term is generated

$$-\mathcal{L}_m^{Dirac} \to -\,\overline{\nu_L}\,\lambda\frac{v}{\sqrt{2}}\nu_R + \text{ h.c. .} \tag{17}$$

The neutrino mass matrix is proportional to the Higgs vev, in complete analogy to the remaining fermions:

$$m_\nu = \lambda\frac{v}{\sqrt{2}}. \tag{18}$$

There are two important consequences of Dirac neutrinos. First, there is a new hierarchy problem in the SM to be explained: why are neutrinos so much lighter than the remaining leptons, even those in the same family (see Fig. 11), if they get the mass in the same way ? Secondly, an accidental global symmetry, lepton number L, that counts the number of leptons minus that of antilepton, remains exactly conserved at the classical level [1], just as baryon number, B, is.

3.2 Massive Majorana neutrinos

Since the combination $\bar{L}\tilde{\phi}$ is a singlet under all gauge groups, the Majorana-type contraction (see Fig. 12):

$$-\mathcal{L}_m^{Majorana} = \bar{L}\tilde{\phi}\,\alpha C\tilde{\phi}^T\bar{L}^T + h.c., \tag{19}$$

is gauge invariant. This term, first writen down by Weinberg [10], gives rise to a Majorana mass term for neutrinos upon spontaneous symmetry breaking:

$$-\mathcal{L}_m^{Majorana} \to \bar{\nu}_L\alpha\frac{v^2}{2}C\bar{\nu}_L^T + h.c., \tag{20}$$

[1] As usual B + L is broken by the anomaly and only B − L remains exact at all orders.

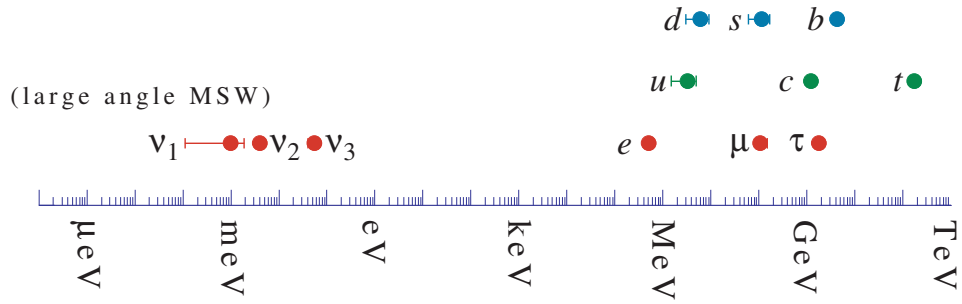

Fig. 11: Fermion spectrum in the Standard Model.

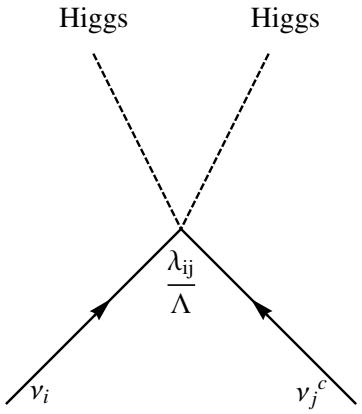

Fig. 12: Weinberg operator.

The neutrino mass matrix in this case is given by:

$$m_\nu = \alpha v^2. \tag{21}$$

The Weinberg operator has dimension 5, and therefore the coupling $[\alpha] = -1$. We can write it in terms of a dimensionless coupling as

$$\alpha = \frac{\lambda}{\Lambda}, \tag{22}$$

where Λ is a new physics scale, in principle unrelated to the electroweak scale.

The consequences of the SM neutrinos being massive Majorana particles are profound.

If the scale Λ is much higher than the electroweak scale v, a strong hierarchy between the neutrino and the charged lepton masses arises naturally. If all dimensionless couplings λ are of the same order, neutrino masses are suppressed by a factor v/Λ with respect to the charged fermions. On the other hand, Weinberg's operator violates lepton number L and provides a new seed for generating the matter/antimatter asymmetry in the Universe as we will see.

Even though the Majorana mechanism to generate neutrino masses does not involve any extra degree of freedom with respect to those in the SM, the existence of the Weinberg coupling implies that cross sections involving for example the scattering of neutrinos and the higgs will grow with energy, ultimately violating unitarity. The situation is analogous to that of the Fermi interaction of Fig. 2. The SM resolved this interaction at higher energies as being the result of the interchange of a heavy vector boson, Fig. 6. The Majorana coupling, if it exists, should also represent the effect at low-energies of the exchange of one or more unknown massive states. What those states are remains one of the most interesting open questions in neutrino physics.

Finally, it is interesting to note that the anomaly cancellation conditions fix all the hypercharges in this case (i.e., there is only one possible choice for the hypercharges that satisfies Eqs. (8)), which implies that electromagnetic charge quantization is the only possibility in a field theory with the same matter content as the SM.

3.3 Neutrino masses and physics beyond-the-standard-model

Any new physics beyond the standard model (BSM) characterized by a high scale, Λ, will induce effects at low energies $E \ll \Lambda$ that can be described by an effective field theory [11, 12]:

$$\mathcal{L}_{\text{eff}} = \mathcal{L}_{\text{SM}} + \sum_i \frac{\alpha_i}{\Lambda} O_i^{d=5} + \sum_i \frac{\beta_i}{\Lambda^2} O_i^{d=6} + ... \tag{23}$$

It is the most general Lagrangian which includes the SM and an infinite tower of operators constructed out of the SM fields respecting Lorentz and gauge symmetries. In principle such a theory depends on infinite new couplings, one per new independent operator, and it is therefore not predictive. However, if the energy we are interested in effects at a given finite order, n, in $\left(\frac{E}{\Lambda}\right)^n$, we can truncate the series to include only operators of dimension $d \leq n+4$. The operators of lowest dimension are the most relevant at low energies.

It turns out that there is only one such operator of the lowest possible dimension, $d = 5$, which is precisely the Weinberg operator of eq. (19). In this perspective, it is natural to expect that the first indication of BSM physics is precisely Majorana neutrino masses, and while many types of BSM theories can give rise to neutrino masses, generically they will induce other new physics effects represented by the operators of $d = 6$ or higher.

4 Neutrino masses and lepton mixing

Neutrino masses, whether Dirac or Majorana, imply lepton mixing [13, 14]. The Yukawa couplings in eq. (16) is a generic complex matrix in flavour space, while that in eq. (19) is a generic complex symmetric matrix, and therefore the same holds for the corresponding mass matrices:

$$-\mathcal{L}_m^{\text{Dirac}} = \overline{\nu_L^i} \left(M_\nu\right)_{ij} \nu_R^j + \overline{l_L^i} \left(M_l\right)_{ij} l_R^j + \text{ h.c.} \tag{24}$$

$$-\mathcal{L}_m^{\text{Majorana}} = \frac{1}{2}\overline{\nu_L^i} \left(M_\nu\right)_{ij} \nu_L^{cj} + \overline{l_L^i} \left(M_l\right)_{ij} l_R^j + \text{ h.c. .} \tag{25}$$

In the Dirac case, the two mass matrices can be diagonalized by a bi-unitary rotation:

$$M_\nu = U_\nu^\dagger \text{Diag}(m_1, m_2, m_3) V_\nu, \;\; M_l = U_l^\dagger \text{Diag}(m_e, m_\mu, m_\tau) V_l, \tag{26}$$

while in the Majorana case, the neutrino mass matrix, being symmetric, can be taken to a diagonal form by

$$M_\nu = U_\nu^\dagger \text{Diag}(m_1, m_2, m_3) U_\nu^*. \tag{27}$$

We can go to the mass basis by rotating the fields as:

$$\nu'_R = V_\nu \nu_R, \; \nu'_L = U_\nu \nu_L, \;\; l'_R = V_l l_R, \; l'_L = U_l l_L. \tag{28}$$

In this basis the charged current interactions are no longer diagonal, in complete analogy with the quark sector (see Fig. 13):

$$\mathcal{L}_{CC}^{\text{lepton}} = -\frac{g}{\sqrt{2}} \overline{l'_i} \gamma_\mu P_L W_\mu^+ \underbrace{\left(U_l^\dagger U_\nu\right)_{ij}}_{U_{\text{PMNS}}} \nu'_j + \text{h.c.} \tag{29}$$

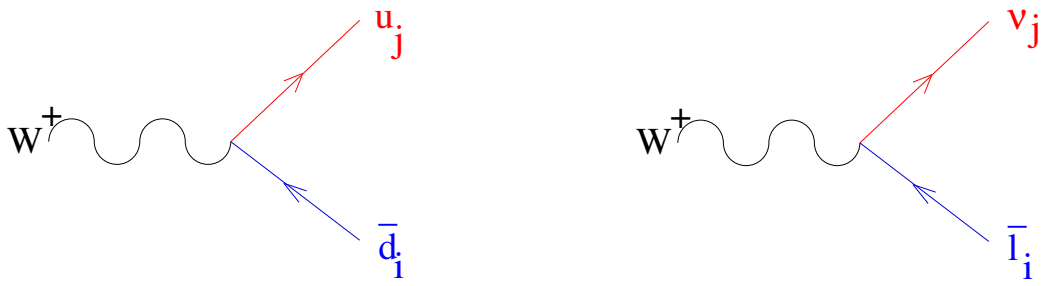

Fig. 13: Quark and lepton mixing.

The mixing matrix in the lepton sector is referred to as the Pontecorvo-Maki-Nakagawa-Sakata (PMNS) matrix, analogous to the CKM one in the quark sector.

The number of physical parameters in the lepton mixing matrix, U_{PMNS}, can easily be computed by counting the number of independent real and imaginary elements of the Yukawa matrices and eliminating those that can be absorbed in field redefinitions. The allowed field redefinitions are the unitary rotations of the fields that leave the rest of the Lagrangian invariant, only those that are not symmetries of the full Lagrangian when lepton masses are included.

	Yukawas	Field redefinitions	$No.\ m$	$No.\ \theta$	$No.\ \phi$
Dirac	$\lambda_l,\ \lambda_\nu$ $4n^2$	$U(n)^3/U(1)$ $\frac{3(n^2-n)}{2},\ \frac{3(n^2+n)-1}{2}$	$2n$	$\frac{n^2-n}{2}$	$\frac{(n-2)(n-1)}{2}$
Majorana	$\lambda_l,\ \alpha_\nu^T=\alpha_\nu$ $3n^2+n$	$U(n)^2$ $n^2-n,\ n^2+n$	$2n$	$\frac{n^2-n}{2}$	$\frac{n^2-n}{2}$

Table 2: Number of real and imaginary parameters in the Yukawa matrices, of those that can be absorbed in field redefinitions. The difference between the two is the number of observable parameters: the lepton masses (m), mixing angles (θ), and phases (ϕ).

In the Dirac case, it is possible to rotate independently the left-handed lepton doublet, together with the right-handed charged leptons and neutrinos, that is $U(n)^3$, for a generic number of families n. However, this includes total lepton number which remains a symmetry of the massive theory and thus cannot be used to reduce the number of physical parameters in the mass matrix. The parameters that can be absorbed in field redefinitions are thus the parameters of the group $U(n)^3/U(1)$ (that is $\frac{3(n^2-n)}{2}$ real, $\frac{3(n^2+n)-1}{2}$ imaginary).

In the case of Majorana neutrinos, there is no independent right-handed neutrino field, nor is lepton number a good symmetry. Therefore the number of field redefinitions is the number of parameters of the elements in $U(n)^2$ (that is n^2-n real and n^2+n imaginary).

The resulting real physical parameters are the mass eigenstates and the mixing angles, while the resulting imaginary parameters are CP-violating phases. All this is summarized in Table 2. Dirac and Majorana neutrinos differ only in the number of observables phases. For three families ($n=3$), there is just one Dirac phase and three in the Majorana case.

A standard parametrization of the mixing matrices for Dirac, $U_{\rm PMNS}$, and Majorana, $\tilde{U}_{\rm PMNS}$, is given by

$$\begin{aligned} U_{\rm PMNS} &= \begin{pmatrix} 1 & 0 & 0 \\ 0 & c_{23} & s_{23} \\ 0 & -s_{23} & c_{23} \end{pmatrix} \begin{pmatrix} c_{13} & 0 & s_{13}e^{-i\delta} \\ 0 & 1 & 0 \\ -s_{13}e^{i\delta} & 0 & c_{13} \end{pmatrix} \begin{pmatrix} c_{12} & s_{12} & 0 \\ -s_{12} & c_{12} & 0 \\ 0 & 0 & 1 \end{pmatrix}, \\ \tilde{U}_{\rm PMNS} &= U_{\rm PMNS}(\theta_{12},\theta_{13},\theta_{23},\delta) \begin{pmatrix} 1 & 0 & 0 \\ 0 & e^{i\alpha_1} & 0 \\ 0 & 0 & e^{i\alpha_2} \end{pmatrix}, \end{aligned} \tag{30}$$

where in all generality $\theta_{ij} \in [0, \pi/2]$ and $\delta, \alpha_1, \alpha_2 \in [0, 2\pi]$.

5 Majorana versus Dirac

It is clear that establishing the Majorana nature of neutrinos is of great importance, since it would imply the existence of a new physics scale. In principle there are very clear signatures, such as the one depicted in Fig. 14, where a ν_μ beam from π^+ decay is intercepted by a detector. In the Dirac case, the interaction of neutrinos on the detector via a charged current interaction will produce only a μ^- in the final state. If neutrinos are Majorana, a wrong-sign muon in the final state is also possible. Unfortunately the rate for μ^+ production is suppressed by m_ν/E in amplitude with respect to the μ^-. For example, for $E_\nu = \mathcal{O}(1)$ GeV and $m_\nu \sim \mathcal{O}(1)$ eV the cross–section for this process will be roughly 10^{-18} times the usual CC neutrino cross-section.

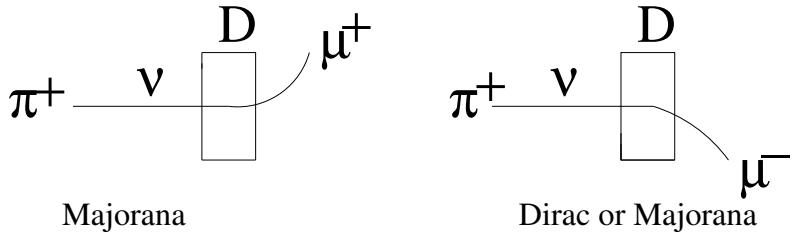

Fig. 14: A neutrino beam from π^+ decay (ν_μ) could interact in the magnetized detector producing a μ^+ only if neutrinos are Majorana.

The best hope of observing a rare process of this type seems to be the search for neutrinoless double–beta decay ($2\beta0\nu$), the right diagram of Fig. 15. The background to this process is the standard double–beta decay depicted on the left of Fig. 15, which has been observed to take place for various isotopes with a lifetime of $T_{2\beta2\nu} > 10^{19}$–10^{21} years.

If the source of this process is just the Majorana ν mass, the inverse lifetime for this process is given by

$$T^{-1}_{2\beta0\nu} \simeq \underbrace{G^{0\nu}}_{\rm Phase} \underbrace{\left|M^{0\nu}\right|^2}_{\rm NuclearM.E.} \underbrace{\left|\sum_i \left(\tilde{U}^{ei}_{\rm PMNS}\right)^2 m_i\right|^2}_{|m_{ee}|^2}. \tag{31}$$

In spite of the suppression in the neutrino mass (over the energy of this process), the neutrinoless mode has a phase factor orders of magnitude larger than the 2ν mode, and as a result present experiments searching for this rare process have already set bounds on neutrino masses in the eV range as shown in Table 3.

Fig. 15: 2β decay: normal (left) and neutrinoless (right).

Experiment	Nucleus	$\lvert m_{ee}\rvert$
EXO-200	^{136}Xe	< 0.19–0.45 eV
NEMO-3	^{100}Mo	< 0.33–0.87 eV
GERDA	^{76}Ge	< 0.2–0.4 eV
KamLAND-Zen	^{136}Xe	< 0.12–0.25 eV
CUORICINO	^{130}Te	< 0.2–0.7 eV

Table 3: Present bounds at 90%CL from some recent neutrinoless double-beta-decay experiments [7].

6 Neutrino Oscillations

The most spectacular implication of neutrino masses and mixings is the macroscopic quantum phenomenom of neutrino oscillations, first introduced by B. Pontecorvo [15]. The Nobel prize in 2015 has been awarded to T. Kajita (from the SuperKakiokande collaboration) and A. B. McDonald (from the SNO collaboration) for the *discovery of neutrino oscillations, which shows that neutrinos have a mass*.

We have seen that the neutrino flavour fields $(\nu_e, \nu_\mu, \nu_\tau)$ that couple via CC to the leptons (e, μ, τ) are unitary combinations of the mass eigenstates fields (ν_1, ν_2, ν_3):

$$\begin{pmatrix} \nu_e \\ \nu_\mu \\ \nu_\tau \end{pmatrix} = U_{\rm PMNS}(\theta_{12}, \theta_{13}, \theta_{23}, \text{phases}) \begin{pmatrix} \nu_1 \\ \nu_2 \\ \nu_3 \end{pmatrix}. \tag{32}$$

In a neutrino oscillation experiment, neutrinos are produced by a source (e.g. pion or μ decays, nuclear reactions, etc) and are detected some macroscopic distance, L, away from the production point. They are produced and detected via weak processes in combination with a given lepton flavour,that is in flavour states. As these states propagate undisturbed in space-time from the production to the detection regions, the different mass eigenstates, having slighly different phase velocities, pick up different phases, resulting in a non-zero probability that the state that arrives at the detector is in a different flavour combination to the one originally produced, see Fig. 16. The probability for this flavour transition oscillates with the distance travelled.

Two ingredients are mandatory for this phenomenom to take place:

– neutrinos must keep quantum coherence in propagation over macroscopic distances, which is only possible because they are so weakly interacting

Fig. 16: Neutrino oscillations.

– there is sufficient uncertainty in momentum at production and detection so that a coherent flavour state can be produced[2]

The master formula for the oscillation probability of ν_α turning into a ν_β is

$$P(\nu_\alpha \to \nu_\beta) = \sum_{i,j} U^*_{\alpha i} U_{\beta i} U_{\alpha j} U^*_{\beta j} e^{-i\frac{\Delta m^2_{ji} L}{2|\mathbf{p}|}}, \tag{33}$$

where $\Delta m^2_{ji} \equiv m^2_i - m^2_j$, $U_{\alpha i}$ are the elements of the PMNS matrix, L is the baseline and $\mathbf{p}$ is the neutrino momentum.

There are many ways to derive this formula. The simplest way that appears in most textbooks uses simple quantum mechanics, where neutrinos are treated as plane waves. A slightly more rigorous method treats neutrinos as wave packets. Finally, it is also possible to derive it from QFT, where neutrinos are treated as intermediate virtual states. The different methods make more or less explicit the basic necessary conditions of neutrino oscillations mentioned above, and therefore are more or less prone to quantum paradoxes.

6.1 Plane wave derivation

Let us suppose that a neutrino of flavor α is produced at t_0. It is therefore a superposition of the mass eigenstates that we assume to be plane waves with spatial momentum $\mathbf{p}$:

$$|\nu_\alpha(t_0)\rangle = \sum_i U^*_{\alpha i} |\nu_i(\mathbf{p})\rangle. \tag{34}$$

The mass eigenstates are eigenstates of the free Hamiltonian:

$$\hat{H}|\nu_i(\mathbf{p})\rangle. = E_i(\mathbf{p})|\nu_i(\mathbf{p})\rangle, \quad E_i(\mathbf{p})^2 = \mathbf{p}^2 + m^2_i. \tag{35}$$

The time evolution operator from $t_0 \to t$ is given by $e^{-i\hat{H}(t-t_0)}$ and therefore the state at time t is given by

$$|\nu_\alpha(t)\rangle = e^{-i\hat{H}(t-t_0)}|\nu_\alpha(t_0)\rangle = \sum_i U^*_{\alpha i} e^{-iE_i(\mathbf{p})(t-t_0)}|\nu_i(\mathbf{p})\rangle. \tag{36}$$

[2]If the momentum uncertainty is sufficiently small one could kinematically distinguish the mass eigenstate being produced/detected.

The probability that at time t the state is in flavour β is

$$P(\nu_\alpha \to \nu_\beta)(t) = |\langle \nu_\beta | \nu_\alpha(t) \rangle|^2 = \left| \sum_i U_{\beta i} U^*_{\alpha i} e^{-iE_i(\mathbf{p})(t-t_0)} \right|^2, \tag{37}$$

where we have used the orthogonality relation $\langle \nu_i(\mathbf{p}) | \nu_j(\mathbf{p}) \rangle = \delta_{ij}$.

Since the neutrinos are ultrarelativistic, we can approximate

$$E_i(\mathbf{p}) - E_j(\mathbf{p}) \simeq \frac{1}{2} \frac{m_i^2 - m_j^2}{|\mathbf{p}|} + \mathcal{O}(m^4), \tag{38}$$

and $L \simeq (t - t_0)$, so that the master formula in eq. (33) is recovered.

The well-founded criticism to this derivation can be summarized in the following questions: 1) why are all mass eigenstates of equal spatial momentum, $\mathbf{p}$? 2) is the plane wave treatment justified when the production and detection regions are localized ? 3) why is it necessary to do the $t - t_0 \to L$ conversion ?

A number of quantum paradoxes can be formulated from these questions, that can be resolved only when the two basic conditions for neutrino oscillations above are made explicit. This can be achieved in a wave packet treatment.

6.2 Wave packet derivation

Many authors have derived the master formula treating neutrinos involved as wave packets. For some recent references see [16, 17].

A neutrino of flavour α is produced at time and position $(t_0, \mathbf{x}_0) = (0, \mathbf{0})$ as a superposition of *source* wave packets, $f_i^S(\mathbf{p})$, one for each mass eigenstate. The state at time and position $(t, \mathbf{x})$ is therefore

$$|\nu_\alpha(t)\rangle = \sum_i U^*_{\alpha i} \int_{\mathbf{p}} f_i^S(\mathbf{p}) e^{-iE_i(\mathbf{p})t} |\nu_i(\mathbf{p})\rangle. \tag{39}$$

For simplicity we will assume gaussian wave packets, with an average momentum $\mathbf{Q}_i$ and width σ_S:

$$f_i^S(\mathbf{p}) \propto e^{-(\mathbf{p}-\mathbf{Q}_i)^2/2\sigma_S^2}. \tag{40}$$

Note that we have lifted the assumption that all mass eigenstates have the same spatial momentum.

A neutrino of flavour β is detected at time and position $(T, \mathbf{L})$ as a superposition of *detector* wave packets, $f_i^D(\mathbf{p})$, created at this space-time position. The state detected is therefore

$$|\nu_\beta(t)\rangle = \sum_j U^*_{\beta j} \int_{\mathbf{p}} f_j^D(\mathbf{p}) e^{-iE_j(\mathbf{p})(t-T)} e^{-i\mathbf{pL}} |\nu_j(\mathbf{p})\rangle, \tag{41}$$

where we also assume gasussian wave packets at detection, with average momentum $\mathbf{Q}'_j$ and width σ_D:

$$f_j^D(\mathbf{p}) \propto e^{-(\mathbf{p}-\mathbf{Q}'_j)^2/2\sigma_D^2}. \tag{42}$$

The probability amplitude for the first state to turn into the second is therefore

$$\mathcal{A}(\nu_\alpha \to \nu_\beta) = \langle \nu_\beta(t) | \nu_\alpha(t) \rangle = \sum_i U^*_{\alpha i} U_{\beta i} \int_{\mathbf{p}} e^{-iE_i(\mathbf{p})T} e^{i\mathbf{pL}} f_i^S(\mathbf{p}) f_i^{D*}(\mathbf{p}) \tag{43}$$

For gaussian wave packets we can rewrite the product of the S and D wave packets as a gaussian wave packet:

$$f_i^{D*}(\mathbf{p}) f_i^S(\mathbf{p}) \propto f_i^{ov}(\mathbf{p}) e^{-(\mathbf{Q}_i - \mathbf{Q}_i')^2/4(\sigma_S^2+\sigma_D^2)}, \tag{44}$$

where the overlap wave packet

$$f_i^{ov}(\mathbf{p}) \equiv e^{-(\mathbf{p}-\bar{\mathbf{Q}}_i)^2/2\sigma_{ov}^2}, \;\; \bar{\mathbf{Q}}_i \equiv \left(\frac{\mathbf{Q}_i}{\sigma_S^2} + \frac{\mathbf{Q}_i'}{\sigma_D^2}\right)\sigma_{ov}^2, \;\; \sigma_{ov}^2 \equiv \frac{1}{1/\sigma_S^2 + 1/\sigma_D^2}. \tag{45}$$

The momentum integral in eq. (43) can be done analytically if we approximate

$$E_i(\mathbf{p}) \simeq E_i(\bar{\mathbf{Q}}_i) + \sum_k \left.\frac{\partial E_i}{\partial p_k}\right|_{\bar{\mathbf{Q}}_i} (p_k - (\bar{Q}_i)_k) + ... = E_i(\bar{\mathbf{Q}}_i) + \mathbf{v}_i(\mathbf{p} - \bar{\mathbf{Q}}_i) + ..., \tag{46}$$

where $\mathbf{v}_i$ is the overlap wave packet group velocity.

The amplitude obtained is

$$\mathcal{A}(\nu_\alpha \to \nu_\beta) \propto \sum_i U_{\alpha i}^* U_{\beta i} e^{-iE_i(\bar{\mathbf{Q}}_i)T} e^{i\bar{\mathbf{Q}}_i \mathbf{L}} e^{-(\mathbf{Q}_i - \mathbf{Q}_i')^2/4(\sigma_S^2+\sigma_D^2)} e^{-(\mathbf{L}-\mathbf{v}_i T)^2\sigma_{ov}^2/2}. \tag{47}$$

Note that the two last exponential factors impose momentum conservation (the average momentum of the source and detector wave packets should be equal up to the momentum uncertainty) and the classical relation $\mathbf{L} = \mathbf{v}_i T$ within the spatial uncertainty, σ_{ov}^{-1}.

Since we usually do not measure the detection time T in a neutrino oscillation experiment, we should integrate the probability over this variable. For simplicity we assume $\mathbf{Q}_i \simeq \mathbf{Q}_i'$ and parallel to $\mathbf{L}$. In this case, the integral gives:

$$\begin{aligned} P(\nu_\alpha \to \nu_\beta) \;&\propto\; \int_{-\infty}^{\infty} dT |\mathcal{A}(\nu_\alpha \to \nu_\beta)|^2 \\ &\propto\; \sum_{i,j} U_{\alpha i}^* U_{\beta i} U_{\alpha j} U_{\beta j}^* e^{-i\frac{\Delta m_{ji}^2 L}{2|\mathbf{p}|}} \underbrace{e^{-\left(\frac{L}{L_{coh}(i,j)}\right)^2}}_{\text{coherence}} \underbrace{e^{-\left(\frac{E_i(\bar{\mathbf{Q}}_i) - E_j(\bar{\mathbf{Q}}_j)}{2\sigma_{ov}}\right)^2}}_{\text{momentum uncertainty}} \end{aligned} \tag{48}$$

where the coherence length

$$L_{\rm coh}(i,j) \simeq \sigma_{ov} \frac{|\mathbf{v}_i - \mathbf{v}_j|}{\sqrt{|\mathbf{v}_i^2 + \mathbf{v}_j^2}}, \tag{49}$$

represents the distance travelled by the two wave packets, moving at slightly different group velocities v_i and v_j, such that the center of the two wave packets have separated spacially a distance of the order of the spatial uncertainty σ_{ov}^{-1}. For $L \geq L_{coh}(i,j)$ the coherence between the wave packets i, j is lost and the corresponding terms in the oscillation probability exponentially suppressed. The last exponential factor in eq. (48) leads to a suppression of the oscillation probability when the difference in average energies of the two wave packets i, j is larger than the momentum uncertainty of the overlap wave packet, σ_{ov}. Note that σ_{ov} is dominated by the smallest of the production and detection uncertainties, and therefore both should be large enough to ensure that the wave packets of the different mass eigenstates remain coherent. To the extent that $L \ll L_{\rm coh}$ and $|E_i - E_j| \ll {\rm Min}(\sigma_S, \sigma_D)$, the probability reduces to the master formula, with one caveat: we have lost the normalization along the way. This is usually unavoidable in the wave packet derivation. The right normalization can be imposed only a posteriori, for example, from unitarity, $\sum_\beta P(\nu_\alpha \to \nu_\beta) = 1$.

In summary, the wave packet derivation is clearly more physical, as it makes explicit the two necessary conditions for neutrino oscillations to take place: coherence and sufficient momentum uncertainty.

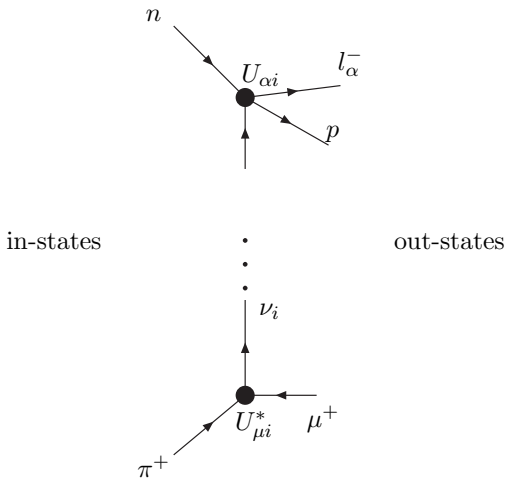

Fig. 17: Neutrino oscillations in QFT.

6.3 QFT derivation

Since we are dealing with relativistic quantum mechanics, QFT should be the appropriate framework to derive the oscillation probability.

In QFT we consider scattering processes where some asymptotic *in-states* that we can prepare in the infinite past come close together at some finite time in an interaction region and scatter off into other asymptotic *out-states* at time $t \to \infty$. The probability amplitude for this process is just the scalar product of the in and out states. In computing this amplitude we usually idealise the asymptotic states as plane waves, which is a good approximation provided the interaction region is small compared to the Compton wavelength of the scattering states. In reality however the proper normalization of the scattering probability as a probability per unit time and volume requires that the initial states are normalized wave packets.

In a neutrino oscillation experiment, the asymptotic states are not the neutrinos, we cannot really prepare the neutrino states, but the particles that produce the neutrino at the source and those that interact with the neutrino in the detector. The neutrino is just a virtual particle being exchanged between the source and detector, see Fig. 17, and in this perspective the interaction region is as large as the baseline and therefore macroscopic, in particular much larger than the Compton wavelength of the asymptotic states involved. It is mandatory therefore to consider the in-states as wave packets to ensure the localization of the source and detector.

Consider for example a neutrino beam produced from pions at rest and a detector some distance apart, where neutrinos interact with nucleons that are also at rest, via a quasi-elastic event:

$$\pi n \to p \mu l_\beta. \tag{50}$$

The in-states therefore will be the two wave packets representing a static pion that decays and is localized at time and position $(0, \mathbf{0})$ within the uncertainty better defined than the decay tunnel, and a nucleon that is static and localized within the detector, at time and position $(T, \mathbf{L})$, when the interaction takes place. The out-states are the muon produced in pion decay and the lepton and hadron produced in the quasi-elastic event. The probability amplitude for the whole process includes the pion decay amplitude, the neutrino propagation and the scattering amplitude at the detector. Therefore in order to extract from the full amplitude an oscillation probability, it must be the case that there is factorization of the whole probability into three factors that can be identified with the flux of neutrino from pion decay, an oscillation probability and a neutrino cross section.

By explicit calculation [18], it is possible to show that such factorization does indeed take place as long as kinematical effects of neutrino masses can be neglected. The oscillation probability defined as the ratio of the probability for the whole process and the product of the neutrino flux from pion decay and the neutrino scattering cross-section is properly normalized.

6.4 Neutrino oscillations in vacuum

Let us analyse more closely the master formula eq. (33). The probability is a superposition of oscillatory functions of the baseline with wavelengths that depend on the neutrino mass differences $\Delta m^2_{ij} = m^2_j - m^2_i$, and amplitudes that depend on different combinations of the mixing matrix elements. Defining $W^{ij}_{\alpha\beta} \equiv [U_{\alpha i} U^*_{\beta i} U^*_{\alpha j} U_{\beta j}]$ and using the unitarity of the mixing matrix, we can rewrite the probability in the more familiar form:

$$\begin{aligned} P(\nu_\alpha \;\to\; \nu_\beta) &= \delta_{\alpha\beta} - 4 \sum_{j>i} \mathrm{Re}[\mathrm{W}^{\mathrm{ij}}_{\alpha\beta}] \, \sin^2\left(\frac{\Delta \mathrm{m}^2_{\mathrm{ij}} \, \mathrm{L}}{4\mathrm{E}_\nu}\right) \\ &\mp \; 2 \sum_{j>i} \mathrm{Im}[\mathrm{W}^{\mathrm{ij}}_{\alpha\beta}] \, \sin\left(\frac{\Delta \mathrm{m}^2_{\mathrm{ij}} \, \mathrm{L}}{2\mathrm{E}_\nu}\right), \end{aligned} \tag{51}$$

where the $\mp$ refers to neutrinos/antineutrinos and $|\mathbf{q}| \simeq E_\nu$.

We refer to an *appearance* or *disappearance* oscillation probability when the initial and final flavours are different ($\alpha \neq \beta$) or the same ($\alpha = \beta$), respectively. Note that oscillation probabilities show the expected GIM suppression of any flavour changing process: they vanish if the neutrinos are degenerate.

In the simplest case of two-family mixing, the mixing matrix depends on just one mixing angle:

$$U_{\text{PMNS}} = \begin{pmatrix} \cos\theta & \sin\theta \\ -\sin\theta & \cos\theta \end{pmatrix} , \tag{52}$$

and there is only one mass square difference Δm^2. The oscillation probability of Eq. (51) simplifies to the well-known expression where we have introduced convenient physical units:

$$\begin{aligned} P(\nu_\alpha \to \nu_\beta) &= \sin^2 2\theta \, \sin^2\left(1.27 \frac{\Delta m^2(\mathrm{eV}^2) \, L(\mathrm{km})}{E_\nu(\mathrm{GeV})}\right), \quad \alpha \neq \beta \, . \\ P(\nu_\alpha \to \nu_\alpha) &= 1 - P(\nu_\alpha \to \nu_\beta). \end{aligned} \tag{53}$$

The probability is the same for neutrinos and antineutrinos, because there cannot be CP violation when there are only two families. Indeed CPT implies that the disappearance probabilities are the same for neutrinos an antineutrinos, and therefore according to eq. (53) the same must hold for the appearance probability. The latter is a sinusoidal function of the distance between source and detector, with a period determined by the oscillation length:

$$L_{\text{osc}} \, (\mathrm{km}) = \pi \frac{E_\nu(\mathrm{GeV})}{1.27 \Delta m^2(\mathrm{eV}^2)} \, , \tag{54}$$

which is proportional to the neutrino energy and inversely proportional to the neutrino mass square difference. The amplitude of the oscillation is determined by the mixing angle. It is maximal for $\sin^2 2\theta = 1$ or $\theta = \pi/4$. The oscillation probability as a function of the baseline is shown on the left plot of Fig. 18.

In many neutrino oscillation experiments the baseline is not varied but the oscillation probability can be measured as a function of the neutrino energy. This is shown on the right plot of Fig. 18. In this case, the position of the first maximum contains information on the mass splitting:

$$E_{\max}(\mathrm{GeV}) = 1.27 \frac{\Delta m^2(\mathrm{eV}^2) L(\mathrm{km})}{\pi/2}. \tag{55}$$

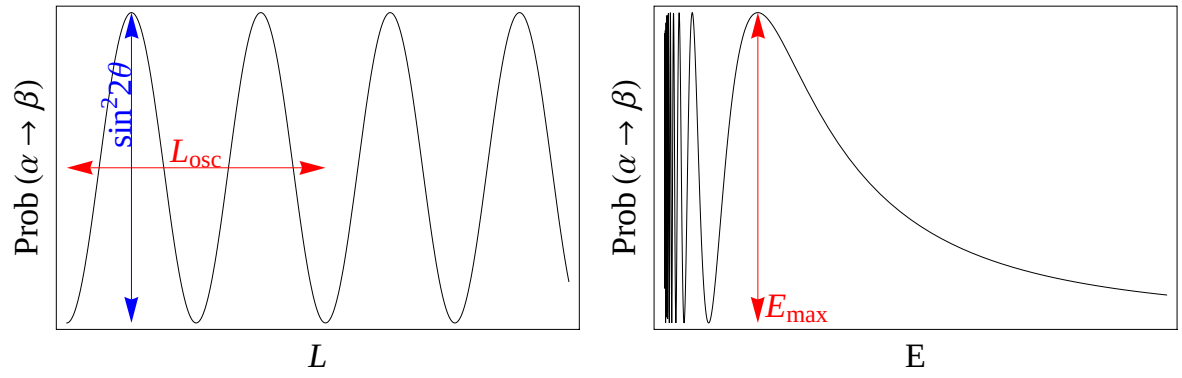

Fig. 18: Left: two-family appearance oscillation probability as a function of the baseline of L at fixed neutrino energy. Right: same probability shown as a function of the neutrino energy for fixed baseline.

An optimal neutrino oscillation experiment in vacuum is such that the ratio of the neutrino energy and baseline are tunned to be of the same order as the mass splitting, $E/L \sim \Delta m^2$. If $E/L \gg \Delta m^2$, the oscillation phase is small and the oscillation probability depends on the combination $P(\nu_\alpha \to \nu_\beta) \propto \sin^2 2\theta(\Delta m^2)^2$, and the mixing angle and mass splitting cannot be disentagled. The opposite limit $E/L \ll \Delta m^2$ is the fast oscillation regime, where one can only measure an energy or baseline-smeared oscillation probability

$$\langle P(\nu_\alpha \to \nu_\beta)\rangle \simeq \frac{1}{2}\sin^2 2\theta. \tag{56}$$

It is interesting, and reassuring, to note that this averaged oscillation regime gives the same result as the flavour transition probability in the case of incoherent propagation ($L \gg L_{\rm coh}$):

$$P\left(\nu_\alpha \to \nu_\beta\right) = \sum_i |U_{\alpha i}U_{\beta i}|^2 = 2\cos^2\theta\sin^2\theta = \frac{1}{2}\sin^2 2\theta. \tag{57}$$

Flavour transitions via incoherent propagation are sensitive to mixing but not to the neutrino mass splitting. The 'smoking gun' for neutrino oscillations is not the flavour transition, which can occur in the presence of neutrino mixing without oscillations, but the peculiar L/E_ν dependence. An optimal experiment that intends to measure both the mixing and the mass splitting requires running $E/L \sim \Delta m^2$.

6.5 Neutrino propagation in matter

When neutrinos propagate in matter (Earth, sun, etc.), their propagation is modified owing to coherent forward scattering on electrons and nucleons [19]:

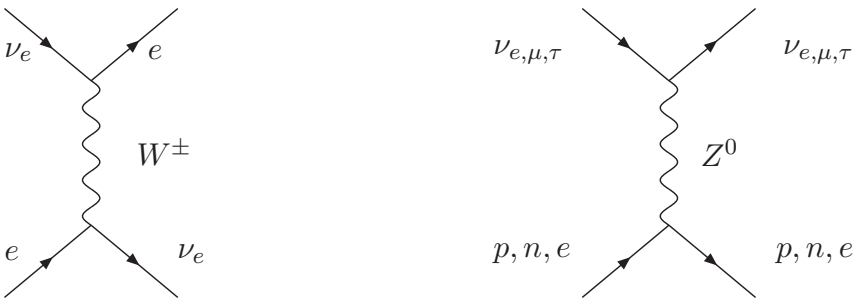

The effective Hamiltonian density resulting from the charged current interaction is

$$\mathcal{H}_{\rm CC} = 2\sqrt{2}G_F\,[\bar{e}\gamma_\mu P_L\nu_e][\bar{\nu}_e\gamma^\mu P_L e] = 2\sqrt{2}G_F\,[\bar{e}\gamma_\mu P_L e][\bar{\nu}_e\gamma^\mu P_L\nu_e]. \tag{58}$$

Since the medium is not polarized, the expectation value of the electron current is simply the number density of electrons:

$$\langle\bar{e}\gamma_\mu P_L e\rangle_{\rm unpol.medium} \;=\; \delta_{\mu 0}\frac{N_e}{2}. \tag{59}$$

Including also the neutral current interactions in the same way, the effective Hamiltonian for neutrinos in the presence of matter is

$$\langle\mathcal{H}_{CC}+\mathcal{H}_{NC}\rangle_{\rm medium} = \bar{\nu}V_m\gamma^0(1-\gamma_5)\nu \tag{60}$$

$$V_m = \begin{pmatrix} \frac{G_F}{\sqrt{2}}\left(N_e-\frac{N_n}{2}\right) & 0 & 0 \\ 0 & \frac{G_F}{\sqrt{2}}\left(-\frac{N_n}{2}\right) & 0 \\ 0 & 0 & \frac{G_F}{\sqrt{2}}\left(-\frac{N_n}{2}\right) \end{pmatrix}, \tag{61}$$

where N_n is the number density of neutrons. Due to the neutrality of matter, the proton and electron contributions to the neutral current potential cancel.

The plane wave solutions to the modified Dirac equation satisfy a different dispersion relation and as a result, the phases of neutrino oscillation phenomena change. The new dispersion relation becomes

$$E - V_m - M_\nu = (\pm|\mathbf{p}| - V_m)\,\frac{1}{E+M_\nu-V_m}\,(\pm|\mathbf{p}|-V_m) \quad h=\pm, \tag{62}$$

where $h=\pm$ indicate the two helicity states and we have neglected effects of $\mathcal{O}(VM_\nu)$. This is a reasonable approximation since $m_\nu \gg V_m$. For the positive energy states we then have

$$E>0 \quad E^2 = |\mathbf{p}|^2 + M_\nu^2 + 4EV_m \quad h=- \quad E^2 = |\mathbf{p}|^2 + M_\nu^2,\; h=+, \tag{63}$$

while for the negative energy ones $V_m \to -V_m$ and $h \to -h$.

The effect of matter can be simply accommodated in an effective mass matrix:

$$\tilde{M}_\nu^2 = M_\nu^2 \pm 4EV_m. \tag{64}$$

The effective mixing matrix $\tilde{V}_{\rm MNS}$ is the one that takes us from the original flavour basis to that which diagonalizes this effective mass matrix:

$$\begin{pmatrix} \tilde{m}_1^2 & 0 & 0 \\ 0 & \tilde{m}_2^2 & 0 \\ 0 & 0 & \tilde{m}_3^2 \end{pmatrix} = \tilde{V}_{\rm MNS}^\dagger \left(M_\nu^2 \pm 4E \begin{pmatrix} V_e & 0 & 0 \\ 0 & V_\mu & 0 \\ 0 & 0 & V_\tau \end{pmatrix} \right) \tilde{V}_{\rm MNS}. \tag{65}$$

The effective mixing angles and masses depend on the energy.

The matter potential in the center of the sun is $V_m \sim 10^{-12}$ eV and in the Earth $V_m \sim 10^{-13}$ eV. In spite of these tiny values, these effects are non-negligible in neutrino oscillations.

6.6 Neutrino oscillations in constant matter

In the case of two flavours, the effective mass and mixing angle have relatively simple expressions:

$$\Delta\tilde{m}^2 \;=\; \sqrt{\left(\Delta m^2\cos 2\theta \mp 2\sqrt{2}E\,G_F\,N_e\right)^2 + (\Delta m^2 \sin 2\theta)^2}, \tag{66}$$

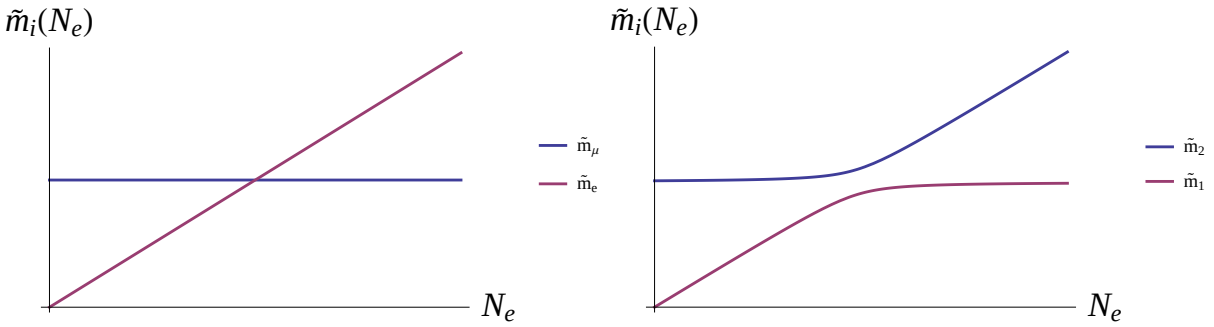

Fig. 19: Mass eigenstates as a function of the electron number density at fixed neutrino energy for $\theta = 0$ (left) and $\theta \neq 0$ (right).

$$\sin^2 2\tilde{\theta} \;=\; \frac{\left(\Delta m^2 \sin 2\theta\right)^2}{(\Delta \tilde{m}^2)^2} \tag{67}$$

where the sign $\mp$ corresponds to neutrinos/antineutrinos. The corresponding oscillation amplitude has a resonance [20], when the neutrino energy satisfies

$$\sqrt{2}\, G_F\, N_e \mp \frac{\Delta m^2}{2E} \cos 2\theta = 0 \quad \Rightarrow \quad \sin^2 2\tilde{\theta} = 1, \quad \Delta \tilde{m}^2 = \Delta m^2 \sin 2\theta. \tag{68}$$

The oscillation amplitude is therefore maximal, independently of the value of the vacuum mixing angle.

We also note that

- oscillations vanish at $\theta = 0$, because the oscillation length becomes infinite for $\theta = 0$;
- the resonance is only there for ν or $\bar{\nu}$ but not both;
- the resonance condition depends on the sign$(\Delta m^2 \cos 2\theta)$:
  resonance observed in $\nu \rightarrow$ sign$(\Delta m^2 \cos 2\theta) > 0$,
  resonance observed in $\bar{\nu} \rightarrow$ sign$(\Delta m^2 \cos 2\theta) < 0$.

The origin of this resonance is a would-be level crossing in the case of vanishing mixing. In the case of two families, for $\theta = 0$, the mass eigenstates as a function of the electron number density, at fixed neutrino energy, are depicted in Fig. 19 for $\Delta m^2 > 0$. As soon as the mixing is lifted from zero, no matter how small, the crossing cannot take place. The resonance condition corresponds to the minimum level-splitting point.

6.7 Neutrino oscillations in variable matter

In the sun the density of electrons is not constant. However, if the variation is sufficiently slow, the eigenstates will change slowly with the density, and we can assume that the neutrino produced in an eigenstate in the center of the sun, remains in the same eigenstate along the trajectory. This is the so-called *adiabatic approximation*.

We consider here two-family mixing for simplicity. At any point in the trajectory, it is possible to diagonalize the Hamiltonian fixing the matter density to that at the given point. The resulting eigenstates can be written as

$$|\tilde{\nu}_1\rangle = |\nu_e\rangle \cos\tilde{\theta} - |\nu_\mu\rangle \sin\tilde{\theta}, \tag{69}$$

$$|\tilde{\nu}_2\rangle = |\nu_e\rangle \sin\tilde{\theta} + |\nu_\mu\rangle \cos\tilde{\theta}. \tag{70}$$

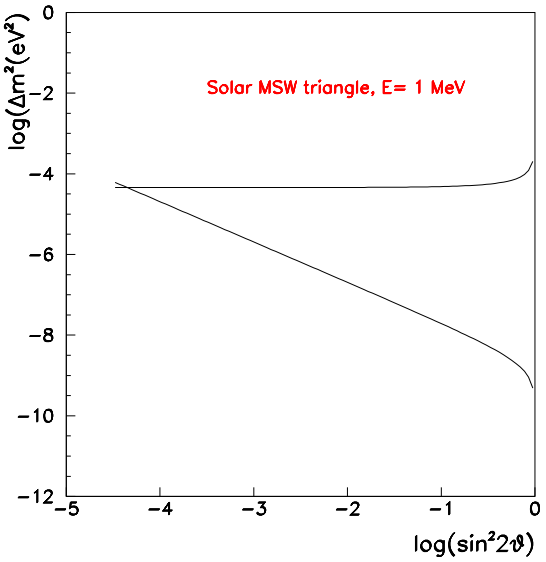

Fig. 20: MSW triangle: in the region between the two lines the resonance and adiabaticity conditions are both satisfied for neutrinos of energy 1 MeV.

Neutrinos are produced close to the centre $x = 0$ where the electron density is $N_e(0)$. Let us suppose that it satisfies

$$2\sqrt{2}G_F N_e(0) \gg \Delta m^2 \cos 2\theta. \tag{71}$$

Then the diagonalization of the mass matrix at this point gives

$$\tilde{\theta} \simeq \frac{\pi}{2} \Rightarrow |\nu_e\rangle \simeq |\tilde{\nu}_2\rangle, \tag{72}$$

in such a way that an electron neutrino is mostly the second mass eigenstate. When neutrinos exit the sun, at $x = R_\odot$, the matter density falls to zero, $N_e(R_\odot) = 0$, and the local effective mixing angle is the one in vacuum, $\tilde{\theta} = \theta$. If θ is small, the eigenstate $\tilde{\nu}_2$ is mostly ν_μ according to Eq. (70).

Therefore an electron neutrino produced at $x = 0$ is mostly the eigenstate $\tilde{\nu}_2$, but this eigenstate outside the sun is mostly ν_μ. There is maximal $\nu_e \to \nu_\mu$ conversion if the adiabatic approximation is a good one. This is the famous MSW effect [19, 20]. The conditions for this to happen are:

– *Resonant condition*: the density at the production is above the critical one

$$N_e(0) > \frac{\Delta m^2 \cos 2\theta}{2\sqrt{2}EG_F}. \tag{73}$$

– *Adiabaticity*: the splitting of the levels is large compared to energy injected in the system by the variation of $N_e(r)$. A measurement of this is given by γ which should be much larger than one:

$$\gamma = \frac{\sin^2 2\theta}{\cos 2\theta} \frac{\Delta m^2}{2E} \frac{1}{|\nabla \log N_e(r)|} > \gamma_{\min} > 1, \tag{74}$$

where $\nabla = \partial/\partial r$.

At fixed energy both conditions give the famous MSW triangles, if plotted on the plane $(\log(\sin^2 2\theta), \log(\Delta m$

$$\log\left(\Delta m^2\right) < \log\left(\frac{2\sqrt{2}G_F N_e(0)E}{\cos 2\theta}\right) \tag{75}$$

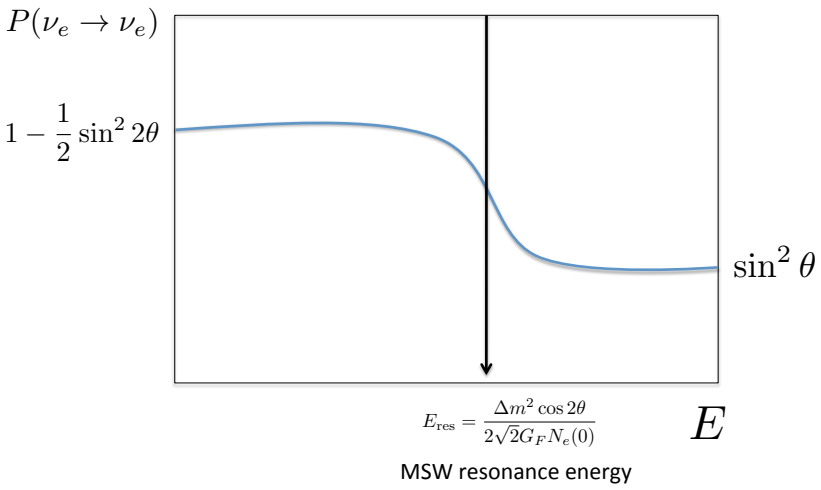

Fig. 21: Schematic survival probability of solar neutrinos as a function of the energy.

$$\log(\Delta m^2) > \log\left(\gamma_{\rm min} 2E\nabla \log N_e \frac{\cos 2\theta}{\sin^2 2\theta}\right). \tag{76}$$

For example, taking $N_e(r) = N_c \exp(-r/R_0)$, $R_0 = R_\odot/10.54$, $N_c = 1.6 \times 10^{26}$ cm^{-3}, $E = 1$ MeV, these curves are shown in Fig. 20.

It should be stressed that neutrino oscillations are not responsible for the flavour transition of solar neutrinos. The survival probability of the solar ν_e in the adiabatic approximation is the incoherent sum of the contribution of each of the mass eigenstates:

$$P(\nu_e \to \nu_e) = \sum_i |\langle \nu_e | \tilde{\nu}_i(R_\odot)\rangle|^2 |\langle \tilde{\nu}_i(0)|\nu_e\rangle|^2, \tag{77}$$

where $\tilde{\nu}_i(r)$ is the i-th mass eigenstate for the electron number density, $N_e(r)$, at a distance r from the center of the sun. If the mass eigenstates contribute incoherently, how can we measure the neutrino mass splitting ? The answer is that the resonance condition of eq. (73) depends on the neutrino energy. If we define

$$E_{\rm res} \equiv \frac{\Delta m^2 \cos 2\theta}{2\sqrt{2} G_F N_e(0)}, \tag{78}$$

the MSW effect will affect neutrinos with $E > E_{\rm res}$, while for $E < E_{\rm res}$, the oscillation probability is close to that in vacuum for averaged oscillations. The spectrum of the solar neutrino flux includes energies both above and below $E_{\rm res}$:

$$\begin{aligned} P(\nu_e \to \nu_e) &\simeq 1 - \tfrac{1}{2}\sin^2 2\theta, \quad E \ll E_{\rm res} \\ P(\nu_e \to \nu_e) &\simeq \sin^2\theta, \qquad E \gg E_{\rm res} \end{aligned} \tag{79}$$

The sensitivity to Δm^2 relies on the ability to locate the resonant energy. This behaviour is esquematically depicted in Fig. 21.

7 Evidence for neutrino oscillations

Nature has been kind enough to provide us with two natural sources of neutrinos (the sun and the atmosphere) where neutrino flavour transitions have been observed in a series of ingenious experiments, that started back in the 1960s with the pioneering experiment of R. Davies. This effort was rewarded with the Nobel prize of 2002 to R. Davies and M. Koshiba *for the detection of cosmic neutrinos*.

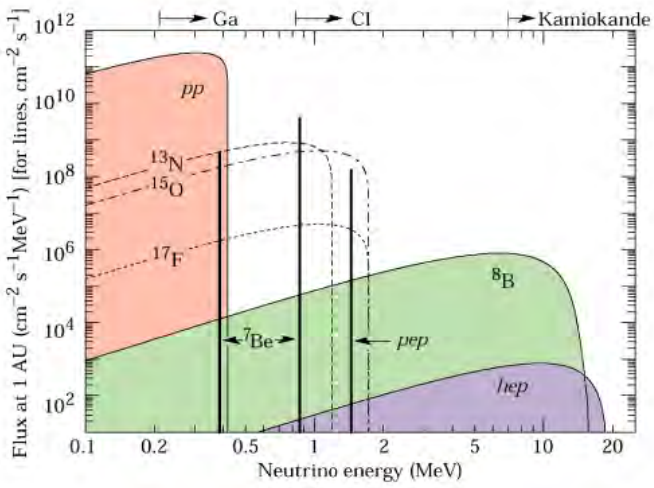

Fig. 22: Spectrum of solar neutrinos [22]. The arrows indicate the threshold of the different detection techniques.

7.1 Solar neutrinos

The sun, like all stars, is an intense source of neutrinos produced in the chain of nuclear reactions that burn hydrogen into helium:

$$4p \longrightarrow {}^4\mathrm{He} + 2e^+ + 2\nu_e. \tag{80}$$

The theory of stelar nucleosynthesis was stablished at the end of the 30's by H. Bethe [21]. The spectrum of the solar ν_e, for massless neutrinos, is shown in Fig. 22. The prediction of this flux, obtained by J. Bahcall and collaborators [22], is the result of a detailed simulation of the solar interior and has been improved over many years. It is the so-called standard solar model (SSM).

Neutrinos coming from the sun have been detected with several experimental techniques that have a different neutrino energy threshold as indicated in Fig. 22. On the one hand, the radiochemical techniques, used in the experiments Homestake (chlorine, ^{37}Cl) [23], Gallex/GNO [24] and Sage [25] (using gallium, ^{71}Ga, and germanium, ^{71}Ge, respectively), can count the total number of neutrinos with a rather low threshold ($E_\nu > 0.81$ MeV in Homestake and $E_\nu > 0.23$ MeV in Gallex and Sage), but they cannot get any information on the directionality, the energy of the neutrinos, nor the time of the event.

On the other hand, Kamiokande [26] pioneered a new technique to observe solar neutrinos using water Cherenkov detectors that can measure the recoil electron in elastic neutrino scattering on electrons: $\nu_e + e^- \to \nu_e + e^-$. This is a real-time experiment that provides information on the directionality and the energy of the neutrinos. The threshold on the other hand is much higher, ~ 5 MeV. All these experiments have consistently observed a number of solar neutrinos between 1/3 and 1/2 of the number expected in the SSM and for a long time this was referred to as the *solar neutrino problem or deficit*.

The progress in this field over the last decade has been enormous culminating in a solution to this puzzle that no longer relies on the predictions of the SSM. There have been three milestones.

1998: The experiment SuperKamiokande [27] measured the solar neutrino deficit with unprecedented precision, using the elastic reaction (ES):

$$\text{(ES)} \qquad \nu_e + e^- \to \nu_e + e^- \qquad E_{\text{thres}} > 5\ \text{MeV}. \tag{81}$$

The measurement of the direction of the events demonstrated that the neutrinos measured definitely come from the sun: the left plot of Fig. 23 shows the distribution of the events as a function of the zenith angle of the sun. A seasonal variation of the flux is expected since the distance between the Earth and the sun

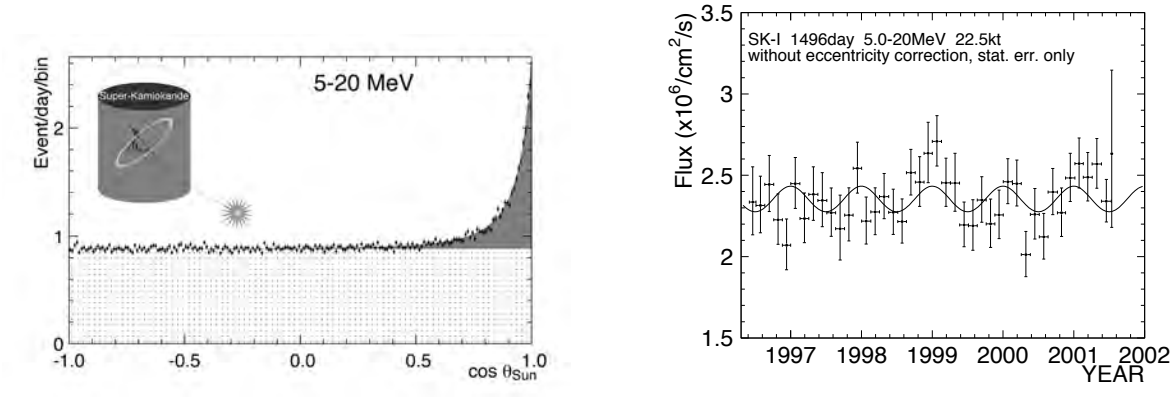

Fig. 23: Left: distribution of solar neutrino events as a function of the zenith angle of the sun. Right: seasonal variation of the solar neutrino flux in SuperKamiokande (from Ref. ([28])).

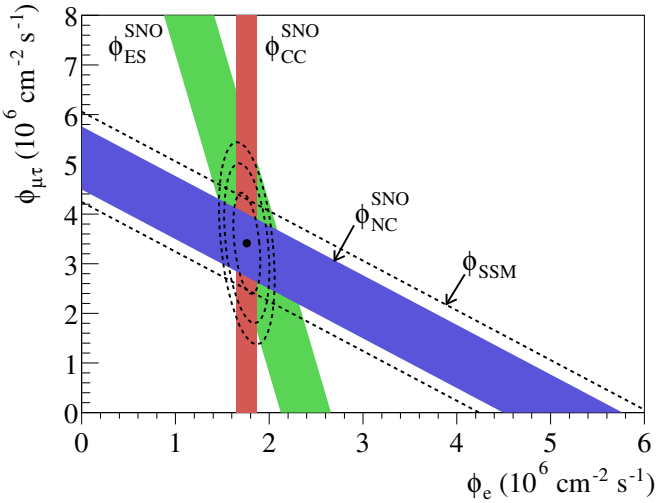

Fig. 24: Flux of ν_μ and ν_τ versus the flux of ν_e in the solar neutrino flux as measured from the three reactions observable in the SNO experiment. The dashed band shows the prediction of the SSM, which agrees perfectly with the flux measured with the NC reaction (from Ref. [30]).

varies seasonally. The right plot of Fig. 23 shows that the measured variation is in perfect agreement with that expectation.

2001: The SNO experiment [29, 30] measured the flux of solar neutrinos using also the two reactions:

$$\text{(CC)} \qquad \nu_e + d \to p + p + e^- \qquad E_{\text{thres}} > 5 \text{ MeV} \tag{82}$$

$$\text{(NC)} \qquad \nu_x + d \to p + n + \nu_x \quad x = e, \mu, \tau \qquad E_{\text{thres}} > 2.2 \text{ MeV} \tag{83}$$

Since the CC reaction is only sensitive to electron neutrinos, while the NC one is sensitive to all the types that couple to the Z^0 boson, the comparison of the fluxes measured with both reactions can establish if there are ν_μ and ν_τ in the solar flux independently of the normalization given by the SSM. The result is shown on the Nobel-prize-winning plot Fig. 24. These measurements demonstrate that the sun shines (ν_μ, ν_τ) about twice more than it shines ν_e, which constitutes the first direct demonstration of flavour transitions in the solar flux! Furthermore the NC flux that measures all active species in the solar flux, is compatible with the total ν_e flux expected according to the SSM.

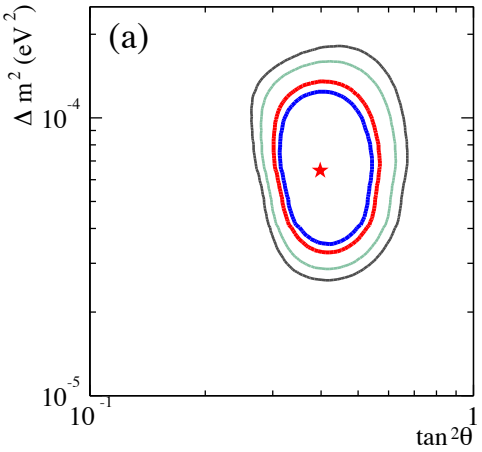

Fig. 25: Analysis of all solar data at SNO in terms of neutrino oscillations (from Ref. [29]).

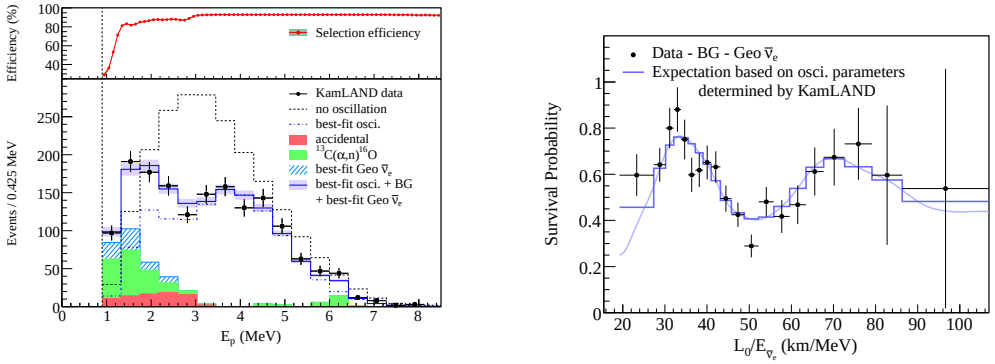

Fig. 26: Spectral distribution of the $\bar{\nu}_e$ events in KamLAND (left) and E_ν/L dependence (right). The data are compared to the expectation in the absence of oscillations and to the best fit oscillation hypothesis (from Ref. [32]).

All solar neutrino data can be interpreted in terms of neutrino masses and mixings. The analysis in terms of two neutrino families is shown in the left plot of Fig. 25. The solar ν_e deficit can be explained for a $\Delta m^2_{\rm solar} \simeq 7$–$8 \times 10^{-5}$eV and a relatively large mixing angle. The fortunate circumstance that

$$\Delta m^2_{\rm solar} \sim \langle E_\nu(1\ {\rm MeV})\rangle / L(100\ {\rm km}) \tag{84}$$

implies that one could look for this oscillation measuring reactor neutrinos at baselines of $\sim$ 100 km. This was the third milestone.

2002: The solar oscillation is confirmed with reactor neutrinos in the KamLAND experiment [31]. This is 1kton of liquid scintillator which measures the flux of reactor neutrinos produced in a cluster of nuclear plants around the Kamioka mine in Japan. The average distance is $\langle L\rangle = 175$ km. Neutrinos are detected via inverse β-decay which has a threshold energy of about 2.6 MeV:

$$\bar{\nu}_e + p \to e^+ + n \qquad E_{\rm th} > 2.6\ {\rm MeV}\ . \tag{85}$$

Figure 26 shows the KamLAND results [32] on the antineutrino spectrum, as well as the survival probability as a function of the ratio E_ν/L. The low-energy contribution of geoneutrinos is clearly visible. This measuremet could have important implications in geophysics.

Concerning the sensitivity to the oscillation parameters, Fig. 27 shows the present determination of the solar oscillation parameters from KamLAND and other solar experiments. The precision in the

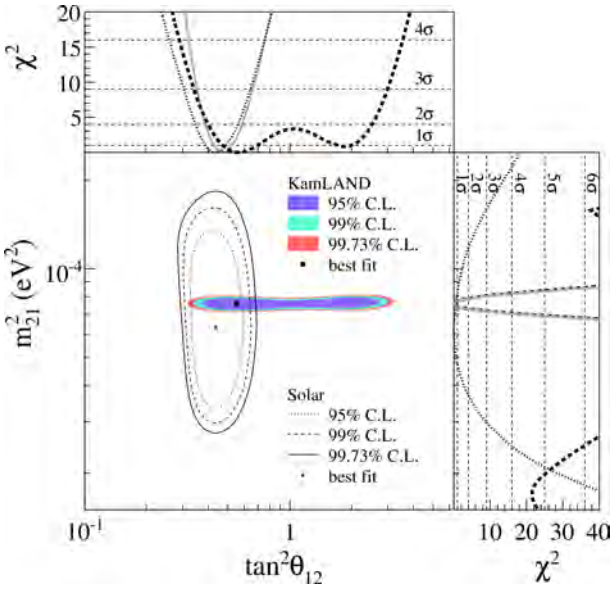

Fig. 27: Analysis of all solar and KamLAND data in terms of oscillations (from Ref. [32]).

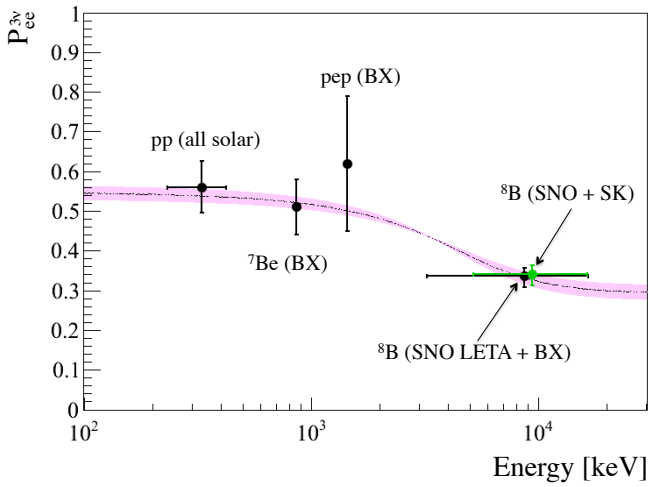

Fig. 28: Comparison of solar neutrino fluxes measured by the different solar neutrino experiments (from Ref. [33]).

determination of $\Delta m^2_{\text{solar}}$ is spectacular and shows that solar neutrino experiments are entering the era of precision physics.

The last addition to this success story is the Borexino [33] experiment. This is the lowest-threshold real-time solar neutrino experiment and the only one capable of measuring the flux of the monocromatic ^{7}Be neutrinos and pep neutrinos. Their recent results are shown in Fig. 28. The result is in agreement with the oscillation interpretation of other solar and reactor experiments and it adds further information to disfavour alternative exotic interpretations of the data. In summary, solar neutrinos experiments have made fundamental discoveries in particle physics and are now becoming useful for other applications, such as a precise understanding of the sun and the Earth.

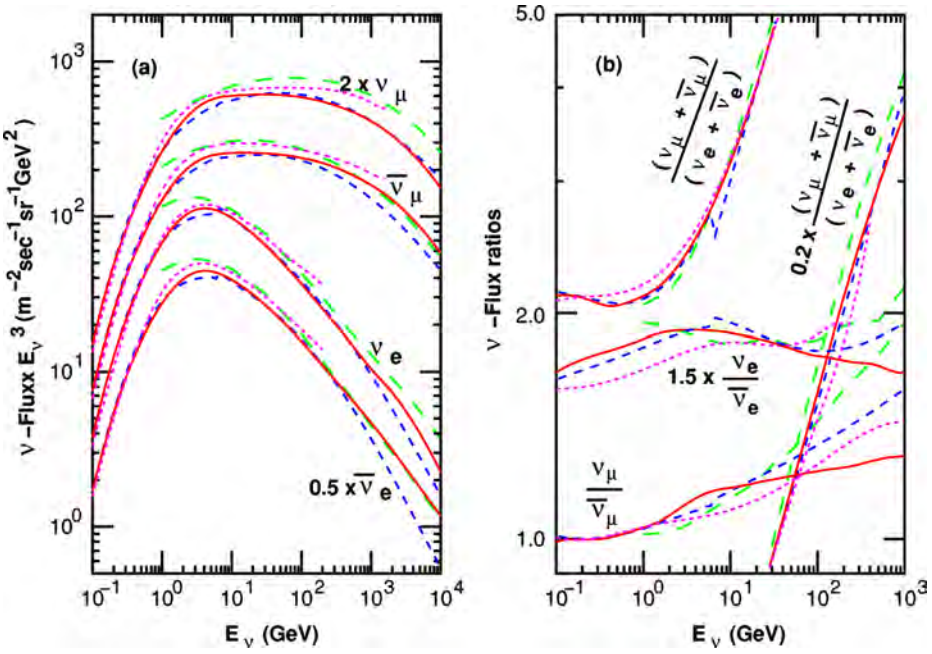

Fig. 29: Comparison of the predictions of different Monte Carlo simulations of the atmospheric neutrino fluxes averaged over all directions (left) and of the flux ratios $(\nu_\mu + \bar{\nu}_\mu)/(\nu_e + \bar{\nu}_e)$, $\nu_\mu/\bar{\nu}_\mu$, and $\nu_e/\bar{\nu}_e$ (right). The solid line corresponds to a recent full 3D simulation. Taken from the last reference in Ref. [34].

7.2 Atmospheric neutrinos

Neutrinos are also produced in the atmosphere when primary cosmic rays impinge on it producing K, π that subsequently decay. The fluxes of such neutrinos can be predicted within a 10–20% accuracy to be those in the left plot of Fig. 29.

Clearly, atmospheric neutrinos are an ideal place to look for neutrino oscillation since the E_ν/L span several orders of magnitude, with neutrino energies ranging from a few hundred MeV to 10^3 GeV and distances between production and detection varying from 10–10^4 km, as shown in Fig. 30 (right).

Many of the uncertainties in the predicted fluxes cancel when the ratio of muon to electron events is considered. The first indication of a problem was found when a deficit was observed precisely in this ratio by several experiments: Kamiokande, IMB, Soudan2 and Macro.

In 1998, SuperKamiokande clarified the origin of this anomaly [35]. This experiment can distinguish muon and electron events, measure the direction of the outgoing lepton (the zenith angle with respect to the Earth's axis) which is correlated to that of the neutrino (the higher the energy the higher the correlation), in such a way that they could measure the variation of the flux as a function of the distance travelled by the neutrinos. Furthermore, they considered different samples of events: sub-GeV (lepton with energy below 1 GeV)), multi-GeV (lepton with energy above 1 GeV), together with stopping and through-going muons that are produced on the rock surrounding Superkamiokande. The different samples correspond to different parent neutrino energies as can be seen in Fig. 30 (left). The number of events for the different samples as a function of the zenith angle of the lepton are shown in the Nobel-prize-winning plot Fig. 31.

While the electron events observed are in rough agreement with predictions, a large deficit of muon events was found with a strong dependence on the zenith angle: the deficit was almost 50% for those events corresponding to neutrinos coming from below $\cos\theta = -1$, while there is no deficit for those coming from above. The perfect fit to the oscillation hypothesis is rather non-trivial given the sensitivity

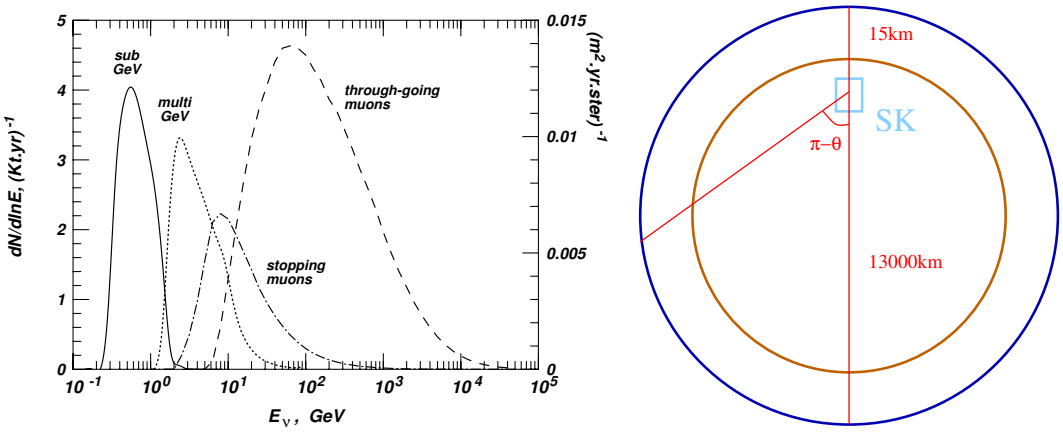

Fig. 30: Left: Parent neutrino energies of the different samples considered in Superkamiokande: sub-GeV, multi-GeV, stopping and through-going muons. Right: Distances travelled by atmospheric neutrinos as a function of the zenith angle.

of this measurement to the E_ν (different samples) and L (zenith angle) dependence. The significance of the E_ν/L dependence has also been measured by the SuperKamiokande Collaboration [37], as shown in Fig. 32. The best fit value of the oscillation parameters indicate $\Delta m^2 \simeq 3 \times 10^{-3}$ eV^2 and maximal mixing.

Appropriate neutrino beams to search for the atmospheric oscillation can easily be produced at accelerators if the detector is located at a long baseline of a few hundred kilometres, and also with reactor neutrinos in a baseline of $\mathcal{O}(1)$km, since

$$|\Delta m^2_{\text{atmos}}| \sim \frac{E_\nu(1-10\text{ GeV})}{L(10^2-10^3\text{ km})} \sim \frac{E_\nu(1-10\text{ MeV})}{L(0.1-1\text{ km})}. \tag{86}$$

A *conventional* accelerator neutrino beam, as the one used in the FSS experiment, is produced from protons hitting a target and producing π and K:

$$p \rightarrow \text{Target} \rightarrow \pi^+, K^+ \rightarrow \nu_\mu(\%\nu_e, \bar{\nu}_\mu, \bar{\nu}_e) \tag{87}$$

$$\nu_\mu \rightarrow \nu_x. \tag{88}$$

Those of a selected charge are focused and are left to decay in a long decay tunnel producing a neutrino beam of mostly muon neutrinos (or antineutrinos) with a contamination of electron neutrinos of a few per cent. The atmospheric oscillation can be established by studying, as a function of the energy, either the disappearance of muon neutrinos, the appearance of electron neutrinos or, if the energy of the beam is large enough, the appearance of τ neutrinos.

Three conventional beams confirmed the atmospheric oscillation from the measurement of the disappearance of ν_μ neutrinos: K2K (L = 235 km), MINOS (L = 730 km) and from the appearance of ν_τ OPERA (L = 730 km). Fig. 33 shows the measurement of the ν_μ survival probability as a function of the reconstructed neutrino energy in the MINOS experiment.

Three reactor neutrino experiments, Daya Bay [39], RENO [40] and Double Chooz [41], have discovered that the electron neutrino flavour also oscillates with the atmospheric wavelength: electron antineutrinos from reactors disappear at distances of $\mathcal{O}(1\text{ km})$, but with a small amplitude.

Finally the T2K experiment has measured for the first time the appearance of ν_e in an accelerator ν_μ beam [42] in the atmospheric range.

The agreement of all these measurements with the original atmospheric oscillation signal was excellent.

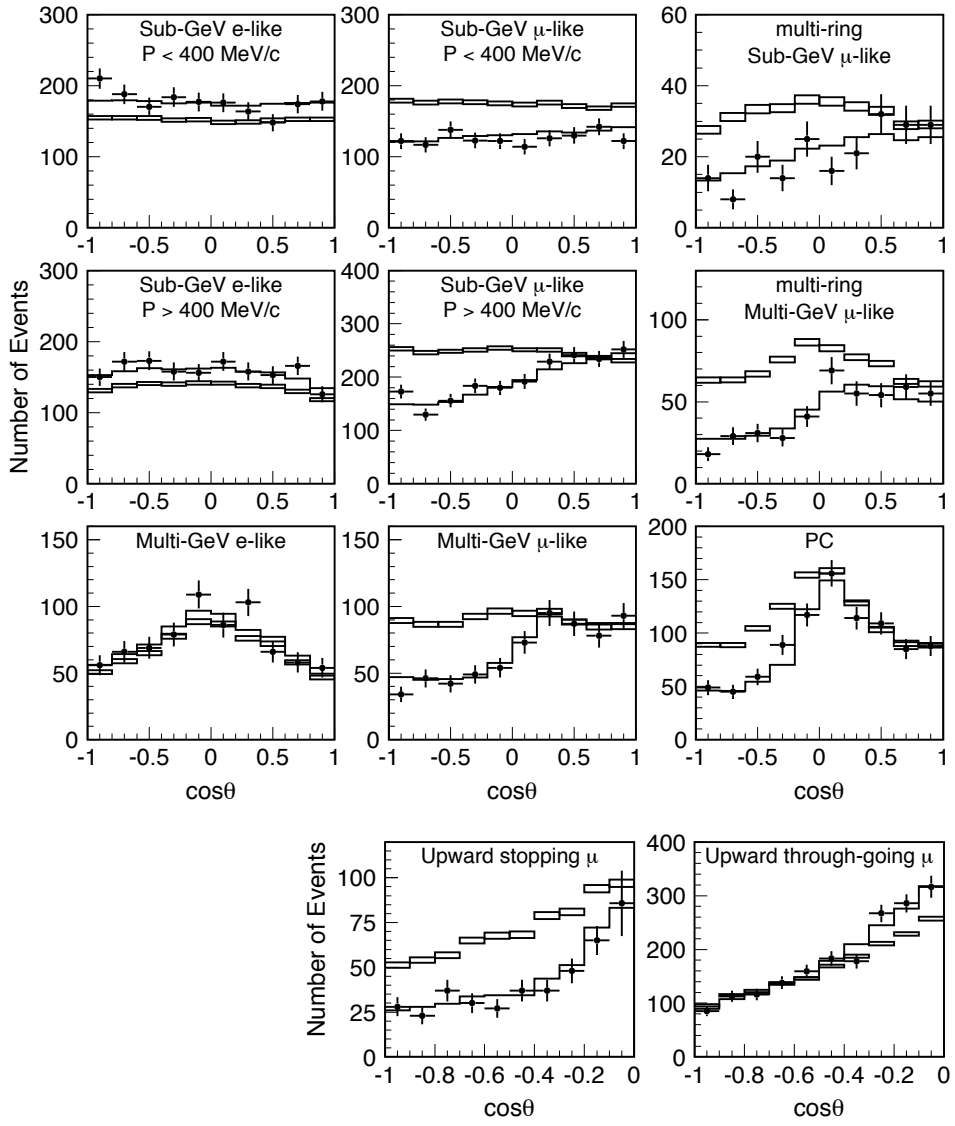

Fig. 31: Zenith angle distribution for fully-contained single-ring e-like and μ-like events, multi-ring μ-like events, partially contained events, and upward-going muons. The points show the data and the boxes show the Monte Carlo events without neutrino oscillations. The solid lines show the best-fit expectations for $\nu_\mu \leftrightarrow \nu_\tau$ oscillations (from Ref. [36]).

8 The three-neutrino mixing scenario

As we have seen the evidence summarized in the previous section points to two distinct neutrino mass square differences related to the solar and atmospheric oscillation frecuencies:

$$\underbrace{|\Delta m^2_{\rm solar}|}_{\sim 8\cdot 10^{-5}\ {\rm eV}^2} \ll \underbrace{|\Delta m^2_{\rm atmos}|}_{\sim 2.5\cdot 10^{-3}\ {\rm eV}^2} \tag{89}$$

The mixing of the three standard neutrinos ν_e, ν_μ, ν_τ can accommodate both. The two independent neutrino mass square differences are conventionally assigned to the solar and atmospheric ones in the following way:

$$\Delta m^2_{13} = m^2_3 - m^2_1 = \Delta m^2_{\rm atmos}, \qquad \Delta m^2_{12} = m^2_2 - m^2_1 = \Delta m^2_{\rm solar}\ . \tag{90}$$

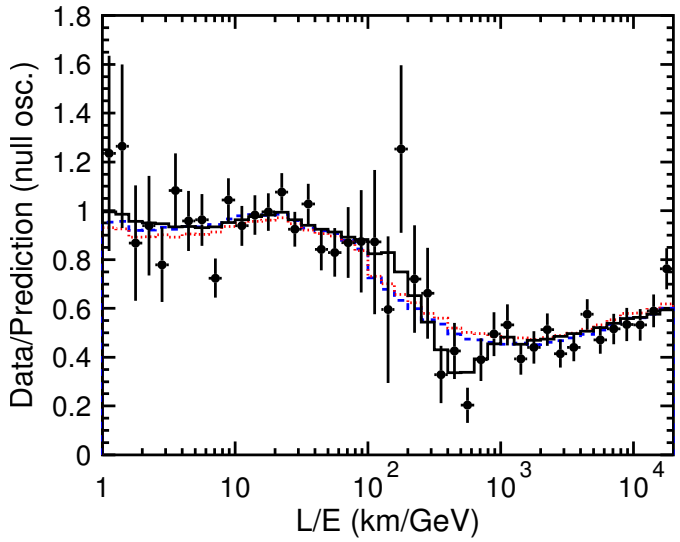

Fig. 32: Ratio of the data to the non-oscillated Monte Carlo events (points) with the best-fit expectation for 2-flavour $\nu_\mu \leftrightarrow \nu_\tau$ oscillations (solid line) as a function of E_ν/L (from Ref. [37]).

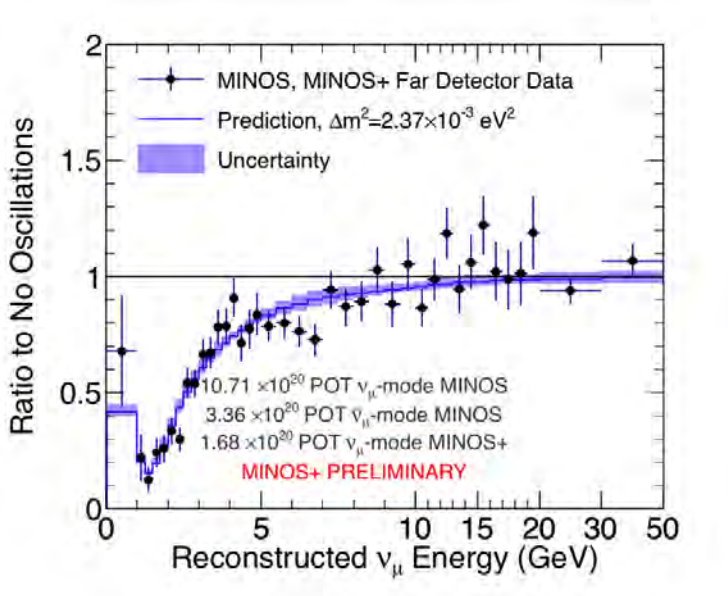

Fig. 33: Ratio of measured to expected (in absence of oscillations) neutrino events in MINOS as a functions of neutrino energy compared to the best fit oscillation solution (from Ref. [38]).

The PMNS mixing matrix depends on three angles and one or more CP phases (see eq. (30) for the standard parametrization). Only one CP phase, the so-called Dirac phase δ, appears in neutrino oscillation probabilities.

With this convention, the mixing angles θ_{23} and θ_{12} in the parametrization of Eq. (30) correspond approximately to the ones measured in atmospheric and solar oscillations, respectively. This is because solar and atmospheric anomalies approximately decouple as independent 2-by-2 mixing phenomena thanks to the hierarchy between the two mass splittings, $|\Delta m^2_{\rm atmos}| \gg |\Delta m^2_{\rm solar}|$, on the one hand, and the fact that the angle θ_{13}, which measures the electron component of the third mass eigenstate element $\sin\theta_{13} = (U_{\rm PMNS})_{e3}$, is small.

To see this, let us first consider the situation in which $E_\nu/L \sim |\Delta m^2_{\rm atmos}|$. We can thus neglect

the solar mass square difference in front of the atmospheric one and E_ν/L. The oscillation probabilities obtained in this limit are given by

$$P(\nu_e \to \nu_\mu) \simeq s^2_{23}\, \sin^2 2\theta_{13}\, \sin^2\left(\frac{\Delta m^2_{13} L}{4E_\nu}\right), \tag{91}$$

$$P(\nu_e \to \nu_\tau) \simeq c^2_{23}\, \sin^2 2\theta_{13}\, \sin^2\left(\frac{\Delta m^2_{13} L}{4E_\nu}\right), \tag{92}$$

$$P(\nu_\mu \to \nu_\tau) \simeq c^4_{13}\, \sin^2 2\theta_{23}\, \sin^2\left(\frac{\Delta m^2_{13} L}{4E_\nu}\right). \tag{93}$$

The results for antineutrinos are the same. All flavours oscillate therefore with the atmospheric frecuency, but only two angles enter these formulae: θ_{23} and θ_{13}. The latter is the only one that enters the disappearance probability for ν_e or $\bar\nu_e$ in this regime:

$$P(\nu_e \to \nu_e) = P(\bar\nu_e \to \bar\nu_e) = 1 - P(\nu_e \to \nu_\mu) - P(\nu_e \to \nu_\tau) \simeq \sin^2 2\theta_{13}\, \sin^2\left(\frac{\Delta m^2_{13} L}{4E_\nu}\right). \tag{94}$$

This is precisely the measurement of reactor neutrino experiments like Chooz, Daya Bay, RENO and Double Chooz. Therefore the oscillation amplitude of these experiments is a direct measurement of the angle θ_{13}, which has been measured to be small.

Note that in the limit $\theta_{13} \to 0$, the only probability that survives in Eq. (93) is the $\nu_\mu \to \nu_\tau$ one, which has the same form as a 2-family mixing formula Eq. (53) if we identify

$$(\Delta m^2_{\text{atmos}}, \theta_{\text{atmos}}) \to (\Delta m^2_{13}, \theta_{23})\,. \tag{95}$$

Therefore the close-to-maximal mixing angle observed in atmospheric neutrinos and the accelerator neutrino experiments like MINOS is identified with θ_{23}.

Instead if we consider experiments in the solar range, $E_\nu/L \sim \Delta m^2_{solar}$, the atmospheric oscillation its too rapid and gets averaged out. The survival probability for electrons in this limit is given by:

$$P(\nu_e \to \nu_e) = P(\bar\nu_e \to \bar\nu_e) \simeq c^4_{13}\left(1 - \sin^2 2\theta_{12}\, \sin^2\left(\frac{\Delta m^2_{12} L}{4E_\nu}\right)\right) + s^4_{13}. \tag{96}$$

Again it depends only on two angles, θ_{12} and θ_{13}, and in the limit in which the latter is zero, the survival probability measured in solar experiments has the form of two-family mixing if we identify

$$(\Delta m^2_{\text{solar}}, \theta_{\text{solar}}) \to (\Delta m^2_{12}, \theta_{12})\,. \tag{97}$$

The results that we have shown in the previous section of solar and atmospheric experiments have been analysed in terms of 2-family mixing. The previous argument indicates that when fits are done in the context of 3-family mixing nothing changes too much.

On the other hand, the fact that reactor experiments have already measured the disappearance of reactor $\bar\nu_e$ in the atmospheric range implies that the effects of $\theta_{13} \simeq 9^\circ$ are not negligible, and therefore a proper analysis of all the oscillation data requires performing global fits in the 3-family scenario. Figure 34 shows the $\Delta\chi^2$ as a function of each of the six parameters from a recent global analysis [43]. There are two parameters in which we observe to distinct minima, these corresponds to degeneracies that cannot be resolved with present data. The first corresponds to the neutrino mass ordering or hierarchy: present data cannot distinguish between the normal (NH or NO) and inverted ordering (IH or IO) represented in Fig. 35. Note that we denote by $\Delta m^2_{13} = \Delta m^2_{\text{atmos}}$ the atmospheric splitting for NO and $\Delta m^2_{23} = -\Delta m^2_{\text{atmos}}$. The second degeneracy corresponds to the octant choice of θ_{23}. Present data are mostly sensitive to $\sin^2 2\theta_{23}$. If this angle is not maximal, there are two possible choices that are roughly

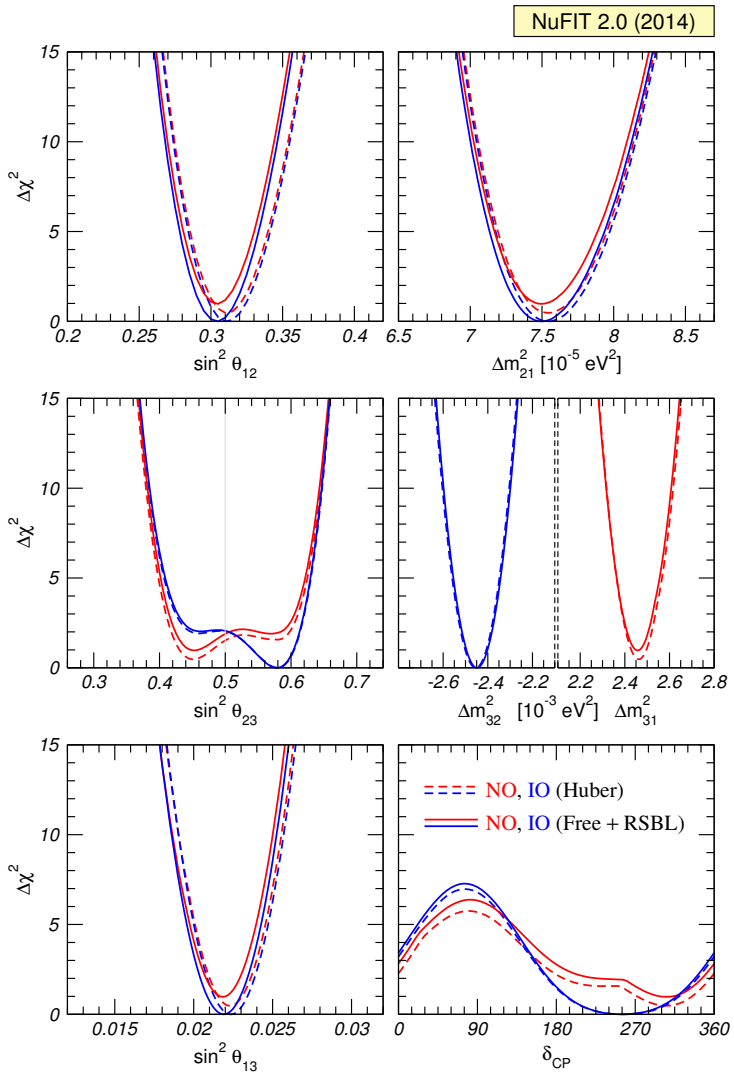

Fig. 34: Fits to the standard 3ν-mixing scenario including all available neutrino oscillation data (from Ref. [43]).

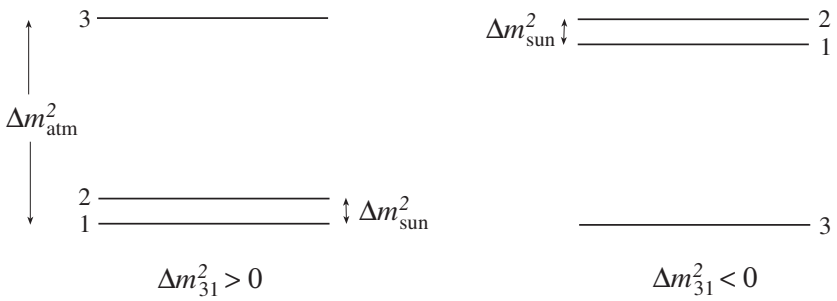

Fig. 35: Possible neutrino spectra consistent with solar and atmospheric data.

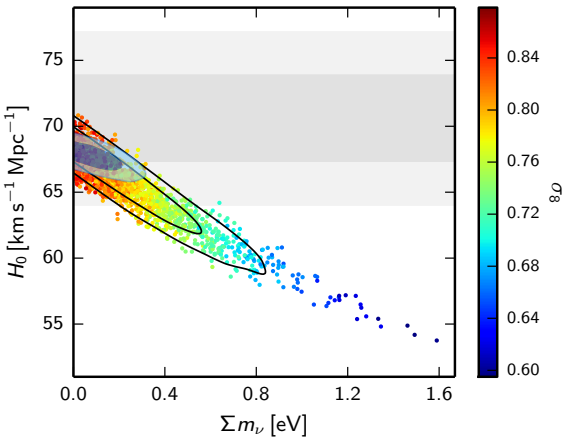

Fig. 36: Constraints on the sum of neutrino masses (in the standard 3ν scenario from cosmology [44]).

equivalent $\theta_{23} \leftrightarrow \pi/4 - \theta_{23}$. Due to this degeneracy, the largest angle is also the one less accurate. The 1σ limits for NO are:

$$\theta_{23}/^\circ = 42^{+3}_{-1.6}, \qquad \theta_{12}/^\circ = 33.5^{+0.78}_{-0.75}, \qquad \theta_{13}/^\circ = 8.5(2),$$
$$\Delta m^2_{12} = 7.5(2) \times 10^{-5}\ \text{eV}^2, \qquad \Delta m^2_{13} = 2.46(5) \times 10^{-3}\ \text{eV}^2. \,. \tag{98}$$

The CP phase δ remains completely unconstrained at 3σ. As we will see, the dependence on the phase requires sensitivity to both frecuencies simultaneously. There is however at 2σ some hint of a preference for $\delta > 180^\circ$. For more details see [43].

Neutrino oscillations cannot provide information on the absolute neutrino mass scale. The best sensitivity to this scale is at present coming from cosmology. Indeed neutrinos properties are imprinted in the history of the universe. In particular the features of the cosmic microwave background (CMB) and the large scale galaxy distribution depends sizeably on the sum of neutrino masses. The last results from Planck [44] are shown in Fig. 36. Their conservative limit at 95%CL is impressive:

$$\sum_i m_i \leq 0.23\text{eV}. \tag{99}$$

9 Prospects in neutrino oscillation experiments

An ambitious experimental program is underway to pin down the remaining unknowns and reach a 1% precision in the lepton flavour parameters. The neutrino ordering, the octant of θ_{23} and the CP violating phase, δ, can be search for in neutrino oscillation experiments with improved capabilities.

Concerning the neutrino ordering, the best hope to identify the spectrum exploits the MSW effect in the propagation of GeV neutrinos through the Earth matter. In the case of three neutrinos propagating in matter, the ν mass eigenstates as a function of the electron density for vanishing θ_{12}, θ_{13} are depicted in Fig. 37 for NO and IO. For NO we see that there are two level crossings giving rise to two MSW resonances. The first one is essentially the one relevant for solar neutrinos, as it affects the smallest mass splitting, with the resonance condition:

$$E^{(1)}_{\text{res}} = \frac{\Delta m^2_{12} \cos 2\theta_{12}}{2\sqrt{2} G_F N_e}. \tag{100}$$

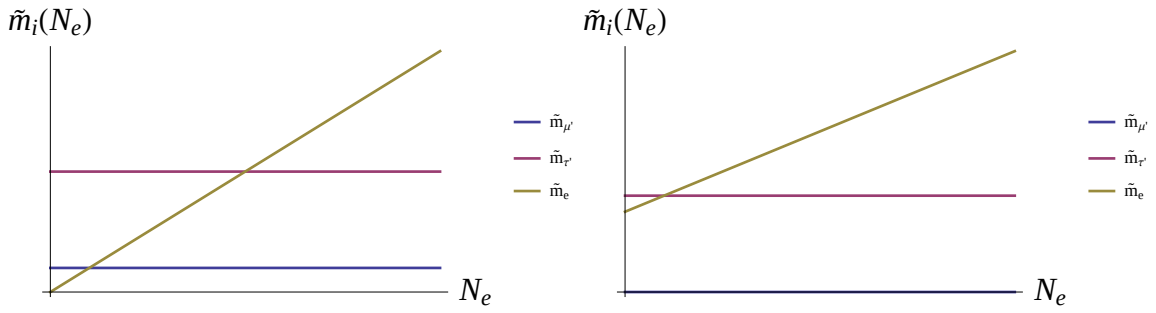

Fig. 37: Level crossings for ν in the three neutrino scenario for NO (left) and IO (right) at vanishing θ_{12} and θ_{13}.

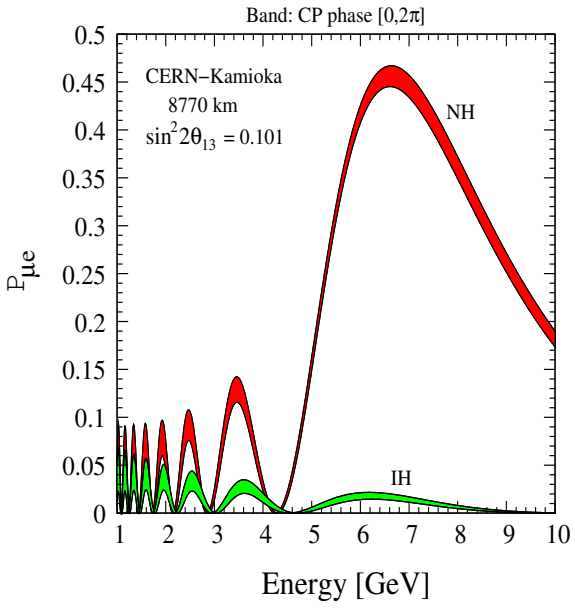

Fig. 38: $P_{\mu e}$ as a function of neutrino energy for L corresponding to the distance CERN-Kamioka for NH/IH. The bands corresponds to the uncertainty in δ (from Ref. [45]).

The second one affects the largest mass splitting

$$E_{\rm res}^{(2)} = \frac{\Delta m_{13}^2 \cos 2\theta_{13}}{2\sqrt{2} G_F N_e}. \tag{101}$$

For IO, only the first resonance appears in the ν channel.

For $\bar{\nu}$ the dependence on N_e of the first eigenstate has a negative slope and therefore only the second resonance appears for IO.

The existence of the atmospheric resonance implies a large enhancement of the oscillation probability $P(\nu_e \leftrightarrow \nu_\mu)$ for NO for energies near the resonant energy and at sufficiently long baseline. For IO the enhancement occurs in $P(\bar{\nu}_e \leftrightarrow \bar{\nu}_\mu)$ instead. For the typical matter densities of the Earth crust and mantle and the value of the atmospheric mass splitting, the resonant energy for neutrinos travelling through Earth is $\simeq 6$ GeV, an energy that can be reached in accelerator neutrino beams. The measurement of the neutrino ordering becomes almost a digital measurement sending a conventional ν beam sufficiently far as shown in Fig. 38, which shows the oscillation probability $P(\nu_\mu \to \nu_e)$ as a function of the neutrino energy at a distance corresponding to the baseline from CERN-Kamioka (8770 km).

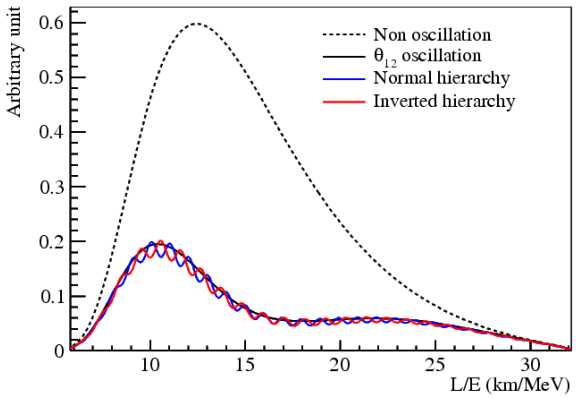

Fig. 39: Reactor neutrino spectrum in JUNO for NO/IO (from Ref. [48]).

The first experiment that will be sensitive to this effect is the NOvA experiment, optimized like T2K to see the ν_e appearance signal, with a baseline of 810km, which is however a bit short to see a large enhancement. Nevertheless if lucky NOvA could discriminate the ordering at 3σ.

The atmospheric resonance must also affect atmospheric neutrinos at the appropriate energy and baseline. Unfortunately the atmospheric flux contains both neutrinos and antineutrinos in similar numbers, and the corresponding events cannot be tell apart, because present atmospheric neutrino detectors cannot measure the lepton charge. If we superimpose the neutrino and antineutrino signals, both orderings will give rise to an enhancement in the resonance region, since no matter what the ordering is, either the neutrino or antineutrino channel will have a resonance. Nevertheless with sufficient statistics, there is discrimination power and in fact the biggest neutrino telescopes, ICECUBE and KM3NeT have proposed to instrument more finely some part of their detectors (PINGU and ORCA projects) to perform this measurement. Also the next generation of atmospheric neutrino detectors, such as HyperKamiokande, with a factor $\mathcal{O}(20)$ more mass than the present SuperKamiokande, or the INO detector that is designed to measure the muon charge in atmospheric events, could discriminate between the two orderings.

A very different strategy has been proposed for reactor neutrino experiments (e.g JUNO project). The idea is to measure very precisely the reactor neutrinos at a baseline of roughly 50 km, where the depletion of the flux due to the solar oscillation is maximal. At this optimal distance, one can get a superb measurement of the solar oscillation parameters, $(\theta_{12}, \Delta m^2_{12})$, and, with sufficient energy resolution, one could detect the modulation of the signal due to the atmospheric oscillation [46, 47]. Fig. 39 shows how this modulation is sensitive to the neutrino ordering. A leap ahead is needed to reach the required energy resolution.

9.1 Leptonic CP violation

As we have seen, the CP phase, δ, in the mixing matrix induces CP violation in neutrino oscillations, that is a difference between $P(\nu_\alpha \to \nu_\beta)$ and $P(\bar{\nu}_\alpha \to \bar{\nu}_\beta)$, for $\alpha \neq \beta$. As we saw in the general expression of Eq. (51), CP violation is possible if there are imaginary entries in the mixing matrix that make $\text{Im}[W^{jk}_{\alpha\beta}] \neq 0$. By CPT, disappearance probabilities cannot violate CP however, because under CPT

$$P(\nu_\alpha \to \nu_\beta) = P(\bar{\nu}_\beta \to \bar{\nu}_\alpha)\,, \tag{102}$$

so in order to observe a CP or T-odd asymmetry the initial and final flavour must be different, $\alpha \neq \beta$:

$$A^{CP}_{\alpha\beta} \equiv \frac{P(\nu_\alpha \to \nu_\beta) - P(\bar{\nu}_\alpha \to \bar{\nu}_\beta)}{P(\nu_\alpha \to \nu_\beta) + P(\bar{\nu}_\alpha \to \bar{\nu}_\beta)}, \quad A^{T}_{\alpha\beta} \equiv \frac{P(\nu_\alpha \to \nu_\beta) - P(\nu_\beta \to \nu_\alpha)}{P(\nu_\alpha \to \nu_\beta) + P(\nu_\beta \to \nu_\alpha)}\,. \tag{103}$$

In the case of 3-family mixing it is easy to see that the CP(T)-odd terms in the numerator are the same for all transitions $\alpha \neq \beta$:

$$A^{\text{CP(T)-odd}}_{\nu_\alpha\nu_\beta} = \frac{\sin\delta c_{13}\sin 2\theta_{13}\overbrace{\sin 2\theta_{12}\frac{\Delta m^2_{12}L}{4E_\nu}}^{\text{solar}}\overbrace{\sin 2\theta_{23}\sin^2\frac{\Delta m^2_{13}L}{4E_\nu}}^{\text{atmos}}}{P^{\text{CP-even}}_{\nu_\alpha\nu_\beta}}. \tag{104}$$

As expected, the numerator is GIM suppressed in all the Δm^2_{ij} and all the angles, because if any of them is zero, the CP-odd phase becomes unphysical. Therefore an experiment which is sensitive to CP violation must be sensitive to both mass splittings simultaneously. In this situation, it is not clear a priori what the optimization of E/L should be.

It can be shown that including only statitistical errors, the signal-to-noise for this asymmetry is maximized for $\langle E_\nu\rangle/L \sim |\Delta m^2_{\text{atmos}}|$. In this case, only two small parameters remain in the CP-odd terms: the solar splitting, $\Delta m^2_{\text{solar}}$ (i.e., small compared to the other scales, $\Delta m^2_{\text{atmos}}$ and $\langle E_\nu\rangle/L$), and the angle θ_{13}. The asymmetry is then larger in the subleading transitions: $\nu_e \to \nu_\mu(\nu_\tau)$, because the CP-even terms in the denominator are also suppressed by the same small parameters. A convenient approximation for the $\nu_e \leftrightarrow \nu_\mu$ transitions is obtained expanding to second order in both small parameters [49]:

$$\begin{aligned} P_{\nu_e\nu_\mu(\bar\nu_e\bar\nu_\mu)} &= s^2_{23}\,\sin^2 2\theta_{13}\,\sin^2\left(\frac{\Delta m^2_{13}\,L}{4E_\nu}\right) && \equiv P^{\text{atmos}} \\ &+ c^2_{23}\,\sin^2 2\theta_{12}\,\sin^2\left(\frac{\Delta m^2_{12}\,L}{4E_\nu}\right) && \equiv P^{\text{solar}} \\ &+ \tilde J\cos\left(\pm\delta - \frac{\Delta m^2_{13}\,L}{4E_\nu}\right)\frac{\Delta m^2_{12}\,L}{4E_\nu}\sin\left(\frac{\Delta m^2_{13}\,L}{4E_\nu}\right) && \equiv P^{\text{inter}}, \end{aligned} \tag{105}$$

where $\tilde J \equiv c_{13}\,\sin 2\theta_{13}\,\sin 2\theta_{12}\,\sin 2\theta_{23}$. The first term corresponds to the atmospheric oscillation, the second one is the solar one and there is an interference term which has the information on the phase δ and depends on both mass splittings.

These results correspond to vacuum propagation, but usually these experiments require the propagation of neutrinos in the Earth matter. The oscillation probabilities in matter can also be approximated by a similar series expansion [49]. The result has the same structure as in vacuum:

$$\begin{aligned} P_{\nu_e\nu_\mu(\bar\nu_e\bar\nu_\mu)} &= s^2_{23}\,\sin^2 2\theta_{13}\left(\frac{\Delta_{13}}{B_\pm}\right)^2\,\sin^2\left(\frac{B_\pm L}{2}\right) \\ &+ c^2_{23}\,\sin^2 2\theta_{12}\left(\frac{\Delta_{12}}{A}\right)^2\sin^2\left(\frac{A\,L}{2}\right) \\ &+ \tilde J\,\frac{\Delta_{12}}{A}\,\sin(\frac{AL}{2})\,\frac{\Delta_{13}}{B_\pm}\,\sin\left(\frac{B_\pm L}{2}\right)\,\cos\left(\pm\delta - \frac{\Delta_{13}\,L}{2}\right), \end{aligned} \tag{106}$$

where

$$B_\pm = |A \pm \Delta_{13}| \qquad \Delta_{ij} = \frac{\Delta m^2_{ij}}{2E_\nu} \qquad A = \sqrt{2}G_F N_e\,. \tag{107}$$

The oscillation probability for neutrinos and antineutrinos now differ not just because of leptonic CP violation, but also due to the matter effects, that as we have seen can be resonant. In particular, the atmospheric term which is the dominant one, shows the expected resonant enhancement in the neutrino or antineutrino oscillation probability (depending on the ordering).

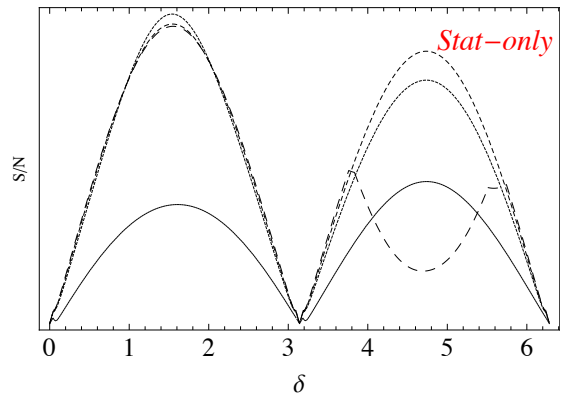

Fig. 40: Signal-to-noise for the discovery of CP violation at fixed $E/L \sim |\Delta m^2_{\rm atm}|$ as a function of the true value of δ for $L = 295$km (long-dashed), $L = 650$km (short-dashed), $L = 1300$km (dotted), $L = 2300$km (solid). The ordering is assumed to be unknown.

The sensitivity to the interference term requires very good knowledge of the leading atmospheric term and the present degeneracies (the octant and the neutrino ordering) directly affect the leading term compromising therefore the δ sensitivity. Either both uncertainties are solved before this measurement, or there must be sufficient sensitivity from the energy dependence of the signal to resolve all unkowns simultaneously.

A rough optimization of L for fixed E/L for discovering CP violation is shown in Fig. 40. It shows the signal-to-noise as a function of the true value of δ, assuming only statistical errors, but including the expected dependence of the cross sections and fluxes. At very short baselines, the sensitivity is compromised due to the lack of knowledge of the neutrino ordering. In a wide intermediate region around $\mathcal{O}(1000)$km the sensitivity is optimal, and at much larger baselines the sensitivity deteriorates because the matter effects completely hide CP-violation.

Several projects have been proposed to search for leptonic CP violation, including conventional beams, but also novel neutrino beams from muon decays (neutrino factories), from radioactive ion decays (β-beams) or from spalation sources (ESS). The relatively large value of θ_{13} has refocussed the interest in using the less challenging conventional beams and two projects are presently being developed: the HyperKamiokande detector, an upscaled version of SuperKamiokande that will measure atmopheric neutrinos with unprecedent precision, and also intercept a neutrino beam from JPARC at a relatively short baseline $L = 295$km, and the DUNE project that involves a ~ 30 kton liquid argon neutrino detector and a neutrino beam from Fermilab to the Soudan mine at a baseline of $L = 1500$km. The expected sensitivities to the neutrino ordering and to CP violation of both projects are shown in Figs. 41., 42.

10 Outliers: the LSND anomaly

The long-standing puzzle brought by the LSND experiment is still unresolved. This experiment [52] observed a surplus of electron events in a muon neutrino beam from π^+ decaying in flight (DIF) and a surplus of positron events in a neutrino beam from μ^+ decaying at rest (DAR). The interpretation of this data in terms of neutrino oscillations, that is a non-vanishing $P(\nu_\mu \to \nu_e)$, gives the range shown by a coloured band in Fig. 44.

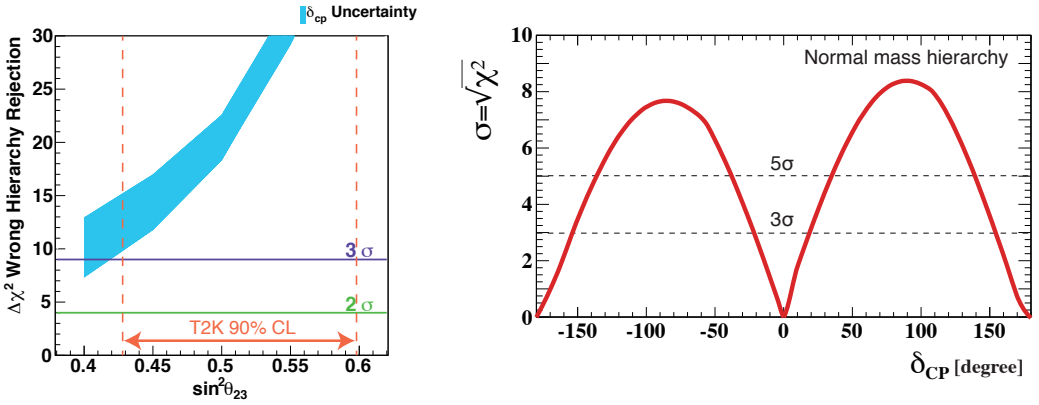

Fig. 41: Prospects for determining the ordering (left) and discovering CP violation (right) in HyperKamiokande (from Ref. [50]).

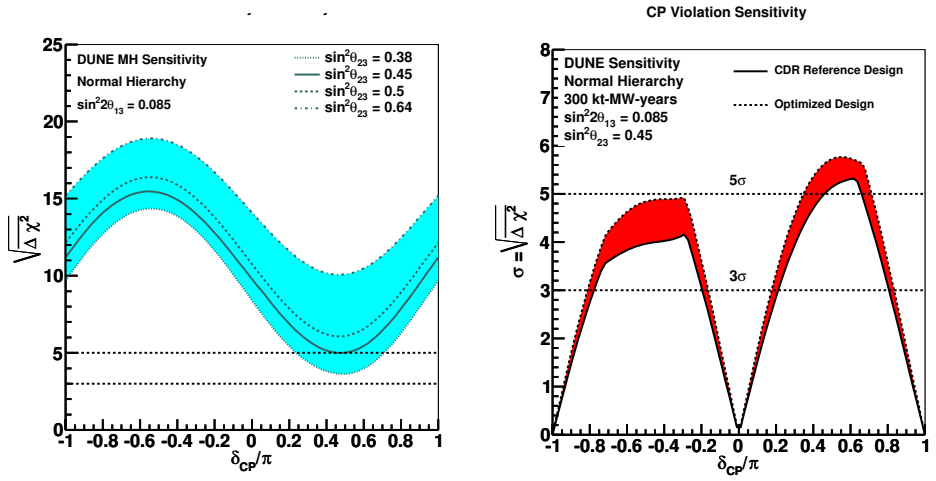

Fig. 42: Prospects for determining the ordering (left) and discovering CP violation (right) in DUNE (from Ref. [51]).

$$
\begin{aligned}
\pi^+ \to \quad & \mu^+ \quad \nu_\mu \\
& \quad\;\; \nu_\mu \to \nu_e \quad \text{DIF } (28 \pm 6/10 \pm 2) \\
& \mu^+ \quad \to e^+ \nu_e \bar{\nu}_\mu \\
& \qquad\;\; \bar{\nu}_\mu \to \bar{\nu}_e \quad \text{DAR } (64 \pm 18/12 \pm 3)
\end{aligned}
$$

A significant fraction of this region was already excluded by the experiment KARMEN [53] that has unsuccessfully searched for $\bar{\nu}_\mu \to \bar{\nu}_e$ in a similar range.

The experiment MiniBOONE was designed to further investigate the LSND signal, with inconclusive results [54]. They did not confirm the anomaly, but found some anomaly at lower energies.

On the other hand, recently the results of various short baseline (tens of meters) reactor neutrino experiments were revised, after an update on the reactor neutrino flux predictions [55–57], which increased theses fluxes by a few per cent. While the measured neutrino flux was found to be in agreement with predictions before, after this revision some reactor neutrinos seem to disappear before reaching near detectors, $L = \mathcal{O}(10)$m. This is the so-called reactor anomaly shown in Fig. 43. This result brought some excitement because if this disappearance is due to oscillations, it might reinforce the oscillation interpretation of the LSND anomaly.

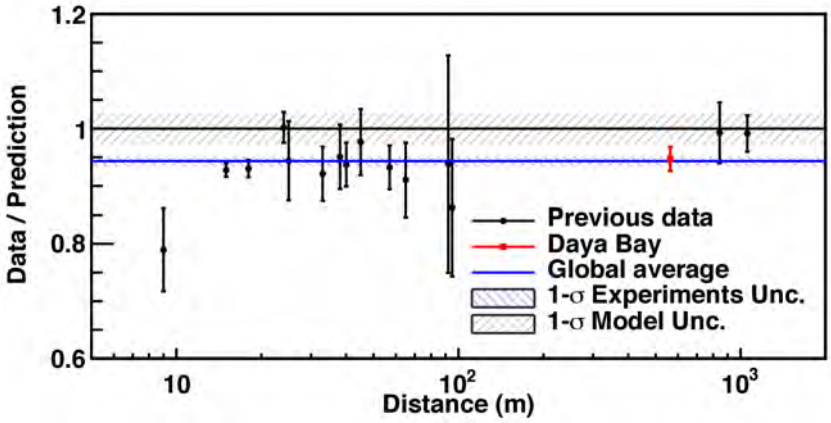

Fig. 43: Reactor neutrino flux measured by various near detectors compared with the recent flux predictions (from Ref. [58]).

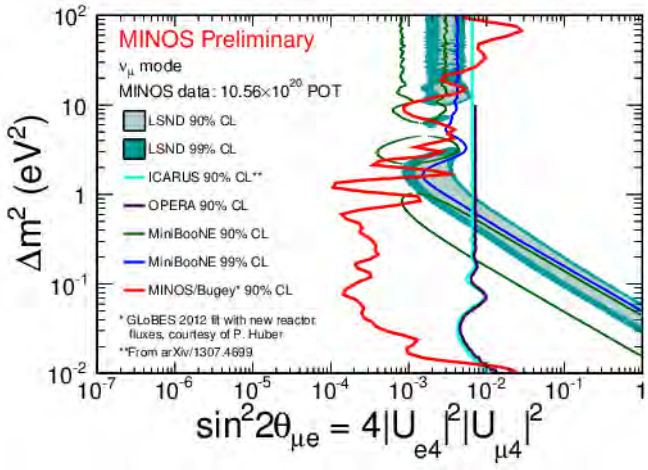

Fig. 44: Sterile neutrino search in the disappearance of ν_μ's in MINOS (from Ref. [59]).

The required mass splitting to describe both anomalies is $\Delta m^2_{\rm LSND} \simeq 1{\rm eV}^2$, which is much larger than the solar and atmospheric, and therefore requires the existence of at least a fourth neutrino mass eigenstate, i. If such a state can explain the LSND anomaly, it must couple to both electrons and muons. Unfortunately the smoking gun would require that also accelerator ν_μ disappear with the same wavelength and this has not been observed:

$$\begin{aligned} P(\nu_\mu \to \nu_e) &\propto |U_{ei}U_{\mu i}|^2 && \text{LSND} \\ 1 - P(\nu_e \to \nu_e) &\propto |U_{ei}|^4 && \text{reactor} \\ 1 - P(\nu_\mu \to \nu_\mu) &\propto |U_{\mu i}|^4 && \text{not observed} \end{aligned}$$

The strongest constraint on the disappearance of ν_μ in the LSND range has been recently set by MINOS+ [59] and is shown in Fig. 44 together with the region favoured by the LSND anomaly. An improvement of this sensitivity is expected also from the measurement of atmospheric neutrinos in ICECUBE.

A number of experiments are being constructed to clarify the reactor anomaly. Hopefully in the near future they will settle this long-standing puzzle.

11 Neutrinos and BSM Physics

The new lepton flavour sector of the SM has opened new perspectives into the flavour puzzle. As we have seen neutrinos are massive but significantly lighter than the remaining charged fermions. Clearly the gap of Fig. 11 calls for an explanation. The leptonic mixing matrix is also very different to that in the quark sector. The neutrino mixing matrix is approximately given by [43]

$$|U_{\rm PMNS}|_{3\sigma} \simeq \begin{pmatrix} 0.80-0.84 & 0.51-0.58 & 0.137-0.158 \\ 0.22-0.52 & 0.44-0.70 & 0.61-0.79 \\ 0.25-0.53 & 0.46-0.71 & 0.59-0.78 \end{pmatrix} . \tag{108}$$

The CKM matrix is presently constrained [7] to be:

$$|V_{\rm CKM}| \simeq \begin{pmatrix} 0.97427(14) & 0.22536(61) & 0.00355(15) \\ 0.22522(61) & 0.97343(15) & 0.0414(12) \\ 0.00886(33) & 0.0405(12) & 0.99914(5) \end{pmatrix} . \tag{109}$$

There is a striking difference between the two (and not only in the precision of the entries...). The CKM matrix is close to the unit matrix:

$$V_{\rm CKM} \simeq \begin{pmatrix} 1 & O(\lambda) & O(\lambda^3) \\ O(\lambda) & 1 & O(\lambda^2) \\ O(\lambda^3) & O(\lambda^2) & 1 \end{pmatrix}, \quad \lambda \sim 0.2, \tag{110}$$

while the leptonic one has large off-diagonal entries. With a similar level of precision, it is close to the tri-bimaximal mixing pattern [60]

$$U_{\rm PMNS} \simeq V_{\text{tri-bi}} \simeq \begin{pmatrix} \sqrt{\frac{2}{3}} & \sqrt{\frac{1}{3}} & 0 \\ -\sqrt{\frac{1}{6}} & \sqrt{\frac{1}{3}} & \sqrt{\frac{1}{2}} \\ \sqrt{\frac{1}{6}} & -\sqrt{\frac{1}{3}} & \sqrt{\frac{1}{2}} \end{pmatrix} .$$

Discrete flavour symmetries have been extensively studied as the possible origin of this pattern. For recent review see [61].

While we do not have yet a compelling explanation of the different mixing patterns, we do have one for the gap between neutrino and other fermion masses. We saw that if the light neutrinos are Majorana particles and get their mass via the Weinberg interaction of Fig. 12, they are signalling BSM physics. Neutrino masses are suppressed because they arise from a new scale of physics that could be $\Lambda \gg v$. Generically such BSM would induce not only neutrino masses but also other effects represented at low-energies by the $d = 6$ effective operators of eq. (23). Unfortunately the list of $d = 6$ operators is too long to be of guidance: which one might be more relevant is to a large extent model dependent.

We could argue that there is not better motivated BSM physics than the one that gives rise to the Weinberg operator. The simplest possibility is that Weinberg's operator, like the Fermi one in Fig.2, arises from the exchange of a massive particle at tree level. The classification of what particles can induce the Weinberg operator at tree level has been done, and reproduces the three types of seesaw models, as depicted in Fig. 45:

- type I see-saw: SM+ heavy singlet fermions [62–65],
- type II see-saw: SM + heavy triplet scalar [66–70],
- type III see-saw: SM + heavy triple fermions [71, 72],

or combinations. The masses of the extra states define the scale Λ.

It is also possible that Weinberg's interaction is generated by new physics at higher orders, such as in the famous Zee model [73] and related ones [74, 75]. In this case, neutrino masses have an additional suppression by loop factors $1/(16\pi^2)$.

The $d = 6$ operators induced at tree level in see-saw models of Types I to III have been worked out [76]. They give rise to a rich phenomenology that could help discriminate between the models. In particular, they could induce beyond-the-standard-model signals in Z and W decays, deviations in the ρ parameter or the W mass, and mediate rare lepton decays, as well as violations of universality and unitarity of the neutrino mass matrix. It would therefore be extremely important to search for these effects. Whether they are large enough to be observed or not depends strongly on how high the scale Λ is, since all these effects are suppressed by two powers of Λ.

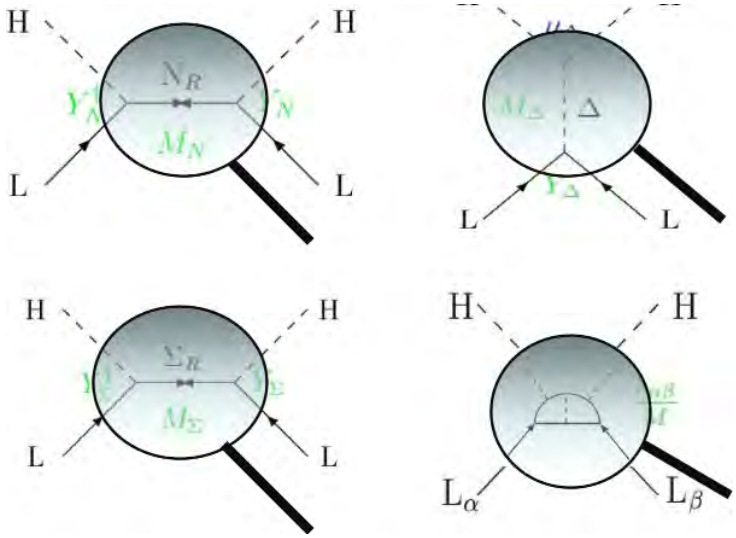

Fig. 45: Magnifying-glass view of Weinberg operator in see-saws Type I (top left), Type II (top right), Type III (bottom left) and Zee–Babu model (bottom right).

Unfortunately, the measurement of Weinberg's interaction leaves behind an unresolved $\lambda \leftrightarrow \Lambda$ degeneracy that makes it impossible to know what the scale of the new physics is, even if we were to know the absolute value of neutrino masses.

The recent discovery of the Higgs field and in particular the value of its mass $m_H = 125$ GeV [77] suggests that the SM is as healthy as ever. In spite of the Landau poles, the value of the SM couplings surprisingly conspire to make the model consistent up to arbitrarily large scales [78].

The most popular choice for Λ has traditionally been a grand-unification scale, given the intriguing fact that the seesaw-type ratio $\frac{v^2}{M_{\rm GUT}} \sim 0.01$–$0.1$ eV, in the right ballpark of the neutrino mass scale. Howeer, in the absence of any stabilizing mechanism such as supersymmetry, however, the electroweak scale needs to be fine-tunned [79, 80] since the Higgs mass receives quadratic loop corrections in Λ. A naturalness argument would then imply that $\Lambda < 10^7$ GeV. The opposite is not true however, the scale Λ would not get corrections from the electroweak scale: any value of $\Lambda \leq v$ is technically natural.

The possibility that the scale Λ might be of the order of the EW scale or lower has recently been studied in more detail, with special emphasis on establishing the existing experimental constraints, and the possibility that this new physics could explain other open problems in the SM such as: the LSND and reactor anomalies, dark matter, leptogenesis, etc. The type I seesaw model is the case better studied so we will concentrate on pinning down the scale Λ in this context.

11.1 Type I seesaw model

It is arguably the minimal extension of the SM allowing for neutrino masses [62–65],. It involves the addition of $n_R \geq 2$ singlet Weyl fermions, ν_R, to the SM. The most general renormalizable Lagrangian which satisfies Lorentz and the gauge symmetries is given by:

$$\mathcal{L}_{\rm TypeI} \;=\; \mathcal{L}_{\rm SM} - \sum_{\alpha,i} \bar{L}^{\alpha} Y_{\nu}^{\alpha i}\, \tilde{\Phi}\, \nu_R^i - \sum_{i,j}^{n_R} \frac{1}{2} \bar{\nu}_R^{ic}\, M_N^{ij}\, \nu_R^j + \text{ h.c. }, \tag{111}$$

where the new parameters involved are a $3 \times n_R$ neutrino Yukawa matrix and a $n_R \times n_R$ symmetric Majorana mass matrix for the singlet fields. Upon spontaneous symmetry breaking these couplings become mass terms, that can be writen in the Majorana basis (ν_L^c, ν_R) as

$$\mathcal{L}_{\rm TypeI} \;\rightarrow\; \mathcal{L}_{\rm SM} - \frac{1}{2} \begin{pmatrix} \bar{\nu}_L & \bar{\nu_R^c} \end{pmatrix} \begin{pmatrix} 0 & m_D \\ m_D^T & M_N \end{pmatrix} \begin{pmatrix} \nu_L^c \\ \nu_R \end{pmatrix} \; + h.c. + ... \tag{112}$$

where

$$m_D = Y_{\nu} \frac{v}{\sqrt{2}}. \tag{113}$$

Note that Dirac neutrinos are a particular case of the model. If we invoke a global lepton number symmetry to force $M_N = 0$, the singlets are exactly equivalent to the right-handed neutrinos in the Dirac case described in sec. 3.1. In the opposite limit $M_N \gg v$, the singlets can be integrated out and give rise to the Weinberg interaction as well as others at $d = 6$, etc. For finite M_N, the spectrum of this theory contains in general $3 + n_R$ Majorana neutrinos, which are admixtures of the active ones and the extra singlets. It is easy to diagonalize the mass matrix in eq. (112) in an expansion in m_D/M_N. The result to leading order in this expansion is

$$U^T \begin{pmatrix} 0 & m_D \\ m_D^T & M_N \end{pmatrix} U \simeq \begin{pmatrix} -m_D \frac{1}{M_N} m_D^T & 0 \\ 0 & M_N \end{pmatrix} + \mathcal{O}(\theta^2), \quad U = \begin{pmatrix} 1 & \theta \\ -\theta^{\dagger} & 1 \end{pmatrix}, \tag{114}$$

where

$$\theta = m_D^* \frac{1}{M_N}. \tag{115}$$

To this order therefore the light neutrino and heavy neutrino masses are given by

$$m_l = \text{Diag}\left[-m_D \frac{1}{M_N} m_D^T \right], \quad M_h = \text{Diag}[M_N]. \tag{116}$$

Fig. (46) depicts the spectrum for the case of $n_R = 3$ as a function of a common M_N. In the limit $M_N \rightarrow 0$ the states degenerate in pairs to form Dirac fermions. As M_N increases three states get more massive proportional to M_N, while three get lighter proportional to M_N^{-1}. This is why the model is called seesaw. The number of new free parameters is large. For the case $n_R = 3$ there are 18 fundamental parameters in the lepton sector: six of them are masses, six mixing angles and six phases. The counting of parameters for general n_R is shown in Table 4. Out of these 18 parameters we have determined only 5: two mass differences and three neutrino mixing angles.

A very convenient parametrization in this model is the so-called Casas-Ibarra [81] parametrization, which allows to write in all generality (up to corrections of $\mathcal{O}(\theta^2)$) the Lagrangian parameters in terms of the parameters that can be measured at low energies: light neutrino masses and mixings, and others that cannot. In particular the phenomenology of this model depends on the spectrum of neutrino mass

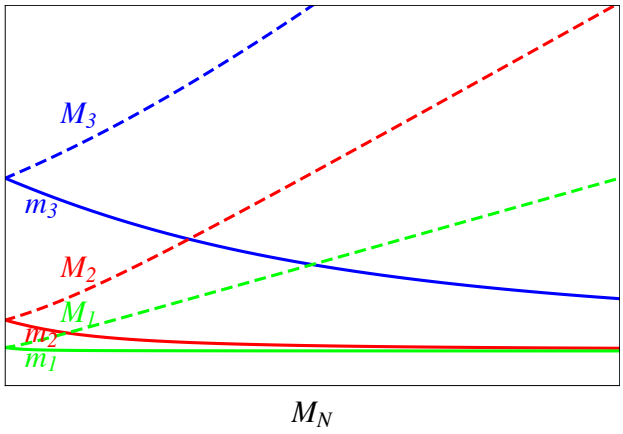

Fig. 46: Spectrum of th type I seesaw model for $n_R = 3$ as a function of a common M_N.

	Yukawas	Field redefinitons	$No.\ m$	$No.\ \theta$	$No.\ \phi$
see-saw $E \geq M_i$	$Y_l, Y_\nu, M_R = M_R^T$ $5n^2 + n$	$U(n)^3$ $\frac{3(n^2-n)}{2}, \frac{3(n^2+n)}{2}$	$3n$	$n^2 - n$	$n^2 - n$
see-saw $E \ll M_i$	$Y_l, \alpha_\nu^T = \alpha_\nu$ $3n^2 + n$	$U(n)^2$ $n^2 - n, n^2 + n$	$2n$	$\frac{n^2-n}{2}$	$\frac{n^2-n}{2}$

Table 4: Number of physical parameters in the see-saw model with n families and the same number of right-handed Majorana neutrinos at high and low energies.

eigenstates, that we denote by $(\nu_1, \nu_2, \nu_3, N_1, N_2, ...N_{n_R})$, and their admixture in the flavour neutrino states which is given by:

$$\begin{pmatrix} \nu_e \\ \nu_\mu \\ \nu_\tau \end{pmatrix} = U_{ll} \begin{pmatrix} \nu_1 \\ \nu_2 \\ \nu_3 \end{pmatrix} + U_{lh} \begin{pmatrix} N_1 \\ N_2 \\ .. \\ N_{n_R} \end{pmatrix} . \tag{117}$$

In the Casas-Ibarra parametrization we have

$$\begin{aligned} U_{ll} &= U_{\rm PMNS} + \mathcal{O}(\theta^2), \\ U_{lh} &= i U_{\rm PMNS} \sqrt{m_l} R \frac{1}{\sqrt{M_h}} + \mathcal{O}(\theta^2). \end{aligned} \tag{118}$$

where R is a general complex orthogonal matrix, $R^T R = 1$, which together with the heavy neutrino masses, M_h, parametrizes the parameter space inaccessible to neutrino oscillation experiments. Note that U_{ll} is the mixing matrix that we measure in neutrino oscillation experiments, assuming the heavy states are too heavy to play a role. This matrix is however no longer unitary, but the unitarity violations are parametrically of $\mathcal{O}(\theta^2) \sim m_l/M_h$.

The Casas-Ibarra parametrization needs to be modified in the presence of large unitarity violations. A similar parametrization valid to all orders in θ is given in [82].

Eqs. (118) indicate that in this model there is a strong correlation between flavour mixings of the heavy states, U_{lh}, and the ratio of light-to-heavy neutrino masses. However the presence of the unknown matrix R, which is not bounded, implies that the naive seesaw scaling, $|U_{lh}|^2 \sim m_l/M_h$, that would hold exactly for one neutrino family, is far too naive for $n_R > 1$. In fact there are regions of parameter space where these mixings can be much larger than suggested by the naive scaling, and these are precisely the regions with more phenomenological interest, as we will see below.

In this model we can ask the question. What is the value of the M_N scale to avoid the hierarchy between neutrinos and the remaining fermions. If we plot the distribution of Yukawa couplings instead of the masses, we find that neutrino masses can be explained with a scale $M_N \simeq$ GUT, if the neutrino yukawa couplings are of $O(1)$ like the top. However if the yukawas are of the order of the electron yukawa, a scale $M_N \sim$ TeV can also explain neutrino masses. Clearly, in both cases we have avoided making neutrinos especial, and the flavour puzzle is no worse than in the charged fermion sector. Note that this wide range of scales between TeV-GUT is the result of the quadratic dependence of the light neutrino masses on the yukawas, as opposed to the linear dependence in the Dirac case.

Let us discuss some phenomenological implications of the different choices of the scale M_N.

Neutrinoless double-beta decay

For $M_N \geq 100$ MeV, the model implies the presence of neutrinoless double beta decay at some level. The amplitude for this process gets contribution from the light and heavy states:

$$m_{\beta\beta} \equiv \sum_{i=1}^{3} (U_{\rm PMNS})_{ei}^2 m_i + \sum_{j=1}^{n_R} (U_{lh})_{ej}^2 M_j \frac{\mathcal{M}^{\beta\beta 0\nu}(M_j)}{\mathcal{M}^{\beta\beta 0\nu}(0)}, \tag{119}$$

where the ratio of matrix elements $\mathcal{M}^{\beta\beta 0\nu}$ for heavy and light mediators satisfy [83]:

$$\frac{\mathcal{M}^{\beta\beta 0\nu}(M_j)}{\mathcal{M}^{\beta\beta 0\nu}(0)} \propto \left(\frac{100\text{MeV}}{M_j}\right)^2, \quad M_j \to \infty. \tag{120}$$

If all the heavy state masses $\gg 100$ MeV, the second term is suppressed and the amplitude contains only the light neutrino masses and mixings:

$$m_{\beta\beta} \simeq |c_{13}^2 (m_1 c_{12}^2 + m_2 e^{i\alpha_1} s_{12}^2) + m_3 e^{i\alpha_2} s_{13}^2| \,, \tag{121}$$

and is quite well constrained from neutrino oscillation experiments. Figure 47 shows the present allowed regions for $m_{\beta\beta}$ neglecting the heavy state contributions as a function of the sum of the light neutrino masses, that can be constrained from cosmology:

$$\Sigma \equiv m_1 + m_2 + m_3. \tag{122}$$

It the neutrino ordering would be inverted or Σ not much smaller than 0.1 eV, there is a good chance that the next generation of $\beta\beta 0\nu$ experiments will see a signal. A plethora of experiments using different technologies have been proposed to reach a sensitivity in $m_{\beta\beta}$ in the range of 10^{-2} eV , which could be sufficient to explore the full parameter space in the case of the IO. The importance of this measurement can hardly be overstated. A non-zero $m_{\beta\beta}$ will imply that neutrinos are Majorana and therefore a new physics scale must exist, that lepton number is violated, and might give very valuable information on the lightest neutrino mass, and even help establishing the neutrino mass ordering. If the heavy states are not too heavy, within 100 MeV-few GeV, they could also contribute to the process significantly and even dominate over the light neutrino contribution for both orderings [85–87].

Mini-seesaw and oscillations

If the scale $M_N \leq$ eV (mini-seesaw models [88]), the extra heavy states could affect neutrino oscillations significantly. Strong constraints can be derived therefore from neutrino oscillation experiments

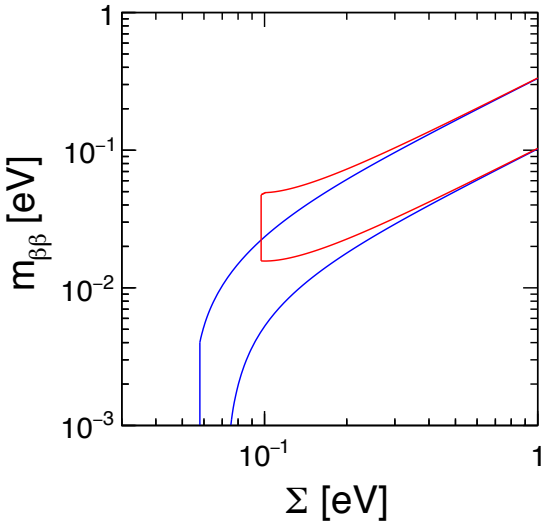

Fig. 47: Allowed region for $m_{\beta\beta}$ for NO (blue contour) and IO (red contour) from a global analysis of neutrino data (from Ref. [84]).

which essentially exclude the possibility that $M_N \in [10^{-9}(10^{-11})\text{ eV}, 1\text{ eV}]$ for NO(IO) [89–91]. The possibility that $M_N \sim 1$ eV could explain the LSND and reactor anomalies has also been studied. It is intriguing that the best fit to the LSND and reactor anomalies [92, 93] point to mixings and masses of the extra neutrino(s) that nicely match the naive seesaw scaling. In fact mini-seesaw models provide similar fits to data [82], with much less parameters, than general phenomenological models with $3+N$ neutrino mixing. Both are affected however by the tension in data between the anomalies and the non-observation of ν_μ disappearance.

Cosmology and the seesaw scale

For $M_N \leq 100$ MeV, the heavy states in seesaw models can sizeably modify the history of the Universe: the abundance of light elements, the fluctuations in the CMB and the galaxy distribution at large scales. This is the case because these extra states contribute to the expansion either as a significant extra component of dark matter (Ω_m) or radiation (ΔN_{eff}).

The singlet states in this mass range are produced at T below the electroweak phase transition via mixing. A simple estimate of their production rate is

$$\Gamma_{s_i}(T) \simeq \sum_\alpha |(\tilde{U}_{lh})_{\alpha i}|^2 \times \Gamma_{\nu_\alpha}(T), \tag{123}$$

where Γ_{ν_α} is the interaction rate of the active neutrinos and the $\tilde{U}_{lh}$ is the light-heavy mixing at T, strongly modified by forward scattering on the plasma particles [94]. The state i will reach thermal equilibrium if $\Gamma_{s_i}(T)$ is larger than the Hubble parameter at some T. If this is the case, the extra species will contribute like one extra neutrino for $T > M_i$ or like an extra component of dark matter for $T < M_i$. The latest results from Planck strongly constrain an extra radiation component at CMB:

$$N_{\text{eff}}(\text{CMB}) = 3.2 \pm 0.5. \tag{124}$$

and also measures the dark matter component to be $\Omega_m = 0.308 \pm 0.012$. Similar bounds are obtained from the abundance of light elements, BBN. These bounds exclude the possibility of having essentially any extra fully thermalized neutrino that is sufficiently long-lived to survive BBN. It can be shown that

the ratio $\frac{\Gamma_{s_i}(T)}{H(T)}$ reaches a maximum at T_{max} [95, 96] and

$$\frac{\Gamma_{s_i}(T_{max})}{H(T_{max})} \sim \frac{\sum_\alpha |(U_{lh})_{\alpha i}|^2 M_i}{\sqrt{g_*(T_{max})}}. \tag{125}$$

The naive seesaw scaling $U_{lh}^2 M_h \sim m_l$, would seem to imply that the thermalization condition depends only on the light neutrino masses and is independent on the seesaw scale. In fact a detailed study shows that indeed this naive expectation holds.

For $n_R = 2$, the heavy states must be $M_i \geq 100$ MeV [97], so that they might decay before BBN. For $n_R = 3$ two things can happen [98]. If the lightest neutrino mass $m_{\rm lightest} \geq 3 \times 10^{-3}$ eV, all the three heavy states thermalize so $M_i \geq 100$ MeV. If $m_{\rm lightest} \leq 3 \times 10^{-3}$ eV two states must be above this limit, but one of the states with mass M_1 might not thermalize and therefore be sufficiently diluted. M_1 may take any value provided $m_{\rm lightest}$, which is presently unconstrained, is tuned accordingly.

The states that could explain the LSND and reactor anomalies will imply $\Delta N_{\rm eff} \geq 1$ which is essentially excluded by cosmology. For a recent detailed analysis see [99]. Exotic extensions involving hidden interactions of the extra singlet states would be needed to make them compatible.

Warm dark matter

For $m_{\rm lightest} \leq 10^{-5}$ eV, M_1 might be $\mathcal{O}($ keV$)$, and a viable warm dark matter candidate [100, 101]. This scenario is the so-called νMSM model [101]. The most spectacular signal of this type of Dark Matter is a monocromatic X-ray line. Two recent analyses [102, 103] have recently shown some evidence for an unexplained X-ray line in galaxy clusters that might be compatible with a 7 keV neutrino. These results are under intense debate. If interpreted in terms of a keV neutrino, the mixing however is too small and some extra mechanism is needed to enhance the production so that it matches the required dark matter density, such as the presence of large primordial lepton asymmetries [104].

Direct searches

In summary, cosmology and neutrino oscillations restrict a huge range of $M_N \in [10^{-17} - 10^2]$ MeV. Naturalness arguments on the other hand point to a scale $M_N \leq 10^{10}$ MeV, suggesting that maybe the scale of M_N is not far from the electroweak scale. States with masses in this range could be produced on the lab and searched for as peaks in meson decays, in beam dump experiments, colliders, etc. [105]. The present experimental bounds on the e, μ mixings of these heavy states are shown in Figs. 48. The shaded regions correspond to existing constraints and the unshaded ones to prospects of various new experiments. For masses below a few GeV, the best constraints come from peak searches in meson decays. In particular the new beam dump experiment SHiP [106] can improve considerably the sensitivity in the region above kaon decays. For the lighter hadrons, improvements can be achieved with the more intense beams expected in long-baseline accelerator neutrino projects such as DUNE [107]. For

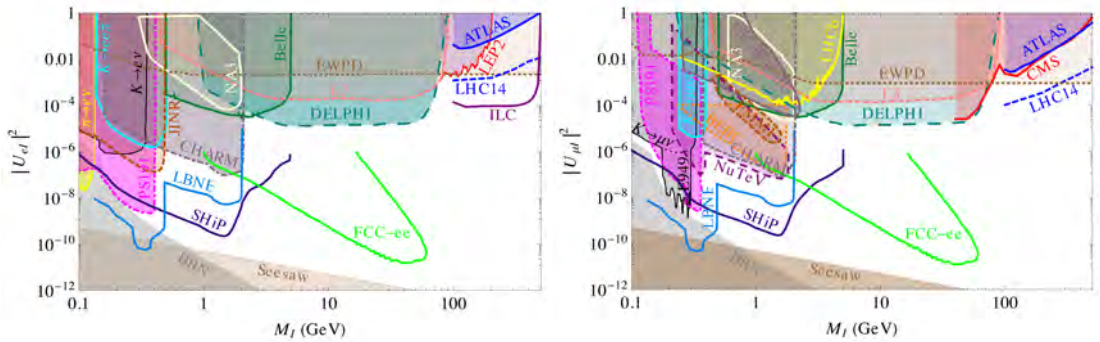

Fig. 48: Constraints from present and future experiments on a heavy neutrino with mixing to the electron (left) and muon (right). Shaded regions are existing bounds and the empty ones are prospects (from Ref. [106]).

masses above the W, Z masses the best constraints are presently coming from LHC searches. Processes with three leptons in the final state as in Fig. 49 seem most promising [108], although other production mechanisms like $W\gamma$ fusion can dominate at higher masses [109]. For a recent review and further references see [106]. For masses below the W mass, it has been pointed out recently that LHC might also improve the present constraints by looking for displaced vertices in the range 1mm-1m [110–112].

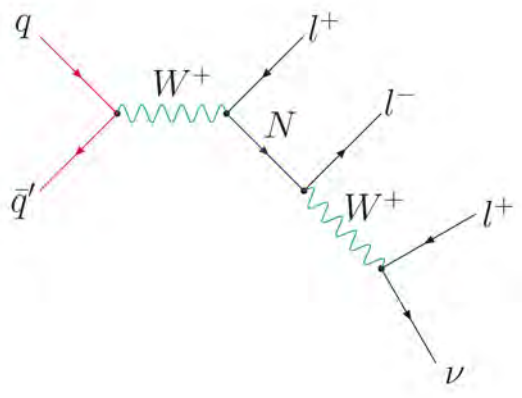

Fig. 49: Process to search for heavy Majoranas at LHC.

Note that present sensitivities are very far from the naive seesaw scaling $|U_{lh}|^2 \sim m_l/M_h$, so they are only exploring a relatively small corner of parameter space.

Lepton flavour violating processes

Massive neutrinos imply that lepton flavour violating processes, such as $\mu \to e\gamma$, eee or $\mu - e$ conversion in atoms, must exist at some level. Heavy Majorana neutrinos around the EW scale can significantly enhance these rates. The constraints on the mixing and mass coming from these searches cannot be included in Figs. 48 without further assumptions, since they depend on the different combination, $|\sum_i U_{ei}U^*_{\mu i}|$. They are shown in Fig. 50 and compared with other present constraints. Future searches will significantly improve present constraints for $M_N \in [1, 100]$ GeV.

11.2 Approximate Lepton Number

Type I seesaw models with a scale around the electroweak scale are very hard to test unless $|U_{lh}|^2 \gg m_l/M_h$. Although this is possible in some corners of parameter space for $n_R \geq 2$, being in such corners might be enforced and technically natural by an approximate lepton number symmetry [113, 114].

Let us consider the simplest case $n_R = 2$ [115]. If the two singlet states have opposite lepton charges and we impose an exact $U(1)$ global symmetry, the 3×2 Yukawa matrix, and the Majorana mass matrix have the following structures:

$$Y_\nu = \begin{pmatrix} Y_{e1} & 0 \\ Y_{\mu 1} & 0 \\ Y_{\tau 1} & 0 \end{pmatrix}, \quad M_N = \begin{pmatrix} 0 & M \\ M & 0 \end{pmatrix}. \tag{126}$$

For this texture, the heavy states form a Dirac pair, while the light neutrino masses vanish identically. The global symmetry can be only approximate if the zero entries in these matrices are small compared to the non-zero ones, but non vanishing. For example if we lift the zero in the 22 element of the M_N matrix to be $\mu \ll M$, we get the type of texture found in the so-called inverse seesaw models[3] [116, 117]. In

[3] In order to get at least two non-zero light neutrino masses by lifting the zeros of M_N only, it is necessary to have two pairs of singlets, each pair with +1 or -1 lepton charge, ie. $n_R = 4$. For $n_R = 2$, the zero's in the Yukawa matrix must be lifted aswell.

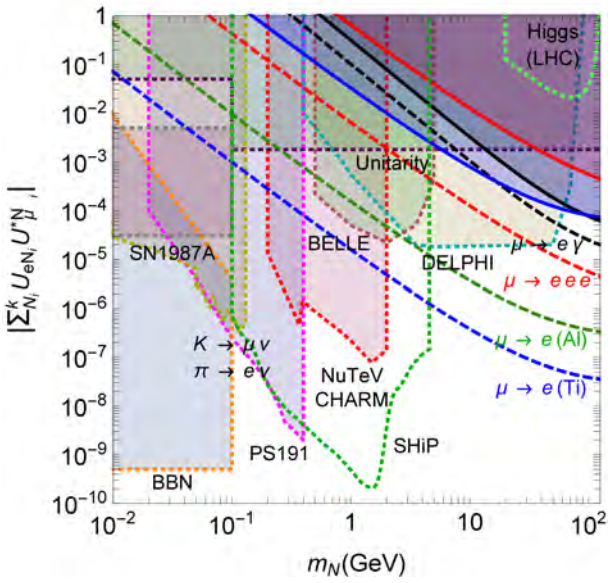

Fig. 50: Present bounds and prospects from lepton $\mu \to e\gamma, \mu \to eee$ and $\mu - e$ conversion searches (from Ref. [106]).

this case the light neutrino mass satisfies $m_l \propto \frac{\mu}{M^2}$. If we integrate out the scale M, the effective field theory describing this type of models is of the form

$$\mathcal{L} = \mathcal{L}_{\rm SM} + \sum_i \frac{\alpha_i}{\Lambda_{\rm LN}} \mathcal{O}_i^{d=5} + \sum_i \frac{\beta_i}{\Lambda^2_{\rm LFV}} \mathcal{O}_i^{d=6} + ..., \tag{127}$$

where the operators that break lepton number ($d = 5$) and those that preserve this symmetry ($d = 6$) are generically suppressed by different scales: $\Lambda_{\rm LN} \simeq \frac{M^2}{\mu} \gg \Lambda_{\rm LFV} \simeq M$. These models therefore have a richer phenomenology if M is at the EW scale, since yukawa's need not be suppressed. Future searches such as those mentioned in the previous section will be particularly important to constraint this subclass of seesaw models.

We have discussed the phenomenological implications of the minimal Type I seesaw model, which will be the hardest to test. The other types of models leading to the Weinberg operator have a richer phenomenology since the extra states couple to gauge fields (e.g the triplet scalar in type II or the fermion in type III), and therefore can be more copiously produced at colliders. In particular lepton number violation could give rise to spectacular signals at LHC, like same-sign lepton resonances in the type II seesaw model [118]:

$$pp \to H^{++}H^{--} \to l^+l^+l^-l^-. \tag{128}$$

Searches for triplet scalar and fermions are now standard LHC analyses.

12 Leptogenesis

The Universe is made of matter. The matter–antimatter asymmetry is measured to be

$$\eta_B \equiv \frac{N_b - N_{\bar{b}}}{N_\gamma} \sim 6.21(16) \times 10^{-10}\ . \tag{129}$$

One generic implication of neutrino mass models is that they provide a new mechanism to explain this asymmetry dynamically.

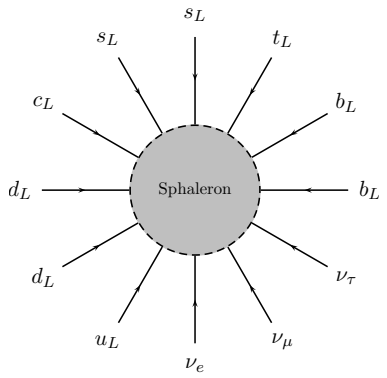

Fig. 51: Artistic view of a sphaleron.

It has been known for a long time that all the ingredients to generate such an asymmetry from a symmetric initial state are present in the laws of particle physics. These ingredients were first put forward by Sakharov [119]:

Baryon number violation

$B + L$ is anomalous in the SM [120] both with and without massive neutrinos. At high T in the early Universe, $B + L$ violating transitions are in thermal equilibrium [121] due to the thermal excitation of configurations with topological charge called sphalerons, see Fig. 51.

These processes violate baryon and lepton numbers by the same amount:

$$\Delta B = \Delta L. \tag{130}$$

In seesaw models, there is generically an additional source of L violation (and $B - L$). If a lepton charge is generated at temperatures where the sphalerons are still in thermal equilibrium, a baryon charge can be generated.

C and CP violation

Any lepton or baryon asymmetry can only be generated if there is C and CP violation. Seesaw models generically include new sources of CP violation. As we have seen in type I seesaw model with $n_R = 3$ there are six new CP phases in the lepton sector. They can be absorbed in the Yukawa matrix, Y_ν of eq. (111). For example, in the Casas-Ibarra parametrization, this matrix is writen as

$$Y_\nu = U^*_{\rm PMNS}\sqrt{m_l}R\sqrt{M_h}\frac{\sqrt{2}}{v}. \tag{131}$$

Three phases can be chosen as those in the PMNS matrix, and therefore accessible via neutrino oscillations and neutrinoless double-beta decay. The other three are the parameters of the general complex matrix R, that we cannot access at low-energies. Note that the combination $Y_\nu^\dagger Y_\nu$ only depends on the latter.

Departure from thermal equilibrium

In seesaw models, $B - L$ violating processes can be out-of-equilibrium at $T \gg T_{\rm EW}$ where the sphalerons are still in thermal equilibrium. In the type I seesaw model two possibilities of non-equilibrium L violation can be realised. In the high scale scenario $M_i \gg v$, the non-equilibrium condition is met at freeze out. The heavy states are thermally produced and freeze out at a temperatures similar to their masses [122]. A net lepton asymmetry can be produced if the decay rate is slower than the expansion of the Universe close to the decoupling temperature, so that the distribution functions of these states differ slightly from the thermal ones, as shown in Fig. 52. It is necessary however that CP

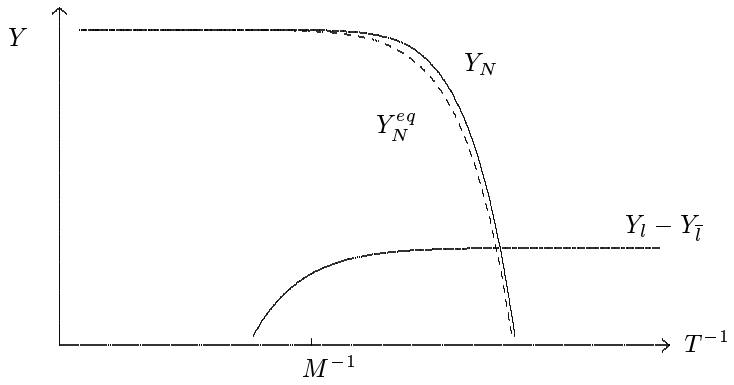

Fig. 52: Abundance of the heavy Majorana singlets at the decoupling temperature and the lepton number generated in the decay.

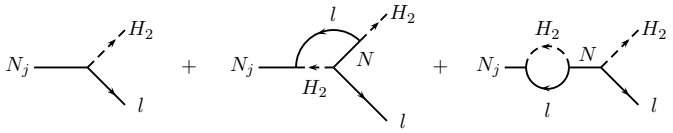

Fig. 53: Tree-level and one-loop diagrams contributing to heavy neutrino decays.

and C be violated in the out-of-equilibrium decays:

$$\epsilon_1 = \frac{\Gamma(N \to \Phi l) - \Gamma(N \to \Phi \bar{l})}{\Gamma(N \to \Phi l) + \Gamma(N \to \Phi \bar{l})} \neq 0 \, . \tag{132}$$

The new CP phases in the Yukawa matrix induce an asymmetry, ϵ_1, at the one-loop level (see Fig. 53). The final asymmetry is given by

$$Y_B = 10^{-2} \overbrace{\epsilon_1}^{\text{CP-asym}} \overbrace{\kappa}^{\text{eff. factor}} \, , \tag{133}$$

where κ is an efficiency factor which depends on the non-equilibrium dynamics. Therefore a relation between the baryon number of the Universe and the neutrino flavour parameters in ϵ_1 exists.

In the low-scale scenario, for $M_i < v$, the out-of-equilibrium condition is met at freeze-in [123] [101, 124]. It is possible that not all the massive states reach thermal equilibrium before T_{EW}. A non-vanishing lepton and baryon asymmetry can survive at T_{EW} and, if this is the case, sphaleron transitions that decouple at this point, can no longer wash it out. It turns out that these conditions can be met naturally in type I seesaw model for masses in the range $[0.1, 100]$ GeV. The relevant CP asymmetries arise in the production of the heavy seesaw states via the interference of CP-odd phases from the Yukawa's with CP-even phases from propagation. A quantum treatment of the corresponding kinetic equations is mandatory in this case.

An interesting question is whether the baryon asymmetry can be predicted quantitatively from the measurements at low energies of the neutrino mass matrix. Unfortunately this is not the case generically, because the asymmetry depends on more parameters than those that are observable at low energies.

For example, in the high-scale scenario, ϵ_1 can be approximated by [125]

$$\epsilon_1 = -\frac{3}{16\pi} \sum_i \frac{\mathrm{Im}[(Y_\nu^\dagger Y_\nu)^2_{i1}]}{(Y_\nu^\dagger Y_\nu)_{11}} \frac{M_1}{M_i} \, , \tag{134}$$

in the minimal model with $M_{2,3} \gg M_1$. It depends only on the CP phases of R, but not those in $U_{\rm PMNS}$.

If the prediction of the lepton asymmetry is not possible, it is possible to constrain the neutrino mass matrix, assuming that the lepton asymmetry explains the measured baryon asymmetry. Indeed, various upper bounds can be derived on the generated asymmetry. In particular ϵ_1 has been shown [126] to satisfy

$$|\epsilon_1| \leq \frac{8}{16\pi}\frac{M_1}{v^2}|\Delta m^2_{\rm atm}|^{1/2}\,, \tag{135}$$

and therefore leptogenesis in this model requires that the lightest heavy neutrino is rather heavy:

$$M_1 \geq \mathcal{O}(10^9\ {\rm GeV})\,. \tag{136}$$

For further details and references see Ref. [125].

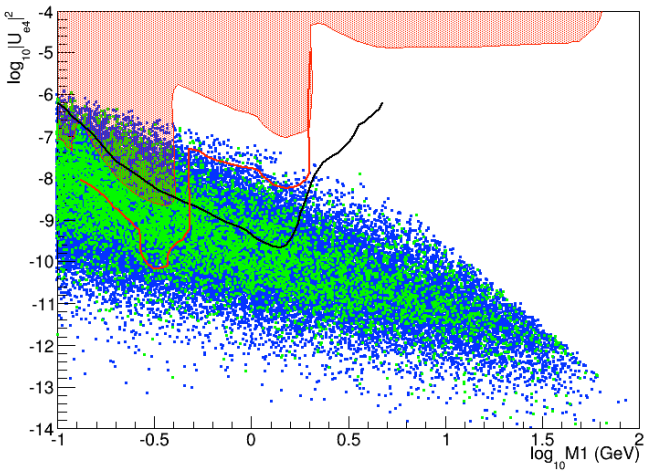

Fig. 54: Points on the plane $|U_{e4}|^2$ vs M_1 for which the baryon asymmetry, Y_B, is in the range $[1/5-1]\times Y_B^{\rm exp}$ (blue) and $[1-5]\times Y_B^{\rm exp}$ (green) for IO (from Ref. [127]). The red band are the present constraints [105], the solid black line shows the reach of the SHiP experiment [106] and the solid red line is the reach of LBNE near detector [107].

Interestingly, in the low-scale scenario, the states responsible for generating the baryon asymmetry might be accessible experimentally. For example, Fig. 54 shows the values of the mixing $|(U_{lh})_{e1}|^2$ and mass M_1 for which the baryon asymmetry can be explained within the type I seesaw model, compared to the sensitivity of future experiments such as SHiP and DUNE.

13 Conclusions

The results of many beautiful experiments in the last decade have demonstrated beyond doubt that neutrinos are massive and mix. The standard 3ν scenario can explain all available data, except that of the unconfirmed signal of LSND. The lepton flavour sector of the Standard Model is expected to be at least as complex as the quark one, even though we know it only partially.

The structure of the neutrino spectrum and mixing is quite different from the one that has been observed for the quarks: there are large leptonic mixing angles and the neutrino masses are much smaller than those of the remaining leptons. These peculiar features of the lepton sector strongly suggest that leptons and quarks constitute two complementary approaches to understanding the origin of flavour in the Standard Model. In fact, the smallness of neutrino masses can be naturally understood if there is new physics beyond the electroweak scale.

Many fundamental questions remain to be answered in future neutrino experiments, and these can have very important implications for our understanding of the Standard Model and of what lies beyond:

Are neutrinos Majorana particles? Are neutrino masses the result of a new physics scale? Is CP violated in the lepton sector? Could neutrinos be the seed of the matter–antimatter asymmetry in the Universe?

A rich experimental programme lies ahead where fundamental physics discoveries are very likely (almost warrantied). We can only hope that neutrinos will keep up with their old tradition and provide a window to what lies beyond the Standard Model.

References

[1] E. Fermi, "Trends to a Theory of beta Radiation. (In Italian)," *Nuovo Cim.*, vol. 11, pp. 1–19, 1934. [,535(1934)].

[2] H. Bethe and R. Peierls, "The 'neutrino'," *Nature*, vol. 133, p. 532, 1934.

[3] B. Pontecorvo, "Inverse beta process," *Camb. Monogr. Part. Phys. Nucl. Phys. Cosmol.*, vol. 1, pp. 25–31, 1991.

[4] F. Reines and C. L. Cowan, "The neutrino," *Nature*, vol. 178, pp. 446–449, 1956.

[5] C. L. Cowan, F. Reines, F. B. Harrison, H. W. Kruse, and A. D. McGuire, "Detection of the free neutrino: A Confirmation," *Science*, vol. 124, pp. 103–104, 1956.

[6] G. Danby, J. M. Gaillard, K. A. Goulianos, L. M. Lederman, N. B. Mistry, M. Schwartz, and J. Steinberger, "Observation of High-Energy Neutrino Reactions and the Existence of Two Kinds of Neutrinos," *Phys. Rev. Lett.*, vol. 9, pp. 36–44, 1962.

[7] K. A. Olive *et al.*, "Review of Particle Physics," *Chin. Phys.*, vol. C38, p. 090001, 2014.

[8] K. Assamagan *et al.*, "Upper limit of the muon-neutrino mass and charged pion mass from momentum analysis of a surface muon beam," *Phys. Rev.*, vol. D53, pp. 6065–6077, 1996.

[9] R. Barate *et al.*, "An Upper limit on the tau-neutrino mass from three-prong and five-prong tau decays," *Eur. Phys. J.*, vol. C2, pp. 395–406, 1998.

[10] S. Weinberg, "Baryon and Lepton Nonconserving Processes," *Phys. Rev. Lett.*, vol. 43, pp. 1566–1570, 1979.

[11] S. Weinberg, "Phenomenological Lagrangians," *Physica*, vol. A96, pp. 327–340, 1979.

[12] W. Buchmuller and D. Wyler, "Effective Lagrangian Analysis of New Interactions and Flavor Conservation," *Nucl. Phys.*, vol. B268, pp. 621–653, 1986.

[13] Z. Maki, M. Nakagawa, and S. Sakata, "Remarks on the unified model of elementary particles," *Prog. Theor. Phys.*, vol. 28, pp. 870–880, 1962.

[14] B. Pontecorvo, "Neutrino Experiments and the Problem of Conservation of Leptonic Charge," *Sov. Phys. JETP*, vol. 26, pp. 984–988, 1968. [Zh. Eksp. Teor. Fiz.53,1717(1967)].

[15] B. Pontecorvo, "Mesonium and anti-mesonium," *Sov. Phys. JETP*, vol. 6, p. 429, 1957. [Zh. Eksp. Teor. Fiz.33,549(1957)].

[16] E. K. Akhmedov and A. Yu. Smirnov, "Paradoxes of neutrino oscillations," *Phys. Atom. Nucl.*, vol. 72, pp. 1363–1381, 2009, 0905.1903.

[17] E. K. Akhmedov and J. Kopp, "Neutrino oscillations: Quantum mechanics vs. quantum field theory," *JHEP*, vol. 04, p. 008, 2010, 1001.4815. [Erratum: JHEP10,052(2013)].

[18] M. Cerdá, "," *Master Thesis University of Valencia*, 2011, 0905.1903.

[19] L. Wolfenstein, "Neutrino Oscillations in Matter," *Phys. Rev.*, vol. D17, pp. 2369–2374, 1978.

[20] S. P. Mikheev and A. Yu. Smirnov, "Resonance Amplification of Oscillations in Matter and Spectroscopy of Solar Neutrinos," *Sov. J. Nucl. Phys.*, vol. 42, pp. 913–917, 1985. [Yad. Fiz.42,1441(1985)].

[21] H. A. Bethe, "Energy production in stars," *Phys. Rev.*, vol. 55, pp. 434–456, 1939.

[22] J. N. Bahcall, M. H. Pinsonneault, and S. Basu, "Solar models: Current epoch and time dependences, neutrinos, and helioseismological properties," *Astrophys. J.*, vol. 555, pp. 990–1012, 2001,

astro-ph/0010346.

[23] B. T. Cleveland, T. Daily, R. Davis, Jr., J. R. Distel, K. Lande, C. K. Lee, P. S. Wildenhain, and J. Ullman, "Measurement of the solar electron neutrino flux with the Homestake chlorine detector," *Astrophys. J.*, vol. 496, pp. 505–526, 1998.

[24] W. Hampel *et al.*, "GALLEX solar neutrino observations: Results for GALLEX IV," *Phys. Lett.*, vol. B447, pp. 127–133, 1999.

[25] J. N. Abdurashitov *et al.*, "Solar neutrino flux measurements by the Soviet-American Gallium Experiment (SAGE) for half the 22 year solar cycle," *J. Exp. Theor. Phys.*, vol. 95, pp. 181–193, 2002, astro-ph/0204245. [Zh. Eksp. Teor. Fiz.122,211(2002)].

[26] Y. Fukuda *et al.*, "Solar neutrino data covering solar cycle 22," *Phys. Rev. Lett.*, vol. 77, pp. 1683–1686, 1996.

[27] Y. Fukuda *et al.*, "Measurement of the solar neutrino energy spectrum using neutrino electron scattering," *Phys. Rev. Lett.*, vol. 82, pp. 2430–2434, 1999, hep-ex/9812011.

[28] J. Hosaka *et al.*, "Solar neutrino measurements in super-Kamiokande-I," *Phys. Rev.*, vol. D73, p. 112001, 2006, hep-ex/0508053.

[29] Q. R. Ahmad *et al.*, "Measurement of the rate of $\nu_e + d \to p + p + e^-$ interactions produced by ^8B solar neutrinos at the Sudbury Neutrino Observatory," *Phys. Rev. Lett.*, vol. 87, p. 071301, 2001, nucl-ex/0106015.

[30] Q. R. Ahmad *et al.*, "Direct evidence for neutrino flavor transformation from neutral current interactions in the Sudbury Neutrino Observatory," *Phys. Rev. Lett.*, vol. 89, p. 011301, 2002, nucl-ex/0204008.

[31] K. Eguchi *et al.*, "First results from KamLAND: Evidence for reactor anti-neutrino disappearance," *Phys. Rev. Lett.*, vol. 90, p. 021802, 2003, hep-ex/0212021.

[32] S. Abe *et al.*, "Precision Measurement of Neutrino Oscillation Parameters with KamLAND," *Phys. Rev. Lett.*, vol. 100, p. 221803, 2008, 0801.4589.

[33] G. Bellini *et al.*, "Final results of Borexino Phase-I on low energy solar neutrino spectroscopy," *Phys. Rev.*, vol. D89, no. 11, p. 112007, 2014, 1308.0443.

[34] M. Honda, T. Kajita, K. Kasahara, and S. Midorikawa, "A New calculation of the atmospheric neutrino flux in a 3-dimensional scheme," *Phys. Rev.*, vol. D70, p. 043008, 2004, astro-ph/0404457.

[35] Y. Fukuda *et al.*, "Evidence for oscillation of atmospheric neutrinos," *Phys. Rev. Lett.*, vol. 81, pp. 1562–1567, 1998, hep-ex/9807003.

[36] Y. Ashie *et al.*, "A Measurement of atmospheric neutrino oscillation parameters by SUPER-KAMIOKANDE I," *Phys. Rev.*, vol. D71, p. 112005, 2005, hep-ex/0501064.

[37] Y. Ashie *et al.*, "Evidence for an oscillatory signature in atmospheric neutrino oscillation," *Phys. Rev. Lett.*, vol. 93, p. 101801, 2004, hep-ex/0404034.

[38] A. Holin, "Results from the MINOS Experiment and New MINOS+ Data," *PoS*, vol. NUFACT2014, p. 028, 2014, 1507.08564.

[39] F. P. An *et al.*, "Observation of electron-antineutrino disappearance at Daya Bay," *Phys. Rev. Lett.*, vol. 108, p. 171803, 2012, 1203.1669.

[40] J. K. Ahn *et al.*, "Observation of Reactor Electron Antineutrino Disappearance in the RENO Experiment," *Phys. Rev. Lett.*, vol. 108, p. 191802, 2012, 1204.0626.

[41] Y. Abe *et al.*, "Indication for the disappearance of reactor electron antineutrinos in the Double Chooz experiment," *Phys. Rev. Lett.*, vol. 108, p. 131801, 2012, 1112.6353.

[42] K. Abe *et al.*, "Observation of Electron Neutrino Appearance in a Muon Neutrino Beam," *Phys. Rev. Lett.*, vol. 112, p. 061802, 2014, 1311.4750.

[43] M. C. Gonzalez-Garcia, M. Maltoni, and T. Schwetz, "Updated fit to three neutrino mixing: status of leptonic CP violation," *JHEP*, vol. 11, p. 052, 2014, 1409.5439.

[44] P. A. R. Ade *et al.*, "Planck 2015 results. XIII. Cosmological parameters," *arXiv:1502.01589[astro-ph.CO]*, 2015, 1502.01589.

[45] S. K. Agarwalla and P. Hernandez, "Probing the Neutrino Mass Hierarchy with Super-Kamiokande," *JHEP*, vol. 10, p. 086, 2012, 1204.4217.

[46] S. T. Petcov and M. Piai, "The LMA MSW solution of the solar neutrino problem, inverted neutrino mass hierarchy and reactor neutrino experiments," *Phys. Lett.*, vol. B533, pp. 94–106, 2002, hep-ph/0112074.

[47] S. Choubey, S. T. Petcov, and M. Piai, "Precision neutrino oscillation physics with an intermediate baseline reactor neutrino experiment," *Phys. Rev.*, vol. D68, p. 113006, 2003, hep-ph/0306017.

[48] F. An *et al.*, "Neutrino Physics with JUNO," *J. Phys.*, vol. G43, no. 3, p. 030401, 2016, 1507.05613.

[49] A. Cervera, A. Donini, M. B. Gavela, J. J. Gomez Cadenas, P. Hernandez, O. Mena, and S. Rigolin, "Golden measurements at a neutrino factory," *Nucl. Phys.*, vol. B579, pp. 17–55, 2000, hep-ph/0002108. [Erratum: Nucl. Phys.B593,731(2001)].

[50] K. Abe *et al.*, "Physics potential of a long-baseline neutrino oscillation experiment using a J-PARC neutrino beam and Hyper-Kamiokande," *PTEP*, vol. 2015, p. 053C02, 2015, 1502.05199.

[51] R. Acciarri *et al.*, "Long-Baseline Neutrino Facility (LBNF) and Deep Underground Neutrino Experiment (DUNE) Conceptual Design Report Volume 2: The Physics Program for DUNE at LBNF," *arXiv:1512.06148 [hep-ex]*, 2015, 1512.06148.

[52] A. Aguilar-Arevalo *et al.*, "Evidence for neutrino oscillations from the observation of anti-neutrino(electron) appearance in a anti-neutrino(muon) beam," *Phys. Rev.*, vol. D64, p. 112007, 2001, hep-ex/0104049.

[53] B. Armbruster *et al.*, "Upper limits for neutrino oscillations muon-anti-neutrino —> electron-anti-neutrino from muon decay at rest," *Phys. Rev.*, vol. D65, p. 112001, 2002, hep-ex/0203021.

[54] A. A. Aguilar-Arevalo *et al.*, "Improved Search for $\bar{\nu}_\mu \to \bar{\nu}_e$ Oscillations in the MiniBooNE Experiment," *Phys. Rev. Lett.*, vol. 110, p. 161801, 2013, 1207.4809.

[55] T. A. Mueller *et al.*, "Improved Predictions of Reactor Antineutrino Spectra," *Phys. Rev.*, vol. C83, p. 054615, 2011, 1101.2663.

[56] G. Mention, M. Fechner, T. Lasserre, T. A. Mueller, D. Lhuillier, M. Cribier, and A. Letourneau, "The Reactor Antineutrino Anomaly," *Phys. Rev.*, vol. D83, p. 073006, 2011, 1101.2755.

[57] P. Huber, "On the determination of anti-neutrino spectra from nuclear reactors," *Phys. Rev.*, vol. C84, p. 024617, 2011, 1106.0687. [Erratum: Phys. Rev.C85,029901(2012)].

[58] F. P. An *et al.*, "Measurement of the Reactor Antineutrino Flux and Spectrum at Daya Bay," *Phys. Rev. Lett.*, vol. 116, no. 6, p. 061801, 2016, 1508.04233.

[59] A. B. Sousa, "First MINOS+ Data and New Results from MINOS," *AIP Conf. Proc.*, vol. 1666, p. 110004, 2015, 1502.07715.

[60] P. F. Harrison, D. H. Perkins, and W. G. Scott, "Tri-bimaximal mixing and the neutrino oscillation data," *Phys. Lett.*, vol. B530, p. 167, 2002, hep-ph/0202074.

[61] S. F. King and C. Luhn, "Neutrino Mass and Mixing with Discrete Symmetry," *Rept. Prog. Phys.*, vol. 76, p. 056201, 2013, 1301.1340.

[62] P. Minkowski, "$\mu \to e\gamma$ at a Rate of One Out of 10^9 Muon Decays?," *Phys. Lett.*, vol. B67, pp. 421–428, 1977.

[63] M. Gell-Mann, P. Ramond, and R. Slansky, "Complex Spinors and Unified Theories," *Conf. Proc.*, vol. C790927, pp. 315–321, 1979, 1306.4669.

[64] T. Yanagida, "HORIZONTAL SYMMETRY AND MASSES OF NEUTRINOS," *Conf. Proc.*, vol. C7902131, pp. 95–99, 1979.

[65] R. N. Mohapatra and G. Senjanovic, "Neutrino Mass and Spontaneous Parity Violation," *Phys.*

Rev. Lett., vol. 44, p. 912, 1980.

[66] M. Magg and C. Wetterich, "Neutrino Mass Problem and Gauge Hierarchy," *Phys. Lett.*, vol. B94, p. 61, 1980.

[67] J. Schechter and J. W. F. Valle, "Neutrino Masses in SU(2) x U(1) Theories," *Phys. Rev.*, vol. D22, p. 2227, 1980.

[68] C. Wetterich, "Neutrino Masses and the Scale of B-L Violation," *Nucl. Phys.*, vol. B187, p. 343, 1981.

[69] G. Lazarides, Q. Shafi, and C. Wetterich, "Proton Lifetime and Fermion Masses in an SO(10) Model," *Nucl. Phys.*, vol. B181, pp. 287–300, 1981.

[70] R. N. Mohapatra and G. Senjanovic, "Neutrino Masses and Mixings in Gauge Models with Spontaneous Parity Violation," *Phys. Rev.*, vol. D23, p. 165, 1981.

[71] R. Foot, H. Lew, X. G. He, and G. C. Joshi, "Seesaw Neutrino Masses Induced by a Triplet of Leptons," *Z. Phys.*, vol. C44, p. 441, 1989.

[72] E. Ma, "Pathways to naturally small neutrino masses," *Phys. Rev. Lett.*, vol. 81, pp. 1171–1174, 1998, hep-ph/9805219.

[73] A. Zee, "A Theory of Lepton Number Violation, Neutrino Majorana Mass, and Oscillation," *Phys. Lett.*, vol. B93, p. 389, 1980. [Erratum: Phys. Lett.B95,461(1980)].

[74] A. Zee, "Charged Scalar Field and Quantum Number Violations," *Phys. Lett.*, vol. B161, p. 141, 1985.

[75] K. S. Babu, "Model of 'Calculable' Majorana Neutrino Masses," *Phys. Lett.*, vol. B203, p. 132, 1988.

[76] A. Abada, C. Biggio, F. Bonnet, M. B. Gavela, and T. Hambye, "Low energy effects of neutrino masses," *JHEP*, vol. 12, p. 061, 2007, 0707.4058.

[77] G. Aad *et al.*, "Combined Measurement of the Higgs Boson Mass in pp Collisions at $\sqrt{s} = 7$ and 8 TeV with the ATLAS and CMS Experiments," *Phys. Rev. Lett.*, vol. 114, p. 191803, 2015, 1503.07589.

[78] G. Degrassi, S. Di Vita, J. Elias-Miro, J. R. Espinosa, G. F. Giudice, G. Isidori, and A. Strumia, "Higgs mass and vacuum stability in the Standard Model at NNLO," *JHEP*, vol. 08, p. 098, 2012, 1205.6497.

[79] F. Vissani, "Do experiments suggest a hierarchy problem?," *Phys. Rev.*, vol. D57, pp. 7027–7030, 1998, hep-ph/9709409.

[80] J. A. Casas, J. R. Espinosa, and I. Hidalgo, "Implications for new physics from fine-tuning arguments. 1. Application to SUSY and seesaw cases," *JHEP*, vol. 11, p. 057, 2004, hep-ph/0410298.

[81] J. A. Casas and A. Ibarra, "Oscillating neutrinos and muon —> e, gamma," *Nucl. Phys.*, vol. B618, pp. 171–204, 2001, hep-ph/0103065.

[82] A. Donini, P. Hernandez, J. Lopez-Pavon, M. Maltoni, and T. Schwetz, "The minimal 3+2 neutrino model versus oscillation anomalies," *JHEP*, vol. 07, p. 161, 2012, 1205.5230.

[83] M. Blennow, E. Fernandez-Martinez, J. Lopez-Pavon, and J. Menendez, "Neutrinoless double beta decay in seesaw models," *JHEP*, vol. 07, p. 096, 2010, 1005.3240.

[84] F. Capozzi, E. Lisi, A. Marrone, D. Montanino, and A. Palazzo, "Neutrino masses and mixings: Status of known and unknown 3ν parameters," *arXiv:1601.07777 [hep-ph]*, 2016, 1601.07777.

[85] A. Ibarra, E. Molinaro, and S. T. Petcov, "TeV Scale See-Saw Mechanisms of Neutrino Mass Generation, the Majorana Nature of the Heavy Singlet Neutrinos and $(\beta\beta)_{0\nu}$-Decay," *JHEP*, vol. 09, p. 108, 2010, 1007.2378.

[86] M. Mitra, G. Senjanovic, and F. Vissani, "Neutrinoless Double Beta Decay and Heavy Sterile Neutrinos," *Nucl. Phys.*, vol. B856, pp. 26–73, 2012, 1108.0004.

[87] J. Lopez-Pavon, E. Molinaro, and S. T. Petcov, "Radiative Corrections to Light Neutrino Masses

in Low Scale Type I Seesaw Scenarios and Neutrinoless Double Beta Decay," *JHEP*, vol. 11, p. 030, 2015, 1506.05296.

[88] A. de Gouvea, "See-saw energy scale and the LSND anomaly," *Phys. Rev.*, vol. D72, p. 033005, 2005, hep-ph/0501039.

[89] A. de Gouvea, W.-C. Huang, and J. Jenkins, "Pseudo-Dirac Neutrinos in the New Standard Model," *Phys.Rev.*, vol. D80, p. 073007, 2009, 0906.1611.

[90] A. de Gouvea and W.-C. Huang, "Constraining the (Low-Energy) Type-I Seesaw," *Phys.Rev.*, vol. D85, p. 053006, 2012, 1110.6122.

[91] A. Donini, P. Hernandez, J. Lopez-Pavon, and M. Maltoni, "Minimal models with light sterile neutrinos," *JHEP*, vol. 07, p. 105, 2011, 1106.0064.

[92] C. Giunti and M. Laveder, "3+1 and 3+2 Sterile Neutrino Fits," *Phys. Rev.*, vol. D84, p. 073008, 2011, 1107.1452.

[93] J. Kopp, P. A. N. Machado, M. Maltoni, and T. Schwetz, "Sterile Neutrino Oscillations: The Global Picture," *JHEP*, vol. 05, p. 050, 2013, 1303.3011.

[94] D. Notzold and G. Raffelt, "Neutrino Dispersion at Finite Temperature and Density," *Nucl. Phys.*, vol. B307, p. 924, 1988.

[95] R. Barbieri and A. Dolgov, "Bounds on Sterile-neutrinos from Nucleosynthesis," *Phys. Lett.*, vol. B237, p. 440, 1990.

[96] K. Kainulainen, "Light Singlet Neutrinos and the Primordial Nucleosynthesis," *Phys. Lett.*, vol. B244, pp. 191–195, 1990.

[97] P. Hernandez, M. Kekic, and J. Lopez-Pavon, "Low-scale seesaw models versus N_{eff}," *Phys.Rev.*, vol. D89, no. 7, p. 073009, 2014, 1311.2614.

[98] P. Hernandez, M. Kekic, and J. Lopez-Pavon, "$N_{\rm eff}$ in low-scale seesaw models versus the lightest neutrino mass," *Phys.Rev.*, vol. D90, no. 6, p. 065033, 2014, 1406.2961.

[99] S. Hannestad, R. S. Hansen, T. Tram, and Y. Y. Y. Wong, "Active-sterile neutrino oscillations in the early Universe with full collision terms," *JCAP*, vol. 1508, no. 08, p. 019, 2015, 1506.05266.

[100] S. Dodelson and L. M. Widrow, "Sterile-neutrinos as dark matter," *Phys. Rev. Lett.*, vol. 72, pp. 17–20, 1994, hep-ph/9303287.

[101] T. Asaka and M. Shaposhnikov, "The nuMSM, dark matter and baryon asymmetry of the universe," *Phys.Lett.*, vol. B620, pp. 17–26, 2005, hep-ph/0505013.

[102] E. Bulbul, M. Markevitch, A. Foster, R. K. Smith, M. Loewenstein, and S. W. Randall, "Detection of An Unidentified Emission Line in the Stacked X-ray spectrum of Galaxy Clusters," *Astrophys. J.*, vol. 789, p. 13, 2014, 1402.2301.

[103] A. Boyarsky, O. Ruchayskiy, D. Iakubovskyi, and J. Franse, "Unidentified Line in X-Ray Spectra of the Andromeda Galaxy and Perseus Galaxy Cluster," *Phys. Rev. Lett.*, vol. 113, p. 251301, 2014, 1402.4119.

[104] X.-D. Shi and G. M. Fuller, "A New dark matter candidate: Nonthermal sterile neutrinos," *Phys. Rev. Lett.*, vol. 82, pp. 2832–2835, 1999, astro-ph/9810076.

[105] A. Atre, T. Han, S. Pascoli, and B. Zhang, "The Search for Heavy Majorana Neutrinos," *JHEP*, vol. 05, p. 030, 2009, 0901.3589.

[106] S. Alekhin *et al.*, "A facility to Search for Hidden Particles at the CERN SPS: the SHiP physics case," *arXiv:1504.04855[hep-ph]*, 2015, 1504.04855.

[107] C. Adams *et al.*, "The Long-Baseline Neutrino Experiment: Exploring Fundamental Symmetries of the Universe," 2013, 1307.7335.

[108] F. del Aguila and J. A. Aguilar-Saavedra, "Distinguishing seesaw models at LHC with multi-lepton signals," *Nucl. Phys.*, vol. B813, pp. 22–90, 2009, 0808.2468.

[109] P. S. B. Dev, A. Pilaftsis, and U.-k. Yang, "New Production Mechanism for Heavy Neutrinos at

the LHC," *Phys. Rev. Lett.*, vol. 112, no. 8, p. 081801, 2014, 1308.2209.

[110] J. C. Helo, M. Hirsch, and S. Kovalenko, "Heavy neutrino searches at the LHC with displaced vertices," *Phys. Rev.*, vol. D89, p. 073005, 2014, 1312.2900.

[111] E. Izaguirre and B. Shuve, "Multilepton and Lepton Jet Probes of Sub-Weak-Scale Right-Handed Neutrinos," *Phys. Rev.*, vol. D91, no. 9, p. 093010, 2015, 1504.02470.

[112] A. M. Gago, P. Hernandez, J. Jones-Perez, M. Losada, and A. Moreno Briceño, "Probing the Type I Seesaw Mechanism with Displaced Vertices at the LHC," *Eur. Phys. J.*, vol. C75, no. 10, p. 470, 2015, 1505.05880.

[113] G. C. Branco, W. Grimus, and L. Lavoura, "The Seesaw Mechanism in the Presence of a Conserved Lepton Number," *Nucl. Phys.*, vol. B312, p. 492, 1989.

[114] J. Kersten and A. Yu. Smirnov, "Right-Handed Neutrinos at CERN LHC and the Mechanism of Neutrino Mass Generation," *Phys. Rev.*, vol. D76, p. 073005, 2007, 0705.3221.

[115] M. B. Gavela, T. Hambye, D. Hernandez, and P. Hernandez, "Minimal Flavour Seesaw Models," *JHEP*, vol. 09, p. 038, 2009, 0906.1461.

[116] D. Wyler and L. Wolfenstein, "Massless Neutrinos in Left-Right Symmetric Models," *Nucl. Phys.*, vol. B218, p. 205, 1983.

[117] R. N. Mohapatra and J. W. F. Valle, "Neutrino Mass and Baryon Number Nonconservation in Superstring Models," *Phys. Rev.*, vol. D34, p. 1642, 1986.

[118] W.-Y. Keung and G. Senjanovic, "Majorana Neutrinos and the Production of the Right-handed Charged Gauge Boson," *Phys. Rev. Lett.*, vol. 50, p. 1427, 1983.

[119] A. D. Sakharov, "Violation of CP Invariance, c Asymmetry, and Baryon Asymmetry of the Universe," *Pisma Zh. Eksp. Teor. Fiz.*, vol. 5, pp. 32–35, 1967. [Usp. Fiz. Nauk161,61(1991)].

[120] G. 't Hooft, "Symmetry Breaking Through Bell-Jackiw Anomalies," *Phys. Rev. Lett.*, vol. 37, pp. 8–11, 1976.

[121] V. A. Kuzmin, V. A. Rubakov, and M. E. Shaposhnikov, "On the Anomalous Electroweak Baryon Number Nonconservation in the Early Universe," *Phys. Lett.*, vol. B155, p. 36, 1985.

[122] M. Fukugita and T. Yanagida, "Baryogenesis Without Grand Unification," *Phys. Lett.*, vol. B174, p. 45, 1986.

[123] E. K. Akhmedov, V. Rubakov, and A. Y. Smirnov, "Baryogenesis via neutrino oscillations," *Phys.Rev.Lett.*, vol. 81, pp. 1359–1362, 1998, hep-ph/9803255.

[124] L. Canetti, M. Drewes, T. Frossard, and M. Shaposhnikov, "Dark Matter, Baryogenesis and Neutrino Oscillations from Right Handed Neutrinos," *Phys. Rev.*, vol. D87, p. 093006, 2013, 1208.4607.

[125] S. Davidson, E. Nardi, and Y. Nir, "Leptogenesis," *Phys. Rept.*, vol. 466, pp. 105–177, 2008, 0802.2962.

[126] S. Davidson and A. Ibarra, "A Lower bound on the right-handed neutrino mass from leptogenesis," *Phys. Lett.*, vol. B535, pp. 25–32, 2002, hep-ph/0202239.

[127] P. Hernandez, M. Kekic, J. Lopez-Pavon, J. Racker, and N. Rius, "Leptogenesis in GeV scale seesaw models," *JHEP*, vol. 10, p. 067, 2015, 1508.03676.